INFORMATION TO USERS

This manuscript has been reproduced from the microfilm master. UMI films the text directly from the original or copy submitted. Thus, some thesis and dissertation copies are in typewriter face, while others may be from any type of computer printer.

The quality of this reproduction is dependent upon the quality of the copy submitted. Broken or indistinct print, colored or poor quality illustrations and photographs, print bleedthrough, substandard margins, and improper alignment can adversely affect reproduction.

In the unlikely event that the author did not send UMI a complete manuscript and there are missing pages, these will be noted. Also, if unauthorized copyright material had to be removed, a note will indicate the deletion.

Oversize materials (e.g., maps, drawings, charts) are reproduced by sectioning the original, beginning at the upper left-hand corner and continuing from left to right in equal sections with small overlaps. Each original is also photographed in one exposure and is included in reduced form at the back of the book.

Photographs included in the original manuscript have been reproduced xerographically in this copy. Higher quality 6" x 9" black and white photographic prints are available for any photographs or illustrations appearing in this copy for an additional charge. Contact UMI directly to order.

UMI

A Bell & Howell Information Company
300 North Zeeb Road, Ann Arbor MI 48106-1346 USA
313/761-4700 800/521-0600

Computer Simulations of Quantum Films on Surfaces

by

Ajit K. S. Jaiswal

A dissertation submitted to the Graduate Faculty in Physics in partial fulfillment of the requirements for the degree of Doctor of Philosophy, City University of New York

1998

This manuscript has been read and accepted for the Graduate Faculty in Physics in satisfaction of the dissertation requirement for the degree of Doctor of Philosophy.

1/20/98 — Date

Chair of Examining Committee
Professor Brian B. Schwartz (Physics)
Brooklyn College, CUNY

1/20/98 — Date

Executive Officer, Physics
Professor Louis S. Celenza

Geoffrey V. Chester
Professor Emeritus (Physics), Cornell University

Marten L. DenBoer
Professor (Physics), Hunter College, CUNY

Micha Tomkiewicz
Professor (Physics), Brooklyn College, CUNY

Paula A. Whitlock
Assoc. Professor (Computer and Information Science), Brooklyn College, CUNY

Supervisory Committee

THE CITY UNIVERSITY OF NEW YORK

ABSTRACT

COMPUTER SIMULATIONS OF QUANTUM FILMS ON SURFACES

by

Ajit Kumar Singh Jaiswal

Adviser: Professor Brian B. Schwartz

In this thesis we present a study of the ground states of helium films, on a range of binding surfaces. We represent the system as a weakly interacting boson gas under the influence of an attenuating external field, which represents the force due to the surface. Monte-Carlo simulations, with periodic boundary conditions have been used to model an infinite system in the plane of the surface, but finite in the normal direction.

We study the film structure and energetics. The surfaces studied range from the experimentally well studied and strongly attracting surface of graphite to the very weak and barely binding surface of cesium. The study ignores the effects of surface structure, specially important for graphite.

Energetics suggests two different types of weak-binding surfaces. Type I are those with a single atom binding energy less than the binding energy per particle in the bulk fluid. Such surfaces will support a fluid monolayer. An example is the surface of lithium, for which we present our calculations. We find that a lithium surface is not strong enough to support a solid monolayer. Those surfaces that have a binding energy greater than the per particle binding energy in the bulk fluid.

we refer to as of Type II. Such surfaces will be non-wetting, and our calculations of the fluid density on this surface seems to indicate this. A good example is the Sodium surface potential, for which we find that the minimum stable coverage corresponds to two layers.

We then calculate the equations of states for the graphite, lithium and sodium surfaces and show different qualitative regimes. For Type I surfaces, there are two qualitatively distinct regimes. Above the equilibrium areal-density there is the regime of stable coverages. Below this density the negative value of the slope signals instability and a phase transition, and our simulation model is no longer valid.

Our data for layering on graphite shows reasonably good agreement with the experimental layer promotion data. Onset and dissappearance of superfluidity in the second layer of graphite, is in good agreement with experimental reports.

Acknowledgements

I thank the members of the supervisory committee for their comments on the draft of the thesis.

My greatest debt is to Prof. Chester for numerous suggestions and comments throughout the course of the calculations presented and in particular on the multilayer work.

I am indebted to Prof. Whitlock for introducing me to the field of Monte Carlo simulations and to Prof. Schwartz for providing encouragement and support.

Much of the computational work was carried out using the computer networks of the Computer Science department and the computer center at Brooklyn College. My special thanks to Bill Goodridge, the SUN system administrator at Brooklyn College, for help with several network related issues and timely installations of computer packages.

I am thankful to Tom MacFarland and Silvio Vitiello for numerous discussions and hospitality during my visit to Cornell, during the summer of 1991.

Finally, I would like to thank Prof. Mate, for encouragement and letting me use the mathematics department computer room, at the most crucial times.

Table Of Contents

List of Tables

List of Figures

CHAPTER I : Introduction

In this thesis we present our calculations and results on the ground state of helium films on a variety of surfaces. We have used computer simulations to solve for the ground state of the many-body Schrödinger wave-equation representing these helium film systems.

In this chapter we first provide the context and overview of the work presented in this thesis. We discuss the basic ideas and approaches that we have taken and describe the scope of our work. We then provide a brief historical review of the field of computer simulations of atomic systems, from the vantage point of the work presented in this thesis. We then briefly review the development of ideas on liquid helium and its modeling in computer simulation work. Finally, we review the low temperature properties of helium and then briefly comment on recent research, both theoretical and experimental, on helium films.

Context and Overview of the Present Work

The interacting Bose gas has been used as a model for the behavior of liquid ^{4}He. Successful calculations have been performed to study the ground state of liquid ^{4}He, using variational and Green's function Monte Carlo methods.

Recently, there has been considerable interest in studying liquid ^{4}He films on well prepared atomic substrates. Such systems may be treated as a weakly interacting Bose gas in the presence of a weak external field that represents the surface. For surface forces much stronger than the helium-helium interatomic force, we expect a layered film structure to emerge. But for surface field strengths

of the order of the interatomic fields, we expect various regimes of film quality. First, the surface interaction must be strong enough to hold the atoms to the surface to form at least a liquid monolayer. Since pressure must be applied to liquid helium to solidify it, the interaction must be stronger still to hold the atoms into a solid layer. A much weaker surface attraction than the interatomic interactions should fail to have even a monolayer form and for weaker and weaker surface force we expect the properties of the film to approach those of the full three dimensional bulk liquid.

Recent theoretical work on studying helium films have used various density functional models (Clements *et. al.*, 1994) (Cheng *et. al.*, 1991). There seems to be qualitative agreement about wetting behavior on a class of surfaces, representing the alkali metals. The range of phenomena predicted is remarkable and there has been a need for a quantitative quantum theory of helium films on surfaces, obtained by direct integration of the many-body equation. Such a task is only feasible using Monte Carlo techniques, and it is the aim of the present work to attempt such a construction. We have confined our interest to studying the ground state of these film systems. Both the variational and Green's function Monte Carlo techniques used in the present work apply only to the ground state.

We describe the thermodynamics of an atomic system in equilibrium under the influence of an external field pointing in a fixed direction (the z axis) and varying along it. One can imagine a large number of atoms in a large box. In the absence of external forces the system will be homogeneous at equilibrium.

When an external attractive force is applied say through one face of the box (the $z = 0$ plane), thus reducing the symmetry of the system from spherical to cylinderical, the atoms in the box will tend to accumulate towards this wall, thus creating inhomogeneity in the spatial distribution of the atoms inside the box. The surface forces we consider depend only on z and not on x and y. Thus we neglect the surface structure and consider it to be strictly planar. Such a system has translational invariance in the plane of the surface (the x-y plane) but not in the direction normal to the surface (the z-direction). In the absence of the external field, the homogenous atomic system in the box (the case of the bulk fluid) is described by distribution functions that are isotropic and depend only on the spherical coordinate r. With the inhomogeniety created by the surface the distributions characterising the system will explicitly depend on z in addition to r. We present expressions for the distribution functions and the structure factor for this inhomogenous case.

We consider a graphite surface as an example of a strongly adsorbing surface, one that is experimentally known to produce at least five layers of helium at temperatures of about a tenth of a Kelvin (Greywall, 1993). The first two layers solidify but the later ones are liquid. The graphite potential has a strong well-depth of about 180 K, compared to the weaker well depth of 10 K of the helium-helium interatomic potential. Our results indicated that for surface potentials with well-depths of about 25 K we still find solid monolayer form. With surface potential well-depths of around 20 K, the surface seems unable to support a solid monolayer.

but forms a well defined stable liquid monolayer. The lithium potential has a well-depth of 17.1 K and supports a liquid monolayer. At higher coverages we show that at least three layers form, after which the systems tends rapidly to the bulk state. For the sodium surface with a well depth of 10.4 K not even a stable liquid monolayer form. For the cesium surface, with a well-depth of 4.4 K, the helium film tends to bulk rapidly, showing little structure.

The Green's function Monte Carlo technique provides an accurate approach for studying the ground states of bosonic many-body systems. For successful convergence, however, it requires a good approximation to the ground state wave-function. The ground state energy that it yields is *exact* up to statistical sampling errors. However, observables that do not commute with the Hamiltonian, like the correlation function, $g(\vec{r})$, can only be approximately calculated. The validity of the approximation depends on the goodness of the approximation to the ground state function that is used as an input (the importance function).

Using the Raleigh-Ritz variational principle, good trial wave-functions have been constructed. The many-variable integral for several sets of parameters in the trial wave function is evaluated using the Variational Monte Carlo technique. The wavefunction with the parameter set that gives the lowest energy represents the best approximation to the ground state of the system. Often much valuable information about the system can be obtained from such a study, and Green's function Monte Carlo calculations can be seen as improving the picture already obtained using the Variational Monte Carlo method.

Such studies for the ground-state of bulk helium have been successfully carried out. The ground-state energy as well as the correlation functions are in excellent agreement with experiment at the equilibrium density of the system. At higher densities, and particularly near freezing, however, the calculations are not so accurate, owing to poor trial wave functions.

There have been several approaches that attempt to incorporate the structure information contained in the pair correlation function, $g(r)$, in the pair-function (Wu *et. al.*, 1961), (Masserini *et. al.*, 1987). However, optimization of the pair function with parameters explicitly depending on density remains an open problem. Reasonably good trial-wave functions have been constructed at least for the equilibrium density. At higher densities an ingeneous trial wavefunction (shadow fuction) has been constructed, with insights borrowed from the path integral formulation of quantum mechanics (Vitiello *et. al.*, 1988). This approach has been used to study near-freezing densities (MacFarland *et. al.*, 1994), and the phase transition to the solid state (Pederiva *et. al.*, 1994, 1995), with good results.

Construction of good trial wave functions for systems of helium films, may be done by simply taking the successful trial wave functions used to study bulk helium, and multiplying it with a z-dependent factor that effectively acts as a cover for the film. Periodic boundary conditions are no longer applied in the z-direction, and the atoms in the simulation are free to move about, contained only by the cover function.

The study and discussion of layered films on helium, has often been charac-

terised by a *layer-by-layer* approach. One studies the first layer on the substrate with the atoms interacting with the single-atom potential of helium on that surface and the helium-helium interatomic potential. After the monolayer has been studied, one estimates the potential that the second layer will see due to the surface, by summing and averaging over the surface and the atoms of the first layer. This second layer is then seen to be interacting in this averaged potential and the interatomic helium-helium potential.

We did not use this approach. Instead, we proposed studying the multilayer system, with each atom interacting with the surface potential and the helium-helium interatomic potential. We expect the multilayer description to emerge from the solution of the full problem.

For a graphite surface, which is the strongest adsorbing surface we consider, we have studied upto three layers. The density profiles obtained represent a reasonable picture of a multilayer system.

The current work is aimed at exploring the possibility of carrying out accurate simulations of the ground state of helium films over the wide range of binding substrates using the ideas and techniques that have proved successful in studying bulk helium. We have established, in this thesis, the basic groundwork for a comprehensive Green's function Monte Carlo study for the range of surfaces, from as strong and well studied one as that of graphite to the weakest surface of cesium.

Most of the work presented in this thesis is variational. Only for studying

the liquid monolayer on lithium have we carried out Green's function Monte Carlo calculations. The lithium surface has a well-depth of 17.1 K and a single-atom binding energy of −9.00 K. which is below the helium-helium binding energy of about −7.14 K. A well formed liquid monolayer is expected and the calculations confirm this.

Historical review

The first Monte Carlo simulation of atomic systems were carried out for classical systems. Metropolis *et. al.*, (1953), established an algorithm to conveniently sample a function of a large number of variables and used it to sample the Boltzmann distribution function for a system of two-dimensional rigid spheres, and calculated the equation of state. They used 224 atoms in their simulation and employed periodic boundary conditions to reduce surface effects. Their approach provided the foundations of much of later simulations of atomic and molecular systems. They extended their work to systems of particles with Lennard-Jones type interactions and to the system of three-dimensional rigid spheres (Rosenbluth *et. al.*, 1954). Their work established the methodological foundations of later simulation work on atomic and molecular systems.

Following up on the methods established by Metropolis *et. al.*, Wood and Parker (1956), reported calculations for the compressibility factor, excess internal energy, excess constant-volume heat capacity, and the radial distribution function of Lennard-Jones (12, 6) molecules at various densities. Phase transitions for simple classical systems, were studied by Adler and Wainright (1957) and Hansen

and Verlet (1969). Extensive work on classical fluids followed. (Rahman. 1964). (Verlet. 1967). (Romano and Singer. 1979). (Anderson. 1980). and several others.

The earliest studies and theoretical modeling of the properties of superfluid helium (helium II) were by London (1938). Tizsa (1938). Landau (1941). Bogolyubov (1947). Feynman (1953. 1954). and others.

The analogy between liquid ^{4}He and an ideal Bose-Einstein gas was first recognized by London (1938). He suggested that the lambda-transition in liquid helium could be understood as the analog for a liquid of the transition which occurs in an ideal Bose-Einstein gas at low temperatures. The fact that no lambda-transition had been found in ^{3}He supported this point of view. Further support came from the works of Matsubara (1951). Feynman (1953). Chester (1955). Penrose and Onsager (1956). Brueckner and Sawada (1957) and others.

Representation of the ground state of ^{4}He as a *product of pair functions* was considered as early as 1940 by Bijl. Bogolyubov and Zubarev (1955). showed that in the weak coupling limit the exact ground state wave function can be written as a product of pair functions.

The first studies of the ground state of bulk helium using variational methods with product of pair function wavefunctions were carried out by Mott (1949). Dingle (1949). and Jastrow (1955).

The first Variational Monte Carlo study of the ground state of bulk helium using Monte Carlo techniques was carried out by McMillan (1964). This was the first attempt to study a quantum system by Monte Carlo methods. At its heart

was the Metropolis algorithm for sampling a function of several variables. In constructing the trial wave function, he built on earlier work and chose a product of pair function form. The implementation of periodic boundary conditions was as in earlier classical work of Metropolis (1953) and others.

Green's function Monte Carlo as an *exact* technique to calculate the ground state energy of a bosonic many body system was developed by Kalos, Verlet, and Levesque (1974). Kalos, applied this technique to study the ground state of Helium (1974), considering interatomic potentials as a repulsive hard core plus an attractive perturbation. With an *exact* theory around, it was for the first time that the interatomic potentials, laboriously fitted from available experimental and ab-initio approaches, could be tested. A systematic study (Kalos *et. al.*, 1981) of available potentials at that time showed that the Aziz potential was the "best" and later studies have favored the use of this potential over the Lennard-Jones potential, which is somtimes used as a reference.

The present work, building on the previous work cited above, is a systematic Monte Carlo study of the ground state of helium films on a wide range of surfaces. It presents a methodologically sound basic approach to the problem and derives a satifactory physical picture, upon which successive improvements can be made.

An extension of our calculations would be to study excited states of helium systems. A start in this direction has been by David Ceperley (1995), who has developed what is called Path Integral Monte Carlo technique, that yields good solutions down to about 1 K, below which one must rely on extrapolations to

Green's function Monte Carlo results for the ground state. Applying Path Integral Monte Carlo to helium films seems to have been attempted, but there seems to be no published account yet. Since Path Integral Monte Carlo seems to be the most promising method to study temperature dependence, it would be an exciting undertaking.

Collateral work

We have excluded from the above listing of major ideas, some recent refinements in the art of constructing good trial wave functions, and considerations in simulating solid helium. We have noted above that for the graphite surface the first two layers have been reported to be solid. Thus for strongly attractive surfaces like graphite we must have a wave function that accomodates a mixed solid and liquid phase. Good and simple trial wave functions at densities close to freezing are not yet available. There has been a feeling that a simple trial wavefunction does not exist. Recently a very sophisticated "shadow trial wave function" has been proposed (Vitiello *et. al.*, 1988). It has been convincingly demonstrated that it gives a good picture of the solid state and is "better" (Tom MacFarland et. al. 1994) than the simple trial functions at densities close to freezing.

A general solution to the fermion problem (the case of helium three for example) has eluded even the best Monte Carlo theorists. It seems about the best one can do is the so called fixed node approximation, which for few body systems may give just passable numbers The difficulty is the following: Monte Carlo techniques essentially are ways to compute an integral. Problems that can be reduced

to quadratures, can therefore be handled by Monte Carlo methods. However in order to be able to sample the distribution function in the integrand, as needed in the integral form of the Schrödinger wave equation (GFMC), one must be able to interpret it as a probability density. Now a probability density, must always be non-negative. The trouble with excited states and anti-symmetric fermionic states is that they have both positive and negative parts. So general methods fail. If one treats the positive and negative parts separately, assuming fixed values of the nodes (which must be varied, since it is yielded by the solution), one may use the usual Monte Carlo methods, for the separate parts. This approach taken by David Arnow (1981), seems to have been successfully applied recently, to study simple chemical few body systems (Anderson and others).

For the problem of simulating solid helium it is firmly believed, though no proof exists, that a simple pair function trial wave function to simulate a quantum solid does not exist. A heuristic argument, due to Hansen, has been around for about twenty five years (Chester, private communication). Hanson, observed that, for classical systems the Lindemann ratio (ratio of root-mean-square deviation of atoms from the lattice sites to the lattice constant) was around 14% and remarkably constant for a wide range of classical solids. In a quantum solid like helium, due to zero point motion this is around 40%, which is remarkably higher. There is a formal analogy between the Boltzmann distribution function used for classical systems, to compute ensamble averages, and the expression for the wave-function (the quantum mechanical distribution function) when written

as an exponential. The exponent of the wavefunction is formally analogous to the potential in the Boltzmann distribution function and it is for this reason that it is called the pseudopotential. Potentials with various structure (one or more local minimas) all yield the same Lindeman ratio. for classical solids studied. Since solid helium is much more diffuse and has a much higher Lindeman ratio. simple pair pseudopotentials cannot be found to simulate solid helium. However. there exists no systematic study of pseudopotentials with enough structure at higher densities. Recent efforts (Moroni *et. al.*, 1995) at obtaining optimized pair functions. have not explicitly incorporated structure information available from the two body correlation function. and they seem to have obtained McMillan like pair functions. Optimization of a pair function with density dependent structure needs to be undertaken. This would have conclusive bearing on whether or not a pair function can successfully represent solid helium.

Review of the Low Temperature Properties of ^{4}He

Atomic ^{4}He is the most inert of all the elements and its interatomic potential is the weakest known. Its two electrons in the 1s orbital are tightly bound and the electron distribution is very nearly spherically symmetric. It acquires a very small polarizability in atomic collisions in the fluid state. The interactions of these atoms among themselves. which arises due to the electromagetic interactions of the closed shell electrons. has essentially two parts: one a highly repulsive part at short range and the other a very weak attractive part at long inter-particle separations. It is this attractive part that gives it a self-bound minimum energy

state at a specific density (the *equilibrium value* at zero pressure and temperature). (The ideal gas under zero pressure would fill all space and go to zero density.) At high temperatures it is the closest example we know to an ideal monoatomic gas.

Ever since the work of deBoer and Michiels (1938) wherein they fit the properties of the inert gases to a Lennard-Jones type of potential, much of the theoretical study of bulk helium (and the other rare gases) has been carried out using this potential which has a well depth of about 10.0 K and a hard core radius of 2.556 Angstroms (more details are given in Appendix III). The potential supports only a very weak bound state.

^{4}He is liquid at zero temperature and the only known substance to be so. It solidifies under a pressure of 26 atmospheres in the fcc closed packing structure. At a temperature of 2.16 K it undergoes a first order phase transition and displays superfluidity (The ideal bose gas of the same mass and density turns superfluid at 3.14 K.) Below, this transition temperature the liquid is referred to as helium II. Zero temperature studies, like the present one, are therefore dealing with this phase of the liquid.

Fermi liquid theory provides a coherent theoretical framework in which to discuss ^{3}He. There is no coherent body of theory for liquid ^{4}He. Interesting developments in the theory of dense classical fluids provided impetus to understanding quantum liquids. The liquids studied were all spherical atoms such as argon, xenon, and krypton, whose interaction is very strongly repulsive at short distances and rather weakly attractive at large distances. The heuristic Lennard-

Jones potential:

$$V(r) = 4\epsilon[(\sigma/r)^{12} - (\sigma/r)^{6}] \tag{1.1}$$

provided a good starting for describing the weak Van der Waals interactions. The attractive part of the potential is strong enough to condense all these fluids at low temperatures.

The classical fluids all obey, rather accurately, a law of corresponding states which says that if ϵ and σ, of the Lennard-Jones potential are used to scale energies and lengths then all physical properties of these substances are universal functions of the reduced temperature and the reduced densities. Thus the equation of state for all of them has the universal form $p_c^* = p_c^*(T^*, V^*)$ where p^* is the reduced pressure $(p\sigma^3/\epsilon)$ and is a universal function of T^*, the reduced temperature (kT/ϵ), and V^*, the reduced volume $(V/N\sigma^3)$. For helium however quantum effects enter through the so called deBoer parameter $\Lambda^* = \hbar/\sigma\sqrt{(m\epsilon)}$. And thus the equation of state for a quantum system has the form: $p_c^* = p_c^*(T^*, V^*, \Lambda^*)$ and is not a universal function; it depends on mass and also depends on the statistics obeyed by the particles.

All these fluids crystallize under pressure. The "classical" fluids crystallize at very low pressures at low temperature. Quantum fluids require a finite pressure even at absolute zero for them to crystallize. It turns out that pressure is not the best variable to understand crystallization - a much better parameter is density.

The basic physical picture we now have of the classical fluids is that to a very good approximation the repulsive part of the potential can be replaced by a hard

sphere potential and the attractive part can be treated as a perturbation whose main effect is to provide a mean attractive potential in which the hard spheres move. In essense this picture tells us that the details of the potential are not important and that one can understand most of the physical properties of dense classical fluids in terms of a fluid of hard spheres moving in a mean free potential.

It has been shown (Kalos, Levesque and Verlet, 1974) that this picture is also applicable to liquid ^{4}He as far as its basic structural properties are concerned i.e. equation of state and spatial correlations. The discussion is confined to absolute zero, as only the ground state can be studied by the Monte Carlo techniques employed. They showed that the equation of state, static correlation function $g(\vec{r})$, and the crystallization density of a Lennard-Jones model of helium could all be accurately calculated from a perturbation scheme in which a hard sphere model was the first approximation and the attractive part of the L-J potential was included as a perturbative correction. This is the same approach as was used in the study of classical fluids.

From both variational and exact calculations of the ground state of the L-J system, the number of particles with zero momentum, or the Bose condensate fraction is $10\% \pm 1\%$. Calculations with the Aziz potential also gives the same result. Further, the number in the zero momentum state depends on density. These considerations are at zero pressure.

Helium adsorbs to all known substances at low enough temperatures, since most substances present much stronger attraction to the helium atoms compared

to the attraction between the helium atoms themselves. Helium readily wets the surface and forms solid layers under pressure. In the case of graphite, a monolayer of helium has been extensively studied. It is known to exhibit several commensurate and incommensurate phases with various crystalline structures.

If, however, the surface presents an attraction of the same order as that of the interatomic attraction, we expect that the layering of the atoms may not be smooth, or well defined. The layers may not be spread flat out, and there may be clusters or "puddles" of atoms all over the surface. If the surface does not provide a stronger attraction than the neighbouring atom, an atom may prefer to cluster around the neighboring atoms rather than adhere to the surface. Uniform wetting will not result in this case and atoms close to the surface may just loosely hang around.

Review of Recent Theoretical Work on Helium Films

The theoretical and experimental study of helium films on weak binding substrates is an active area of study. Since, helium was thought of as a "universal wetting agent", much interest was generated by Cheng, Cole et. al. (1991). Their work was based on Zaremba and Kohns' work (1976) which showed that the depth of the pair potentials between helium and the alkali metals was small. Cheng, Cole et. al. (1991) pointed out that helium will not wet some alkali metal surfaces at zero temperature. They modeled the helium-surface potential by:

$$V(z) = 4C_3^3/(27D^2z^9) - C_3/z^3 \qquad (1.2)$$

where D is the depth of the potential and C_3 is the coefficient of the long range

Van der Waals interaction. This potential form and the numerical values of the constants they used are quite tentative and the numerical constants may be upto 50% in error. However in the absence of both conclusive experimental and theoretical information these potentials have been widely used in the study of these surfaces. The present work uses this potential family too for modeling the weak binding surfaces.

We briefly comment on the major theoretical papers relevant to the properties of helium on surfaces at very low temperatures.

• Cheng *et. al* (PRL, 1991) predict new wetting and nonwetting phenomena for ^{4}He adsorbed on weak-binding substrates such as alkali metals. Specifically, they claim that ^{4}He will *not* wet all the alkali metals; only on Li and Na did they expect to see wetting behaviour, with prewetting.

• Cheng *et. al* (Physica, 1991) predict the adsorption of ^{4}He and para-H_2 to exhibit exotic properties on weak-binding surfaces. For ^{4}He, alternative scenarios including non-wetting, wetting and a Bose gas monolayer. For H_2 they claim that a monolayer superfluid phase can be created by a suitable choice of the substrate. Interesting phenonema are also predicted for ^{3}He/^{4}He mixtures in multilayer films.

• Clements *et. al* (Physica, 1994) study growth of helium films on weakly attractive substrates, using the theory of hypernetted chains for inhomogenous systems. Close to the substrate, they claim, the film grows by formation of well defined liquid layers. Above a minimum stable coverage a liquid monolayer uniformly covers the surface. Upon increasing the coverage a second liquid layer

begins to grow by the formation of two-dimensional liquid "clusters". Above a certain coverage, the second layer leaves vacuum-cluster coexistence, and the system regains the full planar symmetry. The scenario is repeated for a third liquid layer. They interpret data on graphite, using their theoretical conclusions.

• Saarela *et. al* (1993) study growth of helium films on graphite and alkali substrates, and conclude that the growth of a new layer undergoes a phase-transition from a cluster formation into the connected superfluid when the coverage is increased. Based on the connection to the two- dimensional fluid they propose a microscopic theory of quantum vortices in ^{4}He films at zero temperature, in which single vortices are treated as quasiparticles.

• Clements *et. al* (1994) for alkali metal and graphite surfaces, claim the existence of a surface mode for coverages of a monolayer or more and a bulk mode which gains strength as the coverage is increased.

• Clements *et. al* (1993) present a systematic treatment based on density functional theory. In both the two and three dimensional bulk ^{4}He limits, they claim agreement with 2D Monte Carlo and 3D experimental results. Inspite of their methods being approximate and of a qualitative nature, they insist on having uncovered all essential aspects of the physical picture of boson films.

Review of Recent Experimental Work on Helium Films

Helium films are being actively investigated experimentally. The focus of research seems to be on wetting, superfluid and specific heat properties. We briefly comment on the major experimental papers relevant to the properties of

helium on surfaces at very low temperatures.

• Shirron *et. al* (1991) report adsorption isotherms and third-sound resonance of atomically thin ^{4}He films on solid hydrogen. Their third sound mesurements have been carried out at 0.18 K and down to a total helium coverage of 0.45±0.01 atomic layers (and to a maximum of 6 layers), indicating a zero temperature inert coverage of less than 0.3 layers. They plot surface density vs. thickness of the helium film on hydrogen.

• Nacher and Dupont-Roc, (1991) report testing wetting properties of alkali-metallic surfaces by superfluid-helium through heat transport. Appearing as an exception among other substrates, they found cesium to interrupt superfluid film-flow, suggesting nonwetting of cesium by superfluid helium. Their operating temperature was between 1.3 and 1.8 K. Their samples and the surfaces studied may be contaminated, however. They also do not provide data on thicknesses of the films studied.

• Zimmerli *et. al* (1992) report pronounced dips with integral layer periodicity in the third sound velocity. The minimum ^{4}He coverage on graphite needed to support third sound was found to be nearly three layers. They find evidence of layer-by-layer growth of ^{4}He in vapor pressure isotherms down to 1.35 K and third sound isotherms down to 1 K.

• Ketola *et. al* (1992) report wetting of a cesium substrate by more than 9 layers and of a glass substrate by 11.5 layers or more. They find that below the stated thickness third sound does not propagate. Their experiments were carried

out at an operating temperature of 1.38 K .

• Crowell *et. al* (1992) report on torsional oscillator studies of superfluidity in the second and higher layers of ^{4}He films adsorbed on basal plane graphite. They observe a reentrant superfluid phase in the second layer of adsorbed helium. which dissappears before the completion of the second layer and reappears early in the third layer. Their mesurements extend over a range of coverage from 1.5 to 7 atomic layers and temperatures from 20 mK to 1.5 K.

• Greywall (1993) reports heat capacity of ^{4}He adsorbed on graphite for temperatures extending down to 100 mK and for coverages upto five atomic layers. His work focuses mainly on the transitional region between the commensurate structure and the incommensurate phase of the first adsorbed layer. He obtains results that match well with ^{3}He. indicating that at these coverages the overlap between the atomic wavefunctions are not appreciable.

• Wyatt *et. al* (1995) report the prewetting line and estimate the wetting temperature for ^{4}He on Rb. They obtain $T_w = 309$ mK which is much lower than that found for cesium. Based on this low value they claim that rubidium may be the only other alkali element besides cesium that is not wetted by ^{4}He .

• Crowell *et. al* (1996) report conclusion of their study described in the above paper. They conclude that there are several different regimes of superfluid behaviour. Superfluidity in the second layer shows an anamalous temperature dependence and is destroyed by solidification of the film. The superfluid film appears to coexist with a two dimensional surface gas for low coverages in the

third layer. Evidence of a phase transition, which may be the reconstruction of an underlying layer, appears just above the completion of the third layer. Modulation of the superfluid signal with coverage is seen through the completion of the sixth layer.

In this chapter we provided the context of the work presented in this thesis. We also briefly described our ideas and methods and the historical background. We reviewed the field of helium films from the point of view of the work presented in this thesis. In chapter two we present a phenomenological model to describe the system of helium films. This model is constructed using the framework of thermodynamics, and describes the helium film as an inhomogenous system in equilibrium. In chapter three, we describe the computational techniques we used in our calculations. These are mainly the Variational Monte Carlo and Green's function Monte Carlo techniques. We also describe briefly the simplex minimisation technique that we used to improve on the minimum energy parameter set obtained by Variational Monte Carlo . In chapter four we describe the trial wavefunctions that we have used to represent the ground state of the helium film systems that have been studied in this thesis. The results are discussed in chapters five, six and seven. Conclusions and future directions for research are discussed in chapter eight which is the last chapter of this thesis.

CHAPTER II : Statement of the Problem

The Thermodynamic Model

In this chapter we construct a phenomenological description of the fluid phases of the system in the familiar language of thermodynamics. The usual considerations for a homogenous system, need to be modified to obtain a useful thermodynamic description of equilibrium states of a system under the influence of external forces that induce inhomogeneity in the mass density. For, the system under consideration, we have cylinderical symmetry in the problem and the inhomogenity is in the direction normal to the surface. The volume is no longer a descriptive parameter since the atoms of the system aggregate towards the attractive wall leaving empty space towards the opposite sides of the "box". However, "thin" slices of the fluid parallel to the surface may still be considered homogenous.

An important assumption we make is that the equilibrium states of the system can be specified by : U, A, and N, where U is the internal energy, A the area of cross section, and N the total number of atoms in the "box". We will find it convenient to work with the variables U/N, the specific energy or the energy per particle and A/N, the specific area or area per particle, or rather U/N and $\sigma = N/A$, the number of atoms per unit area.

The external field acts like an attractive gravitational force pulling the atoms of the system and at the same time constitutes the conceptual wall that keeps the atoms from falling through, and together with the walls of the sides keeps them contained in a finite volume.

We consider the limit when the area of cross-section, A, and N go to infinity in such a way that, σ, the number of atoms per unit area is finite. At equilibrium σ will be constant throughout the box. In assuming this we ignore the effects due to the walls on the sides, and as long as A is much larger than the average interatomic distance, this is clearly a good assumption.

The pressure on the walls will be due to three factors:

a) the kinetic energy (the ideal gas contribution)

b) the interatomic potential (the Van der Waal contribution)

c) the external field (hydrostatic pressure)

The normal force on the sides of the wall will be a function of $\sigma$and z. There will be a unique value of σat which the system will have zero pressure. In the limit, when the external field goes to zero this value of σwill go to infinity such that σ/height_of_film goes to a finite constant. This constant is the bulk equilibrium density of the liquid.

After these preliminaries, we now describe the thermodynamics of the system. We shall follow the postulatory approach modeled on the one taken in the book titled *Thermodynamics*, by H. B. Callen.

Postulate I :

The equilibrium states of the system are completely specified by the extensive parameters U, A and N.

The equilibrium states exist by virtue of the attractive inter-atomic intertactions, and the fact that the external field does not depend on time.

Postulate II :

The entropy S, of the system, is a function of the extensive parameters of the system and is a maximum for the equilibrium values of the extensive parameters, in the manifold of equilibrium states.

$$S = S(U, A, N) \tag{2.1}$$

This *fundamental relation* contains *all* thermodynamic information about the system. We shall however work in the energy representaion

$$U = U(S, A, N) \tag{2.2}$$

(the fact that this inversion can be done, is postulated later) or in the Helmholtz free energy representation

$$F = F(T, A, N) \tag{2.3}$$

Since we shall mostly be concerned with the system at absolute zero, we note that the two represention are identical at $T = 0$. (since, $F = U - TS$)

Postulate III :

The entropy of a composite system is additive over the constituent, subsystems. The entropy is continuous and differentiable and is a monotonically increasing function of the energy.

The composite systems we consider are identical systems kept side-by-side, each with the same T, A, and N and under the influence of the same external field. We can consider the system to be a composite of slices parallel to the surface. The

entropy, or the internal energy of the entire system will be a sum of the entropies or internal energies of each slice.

This implies that the entropy of the system is a homogeneous first-order function of the extensive parameters:

$$S(\lambda U, \lambda A, \lambda N) = \lambda S(U, A, N) \tag{2.4}$$

Taking λ to be $1/N$, we obtain:

$$S(U, A, N) = Ns(U/N, A/N, 1) \tag{2.5}$$

where $u = U/N$ is the internal energy per atom, $\sigma = N/A$, is the number of atoms per unit area, and $s = S/N$ is the entropy per atom.

Note that in a homogeneous system the analog of $1/\sigma$, is the specific volume ($v = V/N$), where V is the volume of the homogeneous system.

The monotonic property implies that the entropy function can be inverted : $U = U(S, A, N)$.

The internal energy per atom is therefore a function of the specific entropy, s, and the coverage σ.

$$u \equiv \frac{U(S/N, A/N, 1)}{N} \equiv \frac{U(s, 1/\sigma, 1)}{N} \equiv u(s, \sigma) \tag{2.6}$$

It is this quantity that we calculate at $T = 0$, with the Green's function Monte Carlo method.

Postulate IV :

The entropy of the system vanishes in the state for which

$$\left(\frac{\partial U}{\partial S}\right)_{A,N} = 0 \tag{2.7}$$

that is at the zero of temperature.

Intensive parameters of the system

The intensive parameters of the system are the partial derivatives of the internal energy with respect to the extensive parameters.

$$\begin{aligned} dU &= \left(\frac{\partial U}{\partial S}\right)_{A,N} dS + \left(\frac{\partial U}{\partial A}\right)_{S,N} dA + \left(\frac{\partial U}{\partial N}\right)_{S,A} dN \\ &= TdS - \tilde{P}dA + \mu dN \end{aligned} \tag{2.8}$$

where

$$\begin{aligned} T &= \left(\frac{\partial U}{\partial S}\right)_{A,N} \equiv \left(\frac{\partial u}{\partial s}\right)_{A,N} \\ -\tilde{P} &= \left(\frac{\partial U}{\partial A}\right)_{S,N} \equiv \left(\frac{\partial u}{\partial a}\right)_{S,N} \equiv -\sigma^2 \left(\frac{\partial u}{\partial \sigma}\right)_{S,N}, \quad a = A/N \quad \textit{and} \\ \mu &= \left(\frac{\partial U}{\partial N}\right)_{S,A} \end{aligned} \tag{2.9}$$

Since we will be concerned with the limit $N \to \infty, A \to \infty, N/A \to \sigma$ (a constant) the specific internal energy which is a function of the variables s and σ is a more useful quantity:

$$\begin{aligned} du &= \left(\frac{\partial u}{\partial s}\right)_{\sigma} ds + \left(\frac{\partial u}{\partial \sigma}\right)_{s} d\sigma \\ &= Tds + \frac{\tilde{P}}{\sigma^2} d\sigma \end{aligned} \tag{2.10}$$

T and μ have the usual interpretations of temperature and the chemical potential respectively. $\tilde{P}$ however is the force per unit length, where the length is along the perimeter of the cross-section of the system, and the force is outward in this plane. To keep the box in equilibrium at a fixed value of A, this force would have to be applied by the walls on the sides.

We conjecture that :

$$\tilde{P} = \int_0^\infty P(z)dz \tag{2.11}$$

where P(z) is the usual pressure inside the box. Note that we have not yet given a prescription for calculating this pressure. This pressure is due to three contributions as previously noted.

The equations of state of the system

The intensive parameters expressed as functions of the extensive parameters are the equations of state of the system.

$$T = T(S, A, N) \tag{2.12}$$

$$\tilde{P} = \tilde{P}(S, A, N) \tag{2.13}$$

and

$$\mu = \mu(S, A, N) \tag{2.14}$$

The Gibbs-Duhem relation of the system,

$$d\mu = -sdT + \frac{1}{\sigma}d\tilde{P} \tag{2.15}$$

reduces the number of independent equations of state to two. Along an isotherm, we have

$$d\mu = \frac{1}{\sigma}d\tilde{P} \tag{2.16}$$

and since we shall only be interested in the $T = 0$ solution of the system, a knowledge of the second equation of state will yield the third by a direct integration.

Summary of results obtainable from the internal energy, $u(\sigma)$, obtainable from the Monte Carlo calculations

Green's function Monte Carlo calculations for a given surface yield the internal energy per atom at zero temperature as a function of coverage: $u(\sigma)$

Then:

$$\tilde{P}(\sigma) = \sigma^2\left(\frac{du}{d\sigma}\right) \tag{2.17}$$

$$\begin{aligned}\mu(\sigma) &= \mu_o + \sigma(\tilde{P} - \tilde{P}_o) \\ &= \mu_o + \sigma^3\left[\left(\frac{du}{d\sigma}\right) - \left(\frac{du}{d\sigma}\right)_o\right]\end{aligned} \tag{2.18}$$

where the subscript o refers to some reference state.

The isothermal compressibility is given by.

$$\kappa_T = \frac{1}{\sigma}\left(\frac{d\sigma}{d\tilde{P}}\right) = \frac{1}{\sigma}\frac{1}{\left(\frac{d\tilde{P}}{d\sigma}\right)} = \frac{1}{\sigma}\frac{1}{\left[2\sigma\left(\frac{du}{d\sigma}\right) + \sigma^2\left(\frac{d^2u}{d^2\sigma}\right)\right]} \tag{2.19}$$

Hydrostatics of the system From the one-body density matrix, $\rho(z;z')$, the one-body density, $\rho(z;z)$, can be estimated from Monte Carlo calculations and the hydrostatic pressure of the system can be calculated as a function of z. The mass density of the system is easily expressed in terms of the one-body density. $\rho(z) = m\sigma\rho(z;z)$.

Consider an element of the fluid of cross-section area dA and thickness dz. The force balance at equilibrium requires that.

$$-P(z+dz)dA + P(z)dA - \frac{\rho dz dA}{m}\left(\frac{\partial V}{\partial z}\right) = 0 \tag{2.20}$$

or

$$\frac{P(z+dz) - P(z)}{dz} = -\frac{\rho}{m}\left(\frac{\partial V}{\partial z}\right) \tag{2.21}$$

Integrating this expression with respect to z we obtain.

$$P(z) = P(0) - \frac{1}{m}\int_0^z \rho(z')\left(\frac{\partial V(z')}{\partial z'}\right)dz' \tag{2.22}$$

The surface density of atoms will eventually fall to zero at some value of z, say z_∞. At this point the pressure will be zero: $P(z_\infty) = 0$

The surface $z = z_\infty$, may be considered the upper wall of the box. Note that since there is zero pressure at this boundary, no mechanical work is done when this boundary moves as a result of changes introduced through the other walls of the system.

The potential energy of a volume element $dzdA$, due to the external field is:

$$\frac{\rho dz dA}{m} V(z) \tag{2.23}$$

The potential energy of the whole system due to the external field :

$$(P.E.)_{external} = (P.E.)_{external}(0) + \frac{A}{m}\int_0^{z_\infty} \rho(z')V(z')dz' \tag{2.24}$$

The total force per unit length on the sides is given by,

$$\tilde{P} = \int_0^{z_\infty} P(z)dz \tag{2.25}$$

These results are for the entire inhomogenous system. Often we will be interested in the properties of the fluid inside a horizontal slice of a given thickness (a particular "layer", for instance). We must then compute the required properties from the pair-distribution function, which is also obtainable from the Monte Carlo calculations.

The pair distribution Function $g(\rho, z_1, z_2)$

Consider a general N-particle quantum-mechanical system, described by the quantum mechanical state vector $|\Psi\rangle$ or equivalently the density operator $\hat{\rho} =$

$|\Psi\rangle\langle\Psi|$. We shall work in the space representation. Then the density matrix can be written as:

$$\begin{aligned}\rho(r_1,\ldots,r_N;r'_1,\ldots,r'_N) &= \langle r_1,\ldots,r_N|\hat{\rho}|r'_1,\ldots,r'_N\rangle \\ &= \psi^*(r_1,\ldots,r_N)\psi(r'_1,\ldots,r'_N)\end{aligned} \tag{2.26}$$

We can define n-particle density matrices as

$$\rho(r_1,\ldots,r_n;r'_1,\ldots,r'_n) = \langle r_1,\ldots,r_n|\hat{\rho}|r'_1,\ldots,r'_n\rangle \tag{2.27}$$

$$= \int \psi^*(r_1,\ldots r_n,r_{n+1},\ldots r_N)\psi(r'_1,\ldots r'_n,r_{n+1},\ldots r_N)dr_{n+1}..dr_N \tag{2.28}$$

Then, the one-body and the two-body density matrices are defined as

$$\rho(r_1;r'_1) = \int \psi^*(r_1,r_2\ldots r_N)\psi(r'_1,r_2,r_3\ldots r_N)dr_2\ldots dr_N \tag{2.29}$$

$$\rho(r_1,r_2;r'_1,r'_2) = \int \psi^*(r_1,r_2,r_3\ldots r_N)\psi(r'_1,r'_2,r_3\ldots r_N)dr_3\ldots dr_N \tag{2.30}$$

The probability that particle 1 is in the volume dr_1 and particle 2 is in the volume dr_2 is then $\rho(r_1,r_2;r_1,r_2)dr_1dr_2$

If the system is in thermodynamic equilibrium with a reservoir at the absolute temperature T then it can be shown that the density operator is

$$\hat{\rho} = Z^{-1}e^{-H/kT} \tag{2.31}$$

The normalization coefficient Z is chosen to make the trace of ρ equal to one.

$$Z = \mathrm{Tr}\ \{e^{-H/kT}\} \tag{2.32}$$

Since all physical observables can be calculated using either the wavefunction Ψ or the density operator $\hat{\rho}$, and since the density operator can be defined in terms

of the wave-function, a knowledge of the wavefunction of the system can be used to calculate thermodynamic properties of the system.

It is however convenient to define n-particle distribution functions in terms of the n-particle density matrices as:

$$g_N^{(n)}(r_1,\ldots r_2) = \frac{\rho(r_1,\ldots,r_n;r_1,\ldots,r_n)}{\prod_{i=1}^{n}\rho(r_i;r_i)} \tag{2.33}$$

or in terms of the wavefunctions as:

$$g_N^{(n)}(r_1,\ldots r_2) = \frac{\int |\psi(r_1,\ldots,r_n,r_{n+1},\ldots,r_N)|^2 dr_{n+1}dr_N}{\prod_{i=1}^{n}\int |\psi(r_1,\ldots,r_{i-1},r_i,r_{i+1},\ldots,r_N)|^2 dr_1\ldots dr_{i-1}dr_{i+1}dr_N} \tag{2.34}$$

As the mutual distances between the n particles increase, the correlations between their positions are expected to decrease. Consequently, in the limit $|r_i - r_j| \rightarrow \infty$ for all $1 \leq i,j \leq n$, the n-particle probability densities $\rho(r_1,\ldots,r_n;r_1,\ldots,r_n)$ will factorize into the product of n single-particle densities:

$$\rho(r_1,\ldots,r_n;r_1,\ldots,r_n) \approx \rho(r_1;r_1)\ldots\rho(r_N;r_N) \tag{2.35}$$

In this limit the position of each of the n particles is independent of the positions of the remaining $n-1$ particles. In this case, it can be seen that $g_N^{(n)}(r_1,\ldots r_2) \rightarrow 1$ for all n as the mutual distance between the n particles increase indefinitly. Strictly speaking the limit of mutual distances makes sense only in the thermodynamic limit. For systems of macroscopic size, however, the asymptotic limit is reached for all practical purposes when $|r_i - r_j| \sim V^{1/3}$, the distance $V^{1/3}$ being many order of magnitudes larger than typical interatomic distances. The most important

distribution functions are the single-particle density function, $\rho(r_1 : r_1')$ and the pair function, $g_N^{(2)}(r_1, r_2)$

Some of the important quantities that can be determined using these distribution functions, are summarized below:

The case of an isotropic system with only pair potentials, is worked out in Hansen (1976, pages 40-43) The generalization to the case when the system is cylindrically symmetric (translational invariance in the x-y plane but not in the z-direction), and there is an external field, depending on z,) is listed along side. The excess energy in the isotropic case is given by,

$$\frac{U^{ex}}{N} = 2\pi\rho \int_0^\infty g(r)v(r)r^2 dr \tag{2.36}$$

The excess energy in the case of cylinderical symmetry, with z dependent external force, and for the slab ($z_a < z < z_b$), is given by,

$$\frac{U^{ex}(z_a, z_b)}{N} = \pi\sigma \int_{z_a}^{z_b} \rho(z_1 : z_1)dz_1 \int_{z_a}^{z_b} \rho(z_2 : z_2)dz_2 \int_0^\infty g(r_{12}, z_1, z_2)v(r_{12})\rho_{12}d\rho_{12} + \int_{z_a}^{z_b} v_s(z)\rho(z : z)dz \tag{2.37}$$

where,

$$g(r_{12}, z_1, z_2) = g_N^{(2)}(r_1, r_2) \tag{2.38}$$

Thus knowing $g(r_{12}, z_1, z_2)$ and $\rho(z : z)$, one can calculate the internal energy of a slab of arbitrary thickness of the full inhomogenous system at any given σ.

The equation of state in the isotropic case is given by,

$$\frac{\beta P}{\rho} = 1 - \frac{2}{3}\pi\beta\rho \int_0^\infty g(r)r^3 \frac{dv(r)}{dr} dr \tag{2.39}$$

The compressibility equation in the isotropic case is given by.

$$1 + \rho \int [g^{(2)} - 1] dr = \frac{< N^2 > - < N >^2}{< N >} = k_B T \chi_T \tag{2.40}$$

The structure factor in the isotropic case is given by.

$$S(\vec{k}) = 1 + \rho \int exp(-i\vec{k} \cdot \vec{r}) g(\vec{r}) d\vec{r} \tag{2.41}$$

The structure factor in the case of cylinderical symmetry, with z dependent external force, and for the slab ($z_a < z < z_b$), is given by.

$$S(k_\rho, k_z) = 1 + 2\pi\sigma \int_{z_a}^{z_b} dz_1 \int_{z_a}^{z_b} dz_2 \; e^{-i[k_\rho \rho + k_z (z_1 - z_2)]} g(r_{12}, z_1, z_2) \rho d\rho \tag{2.42}$$

where

$$r_{12} = \sqrt{\rho^2 + (z_1 - z_2)^2} \tag{2.43}$$

Monte Carlo simulations of physical systems described by the Schrödinger wave equation, give the solution, $\Psi(R)$ not as an analytical function but as a set of particle configurations sampled from $\Psi(R)$. We must therefore establish procedures to process these configurations to yield the distribution functions of interest.

General Schematics of Surface Energetics

In this section we consider the different types of surfaces potentials based on considerations of energetics.

We consider a surface that has no structure and is flat, and its effect on the atoms on it are completely representable by a surface to atom potential. In this

case the ground state of the system, that comes from the solution to the many body Schrödinger wave equation depends only on the parameters in the surface potential, the parameters in the interatomic potential, the mass of the atoms and the coverage. Throughout this work the term coverage is used to mean the atoms per unit area on the surface. Below the ground state coverage, σ_o, the system will be unstable and breakup into a liquid-gas phase. We may also speak of σ_o as the *minimum stable coverage*. We say *minimum* because for $\sigma \geq \sigma_o$, we have well-defined solutions of the many body Schrödinger wave-equation.

A surface-to-atom potential is repulsive at short range and weakly attractive at large distances, going through a minimum at a distance z_{min} which we may think of as the location of the surface. Beyond this minimum the potential is a monotonically decreasing function of z.

A single atom bound to the surface has a ground state energy, E_o, obtained by solving the one-dimensional Schrödinger wave equation with the atom interacting in the surface potential. This single-atom binding, is as we shall see, a characteristic input in the understanding of the film structure. The width at half height of the square of the wave-function for this single-atom on the surface problem, w, gives a measure of the z-motion of the atoms on the surface.

As the coverage is increased (more and more atoms are put on the surface) the atoms on the surface interact with the Van der Waals attractive force, and lower the total energy of the system. The minimum value of the lowering is given by the ground state energy of the two dimensional helium system E_{2D} (approximately

-0.9 K).

At coverages less than σ_o the system is unstable. However, variational calculations yield a value of the energy for a hypothetical low density system. The particle configurations, as we have remarked earlier, may not present the picture of a homogenous system in the x-y plane, none-the-less the per atom energy will be well-defined, though with large Monte Carlo sampling fluctuations, in some average sense. We use this variational energy in the qualitative considerations below.

If there was no surface and atoms interacted only among themselves then in the thermodynamic limit there would be a self bound equilibrium state at a density ρ_o (0.022 atoms/Å^3 for ^{4}He) and with a binding energy E_{bulk} (-7.12 K for ^{4}He). The existence of this bound state depends only on the short range repulsive hard core plus the long range attractive Van der Waal force between the atoms and not on the detailed form of the interatomic interaction. For helium, the adsorbate atom studied in the present work, the form of the interaction is quite accurately known but the general picture that we present here depends only on the existence of the bound state.

Two characteristics of the atom-surface interaction seem to capture most of the gross features of film growth. They are the *single-atom binding energy*, E_o, and the width (at half-height) of the single atom wavefunction, w. The depth of the well is not as good a measure of the surface interaction strength as E_o, and the width of the potential is not as good a measure of the z-motion of the atoms

than w.

As the coverage is increased, the energetics will exhibit two qualitatively different patterns. We first consider the case the atom is bound stronger to the surface than to the bulk liquid ($E_o < E_{bulk}$). We will refer to such a surface as of Type I. In this case the binding energy per atom of the system will first fall due to the atoms acquiring at least some interatomic binding energy over and above their surface binding. Eventually, the binding energy will rise as at higher and higher coverages, the atoms are further and further away from the bottom of the potential well, and the gain in interatomic binding energy is not as much. Eventually the bulk value, E_{bulk}, will be reached in the limit of infinite coverage. The minimum in the binding energy per atom, E_{min}, is a signal of the minimum stable coverage. This minimum stable coverage will be a monolayer if w, is of the order of interatomic distances in the bulk fluid or less. For surfaces with a larger w the minimum stable coverage will correspond to greater than monolayer structure. We expect and show that the lithium potential has a small enough width for a monolayer minimum stable coverage.

Let us consider the energy difference, $E_{min} - E_o$. For the 2-D liquid it is about -0.85 K, for the graphite surface it is about -0.9 K, and for the lithium surface it is about -1.3 K. For wider potentials this value will be even lower. However above some critical value, say ΔE_c (maybe around -2.0 K) we expect the minimum stable structure to look like more than a monolayer.

If on the other hand the atom is bound weaker to the surface than to the bulk

liquid ($E_o > E_{bulk}$), then with increasing coverage, the binding energy will fall, reach E_{bulk} at some coverage, go through a minimum at σ_o and eventually reach the limiting bulk value again. We will refer to such a surface as of Type II.

A monolayer may still form, if the absolute value of $(E_o - E_{bulk})$ is less than the absolute value of E_{c1}, for small enough w. If the absolute value of $(E_o - E_{bulk})$ is more than E_{c1}, then the minimum stable coverage will be more than monolayer, regardless of the width of the well.

In the limit of infinite coverage, the energy per atom will reach the bulk value, E_{bulk}. Before reaching this value, it will be less than E_{bulk}, as the system will acquire some binding due to the surface, regardless of how weak the surface interaction is. Together with the fact that, in the limit of zero coverage (the single atom case) the binding energy was greater than E_{bulk}, this implies that there will be a minimum in the per atom energy. Thus we can say that for a given abs $(E_o - E_{bulk})$, there will be a critical σ_o , above which the gain in binding due to the interatomic interaction will be enough to overcome the difference abs $(E_o - E_{bulk})$ and there will be stable coverage. From these considerations we can say that the fluid will wet all surfaces, regardless of their strength. Given a particulaer surface the only questions is: how many layers will build up before it wets (reaches E_{min}).

By instability of the coverage we mean that the system will be thermodynamically unstable, and split up into a liquid-gas coexistence phase with droplet formation. Under such circumstances, the treatment in the present work cannot be used. Below reaching E_{min}, the system is in such a state.

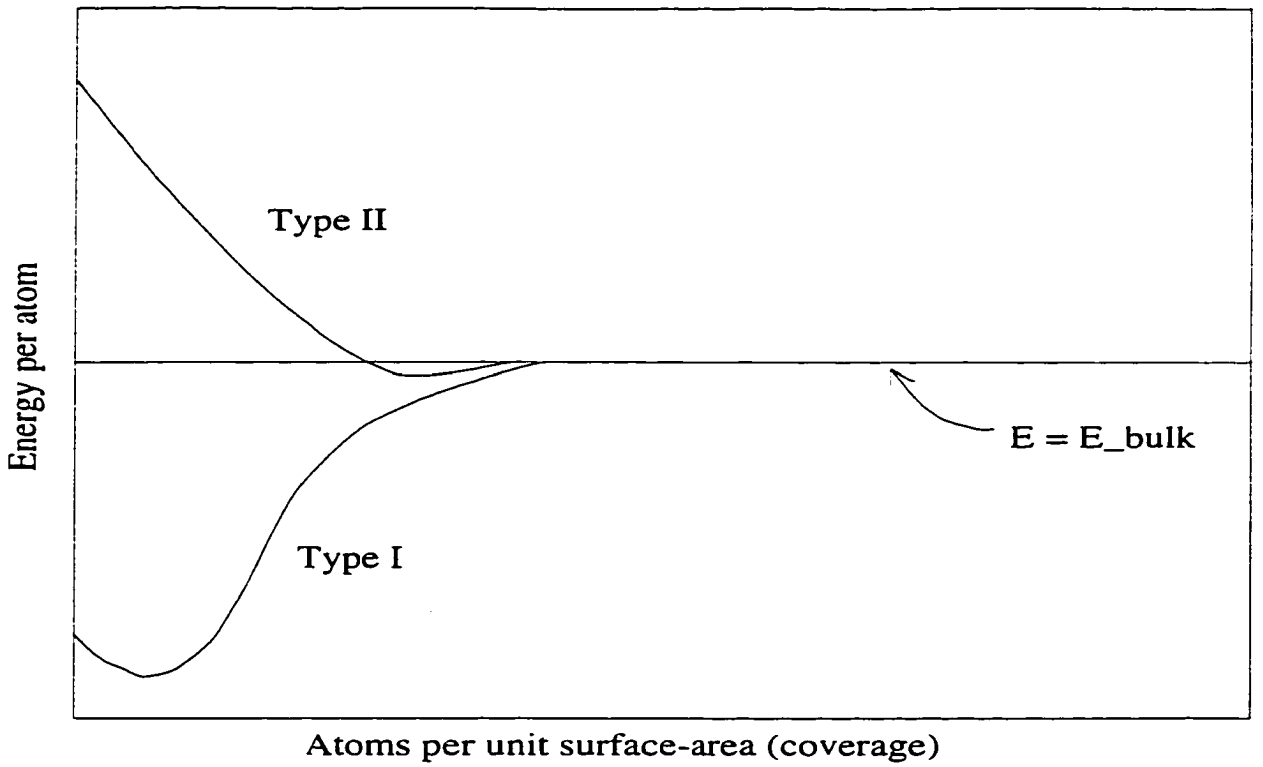

Fig. 2.1 Qualitative forms of the Equations of State for atomic films on a surface. The graphs are not drawn to scale. The Energy per atom is on the y axis and the coverage is on the x-axis. There are essentially two different types of surfaces with respect to adsorption: Type I with single atom binding energies higher than E_{bulk}, and Type II which have single atom binding energies lower than E_{bulk}.

We now describe some of the above considerations graphically. Fig. 2.1 shows the qualitative form of the equation of states for a typical Type I and a typical Type II surface. The figures are not drawn to scale, and are intended to show the shape of the curves. The curve for a Type I surface starts from below the E_{bulk} line, whereas the curve for a Type II surface starts from above the E_{bulk} line. Note that both the curves first monotonically decrease and then monotonically increase until they reach the bulk value. Note also, that the curve representing a Type II surface goes below the E_{bulk} line and then goes through a minimum. We have

discussed this feature above.

Fig. 2.2 shows the equation of states of two surfaces of Type I that have the same single atom binding energy but their potentials have different widths. Note that the wider the surface potential well, the more atoms it can accomodate and consequently the energy lowering will be greater. In this case, the energy per atom will approach the bulk value at a higher coverage.

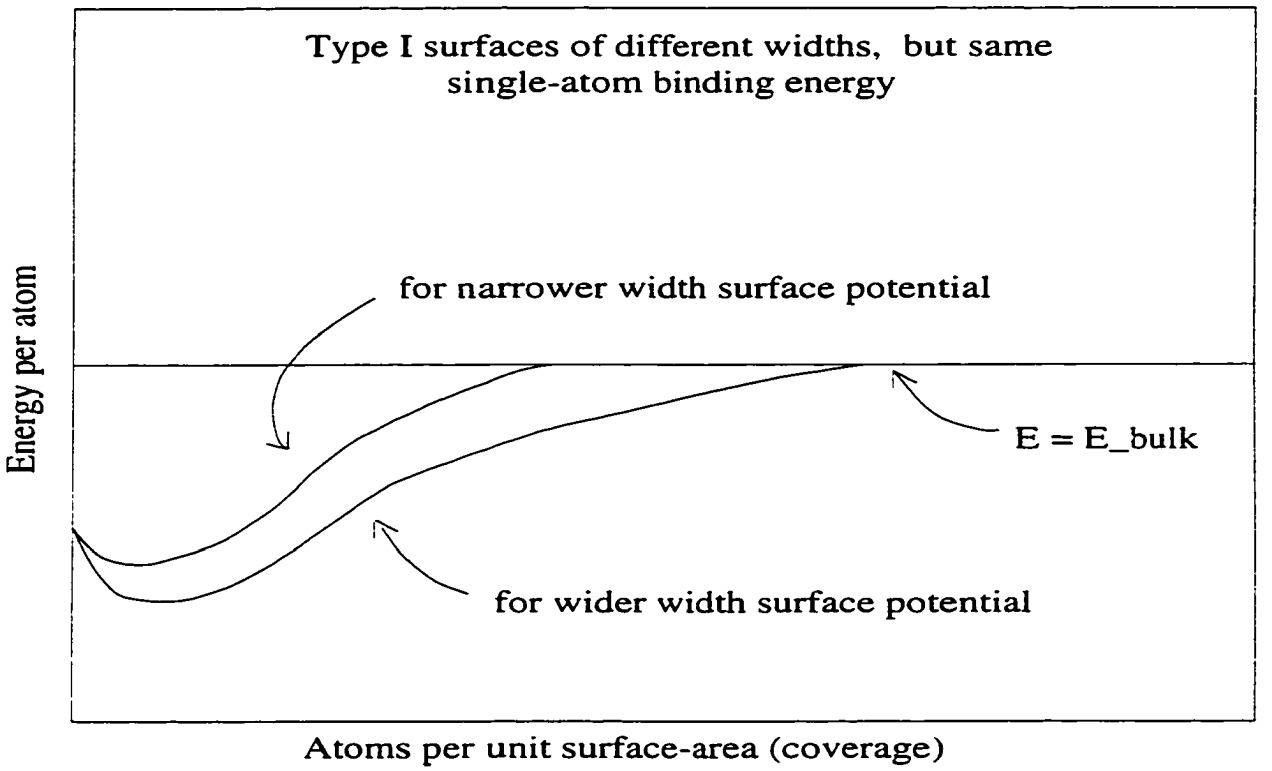

Fig. 2.2 Qualitative forms of the Equations of State for atomic films on a surface. The graphs are not drawn to scale. The Energy per atom is on the y axis and the coverage is on the x-axis. The curves correspond to two surfaces of Type I with the same single atom binding energy but with differing widths. The lower curve is for the surface with a wider potential well.

Fig. 2.3 shows the equation of states of two surfaces of Type II that have the same single atom binding energy but their potentials have different widths. As in

the case of Type I surfaces described in the previous figure, the wider the surface potential well, the more atoms it can accomodate and consequently the energy lowering will be greater. In this case, the energy per atom will approach the bulk value at a higher coverage.

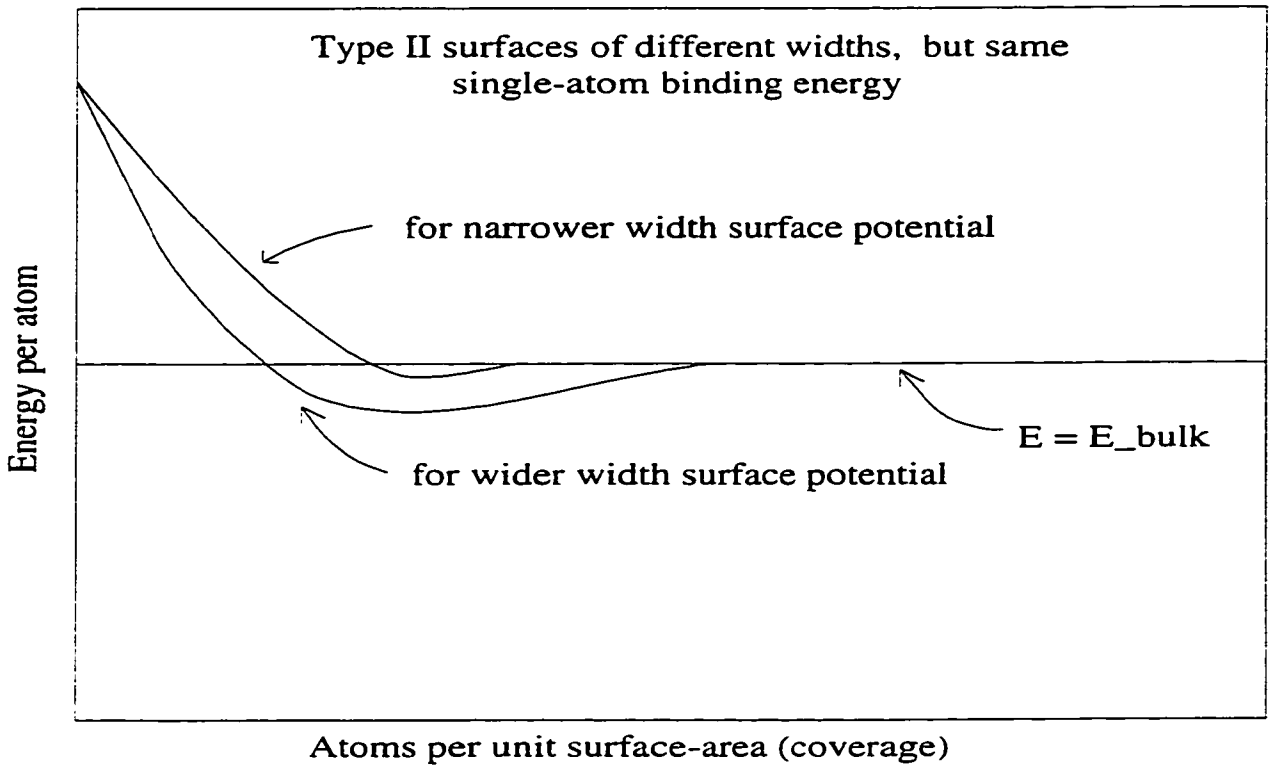

Fig. 2.3 Qualitative forms of the Equations of State for atomic films on a surface. The graphs are not drawn to scale. The Energy per atom is on the y axis and the coverage is on the x-axis. The curves correspond to two surfaces of Type II with the same single atom binding energy but with differing widths. The lower curve is for the surface with a wider potential well.

Type II surfaces with a relatively high binding energy may have an equation of state with a flat minima. In such cases, for coverages below the minimum stable coverage, σ_o , we may see a pre-wetting phase, before wetting takes place.

In chapters five and six, we discuss the results that we have obtained for

the surfaces of graphite, lithium and sodium. The graphite surface is a case of a strongly adsorbing surface, and is of Type I according to our criterion discussed above. The lithium surface is of Type I and its minimum stable coverage represents a liquid monolayer. The sodium surface is of Type II and its minimum stable coverage represents a liquid bilayer.

CHAPTER III : Computational Techniques used

This chapter gives a review of the two Monte Carlo methods used in this work, namely Variational Monte Carlo and Green's function Monte Carlo . The simplex minimization technique is briefly described later in the chapter.

Variational Monte Carlo

Variational Monte Carlo was the first Monte Carlo technique to be used in the simulation of helium (McMillan, 1965). A trial wave-function, ψ_T, is used, usually of the pair product form, $\psi_T = exp[-\Sigma_{i<j} u(r_{ij})]$.

The Hamiltonian for a multiparticle system is written as

$$H = -\frac{\hbar^2}{2m}\sum_i \nabla_i^2 + \sum_{i<j} V(|r_i - r_j|) \tag{3.1}$$

We calculate the expectation value of the Hamiltonian, which is an upper bound to the ground-state energy E_o.

$$E_o \leq \int dR \frac{\psi_T(R) H(R) \psi_T(R)}{\int dR |\psi_T(R)|^2} \tag{3.2}$$

which can be rewritten as

$$\int dR \frac{H\psi_T(R)}{\psi_T(R)} \frac{\psi_T(R)\psi_T(R)}{\int dR' \psi_T(R')\psi_T(R')} \tag{3.3}$$

The second form of the integral is estimated by a Monte Carlo calculation that samples $\psi_T^2(R)$ using the method of Metropolis *et. al.*, 1953. If $\psi_T(R)$ is close to the true ground-state wave function this Monte Carlo estimate will give a low variance answer since $\frac{H\psi_T(R)}{\psi_T(R)}$ will be nearly constant. A good trial wave

function will be the one that minimizes equation [2] with respect to parameters in $\psi_T(R)$. The minimum energy is the best estimate of E_o for that class of trial function.

An advantage of the method is that it is both simple to understand and to program. The calculations are one to two orders of magnitude faster than Green's function Monte Carlo and Path Integral Monte Carlo . States that are a ground state of a given symmetry, such as bosons, fermions, photons, rotons, and vortices can be treated by constructing appropriate trial wave functions. With Variational Monte Carlo one can tell how important a given correlation is by systematically adding terms to the trial function. One ends up with an explicit function, however approximate, that helps picture and understand the quantum system.

But Variational Monte Carlo is hardly a black-box. To get reliable results one must very carefully optimize trial wave functions and systemetically add more complicated effects. There is nothing internal to the method that tells you when to stop introducing more correlations (or effects) in the trial wave function. And in any case, the value of the energy obtained is only an upper bound to the energy and one cannot know how close to the exact energy one is, unless there are other methods that furnish it. Even the best pair product trial functions used to date are off by about 1.2 K in bulk liquid helium, which is about 17% of the total. Taking into account three body correlations one gets another 0.7 K, thus accounting for 10% of the descrepancy, leaving the remaining 7-8% to be obtained by additional enhancements (higher order correlations) to the trial function. At a given level

of the sophistication of the wave function there is therefore a systematic bias or error. This variational bias is generally different at different densities, for a given functional form of the trial function, and the density at which this form will give a minimum will be different (usually lower) than the experimental minimum. Variational Monte Carlo becomes increasingly unreliable as the physical system become more dense or complex because a high-quality trial function has too many possible variational parameters to optimize easily. Both Green's function Monte Carlo and Path Integral Monte Carlo build this complexity into the algorithm, rather than requiring guesses as to which terms are needed.

We model a film as an upper half plane filled with atoms at a given coverage (number of atoms per unit area) in a rectangular box open in the normal direction. We impose periodic boundary conditions on the lateral sides of the box, to eliminate surface effects. This is equivalent to extending the system periodically in the lateral directions with the periodicity of the box. Each particle in the simulation box (eg. one at (x,y,z)) will have an image at the same relative position in every other box (ie. at (x±L,y±L,z±L)). If we define the distance between particles i and j, r_{ij}, to be the distance from particle i to the nearest image of particle j, the trial wave function is periodic and satisfies the boundary conditions. This choice of boundary conditions is important since we do not wish to take the usual limit $N, V \rightarrow \infty$ with $\rho = N/V$. In this thesis we perform the integrations for N of the order of 100 particles so as to eliminate surface effects in so far as this is possible. Since, we hope to study the solid as well the liquid phase, we will choose the par-

ticle number N to permit condensation into the cubic-close-packed configuration in the periodic cube.

Green's function Monte Carlo

The first exact calculation of the ground state of liquid ^{4}Heusing the Green's function Monte Carlo method was by Kalos, Levesque, and Verlet (1974).

In this method, the Schrödinger equation is transformed into an integral equation by a Green's function for the Hamiltonian with a shifted energy scale. The integral equation is solved by a Neumann series, and the iterations are carried out by Monte Carlo technique. The iteration of the Neumann series to solve the integral equation is initiated with a trial wave function $\psi_o(R)$, R being a point in 3N dimensional configuration space.

i) Schrödinger equation in integral form

Consider the Schrödinger equation for a many-body system.

$$\Big[-\sum_{i=1}^{N}\frac{\hbar^2}{2m}\nabla_i^2 + V(r, r_2, \ldots, r_i)\Big]\psi(r, r_2, \ldots, r_i) = E\psi(r, r_2, \ldots, r_i) \qquad (3.4)$$

Setting $\hbar^2/2m = 1$ and denoting the point $(r, r_2, \ldots, r_N)$ in $3N$ dimensional configuration space by R we write succinctly

$$\big[-\nabla_i^2 + V(R)\big]\psi(R) = E\psi(R) \qquad (3.5)$$

To guarantee a positive spectrum of eigenvalues, let $V_o + V(R) \geq 0$. Then

$$\big[-\nabla_i^2 + V(R) + V_o\big]\psi(R) = (E + E_o)\psi(R) \qquad (3.6)$$

We seek an integral formulation of this Schrödinger equation. Accordingly, we consider Green's function for the operator on the left side of (3.6), namely

$$\left[-\nabla_i^2 + V(R) + V_o\right] G(R, R_o) = \delta(R - R_o) \tag{3.7}$$

Appropriate boundary conditions for the problem must be contained in G. For the treatment of an isolated system of interacting particles, $G(R, R_o)$ vanishes as the separation of any pair of particles $|r_i - r_j|$ increases without limit. On the other hand in calculations modelling a large system by the use of a finite number of particles in a box of side L, ψ and G must be multiply periodic in the sense that

$$\psi(R + P_j) = \psi(R) \tag{3.8}$$

$$G(R + P_j; R_o) = G(R; R_o) \tag{3.9}$$

and P_j is a vector all of whose 3N components are zero except the j^{th} which is L.

Substituting eqn. (3.7) in (3.6) yields an integral equation

$$\psi(R) = (E + V_o) \int G(R, R')\psi(R')dR' \tag{3.10}$$

Given an initial $\psi^o(R)$, Eq. (3.10) can be solved by iteration:

$$\psi^{(n+1)}(R) = (E + V_o) \int G(R, R')\psi^{(n)}(R')dR' \tag{3.11}$$

When the spectrum of the hamiltonian is discrete near the ground state $\psi_o(R)$ of the Schrödinger equation, Eq. (3.4) then $\psi_o(R)$ is the limiting value of $\psi^{(n)}(R)$ for large n.

It is possible to device a Monte Carlo method which produces populations drawn in turn from the successive $\psi^{(n)}$. Suppose that a set of configurations $\{R^{(o)}\}$ is drawn at random from the given function $\psi^{(o)}(R)$. Then for each configuration $R_k^{(o)}$, let new configurations $R_l^{(1)}$ be selected at random from the density function $(E+V_o)G(R_l^{(1)}, R_k^{(o)})$ conditional on $R_k^{(o)}$. Note that the number of configurations is not conserved. The expected number of configurations appearing in a unit neighborhood of R, averaged over all possible $\{R^{(o)}\}$ is

$$(E + V_o) \int G(R, R')\psi^{(o)}(R')dR' = \psi^{(1)}(R) \tag{3.12}$$

which is Eq. (3.11) for n = 1. Thus the sampling of $G(R_l^{(1)}, R_k^{(o)})$ produces a population of configurations $\{R^{(1)}\}$ drawn from $\psi^{(1)}(R)$ Clearly, repetition leads to a population whose density is $\psi^{(2)}$ and further iteration to samples drawn from $\psi^{(n)}$ from any n. We call the population drawn from $\psi^{(n)}$ the n^{th} "generation".

Unfortunately, E_o , the exact eigenvalue of the ground state, is not known in advance. Equation (3.11) requires the correct eigenvalue to yield $\psi^{(n)}$ asymptotically equal to $\psi_o(R)$. On the other hand it is equally clear from (3.11) that if one uses, for computational purposes, a trial eigenvalue E_t larger than E_o, the $\psi^{(n)}$ grow in normalization reflected in a growth in the population of configurations. If E_t is too small the population declines. Thus the distribution of configurations has the correct marginal distribution and, in addition, the eigenvalue E may be estimated from the change in population size

$$E + V_o = \frac{(E_t + V_o) \int \psi^{(n)}(R)dR}{\int \psi^{(n+1)}(R)dR} \tag{3.13}$$

A Monte Carlo estimator for E_o is then E_1 given by

$$E_1 + V_o \approx (E_t + V_o)N_n/N_{n+1} \tag{3.14}$$

where N_n is the number of configurations in the population drawn from $\psi^{(n)}$ according to (3.11) and the symbol $\approx$ indicates that the quantity is a statistical estimator, that is asymptotically accurate. However, this estimator is biased as the expectation value of the quotient of two integrals is not the quotient of the expected values. An estimator, E_2 for which the second kind of bias is smaller is

$$(E_2 + V_o) \approx (E_T + V_o)\frac{\sum_{k=n_1}^{n_2} N_k}{(\sum_{k=n_1}^{n_2} N_{k+1})} \tag{3.15}$$

In any case the magnitude of the bias must be evaluated or bounded in obtaining practical results. Including the size of more generations decreases the bias as a consequence of the increased statistical correlation and reduced fluctuation of numerator and denominator.

The bias can be eliminated completely and the statistical error reduced in magnitude by the following method, known as importance sampling. Multiply (3.5) by some known $\psi_T(R)$ which satisfies the boundary conditions. It has beeen found effective to use a trial function which minimized the energy in a variational study of the same problem. Upon integrating over the full space of R and using the hermiticity of the Hamiltonian, one obtains

$$E = \frac{\int \psi_o(R)[-\nabla^2 + V(R)]\psi_T(R)dR}{\int \psi_o(R)\psi_T(R)dR} \tag{3.16}$$

If one samples a population $R_1, \ldots, R_N$ from the density function $\psi_o(R)\psi_T(R)$ then

$$E_3 \approx \frac{1}{n}\sum_{k=1}^{n} \psi_T(R_k)^{-1}(-\nabla^2 + V)\psi_T(R_k) \tag{3.17}$$

is an unbiased estimator of E. It has the property that as ψ_T approaches ψ_o, E_3 becomes exact, independent of the values of R_k. Thus one expects that for "reasonable" ψ_T, the estimator E_3 will exhibit less variance than E_2 before the convergence of $\psi^{(n)}$ to $\psi^{(\infty)}$. Estimator E_2 is called a "growth" estimate, E_3 a "variational" estimate.

The iteration process (3.11) does not converge to $\psi_T\psi_o$ but, formally it is easy to change it so that it will do so. Simply multiply (3.11), through by $\psi_T(R)$ and introduce $\psi_T(R')/\psi_T(R')$ into the integral. The sequence

$$\psi_T(R)\psi^{(n+1)}(R) = (E_t + V_o)\int [\psi_T(R)G(R,R')/\psi_T(R')]\psi_T(R')\psi^{(n)}(R')dR' \tag{3.18}$$

can be sampled randomly as before and converges to $\psi_T\psi_o$ where ψ_o is the lowest state not orthogonal to ψ_T. The growth estimator, Eq. (3.15) may also be used with N_k referring to the size of the population generated with $\psi_o\psi_T$.

ii) Sampling Green's Function by Random Walks

The development of the preceding section rests upon a crucial technical assertion, that it is possible to sample $(E_t + V_o)G(R,R')$ or $(E_t + V_o)\psi_T(R)G(R,R')/\psi_T(R')$ for R conditional on R'. Now for some simple problems - e.g., a particle in a box - one can construct the analytic form of G and hence an algorithm for sampling it. For interesting problems of statistical physics an analytical form is

not possible, but we now sketch how it is possible to sample $G(R, R')$ without knowing it explicitly. This algorithm is, of course, the heart of the method.

Let D be the full domain in configuration space in which the particlea move. Consider some $D_o(R_o) \subset D$ and suppose that

$$U_o > V(R) + V_o \qquad for \qquad R \in D_o \tag{3.19}$$

We introduce the Green's function on the domain D_o, a "partial" Green's function

$$(-\nabla^2 + U_o)G_U(R_1, R_o) = \delta(R_1 - R_o) for R_1, R_o \notin D_o \tag{3.20}$$

with the boundary condition

$$G_U(R_1, R_o) = 0 \qquad for \qquad R_1, R_o \notin D_o \tag{3.21}$$

In principle U_o could be a function of R, but in practice only constant values have been used. The Green's functions introduced here are symmetric because of the boundary conditions. Equation (3.7) can be rewritten for a source at R_1 as

$$\left[-\nabla_i^2 + V(R_1) + V_o\right] G(R, R_1) = \delta(R - R_1) \tag{3.22}$$

On multiplying (3.20) by $G(R, R_1)$, (3.22) by $G_U(R_1, R_o)$, subtracting and integrating, one finds

$$G(R, R_o) = G_U(R, R_o) + \int_{\partial D_o(R_o)} [-\nabla_{n_1} G_U(R_1, R_o)] G(R, R_1) dR_1$$

$$+ \int_{D_o(R_o)} \{[U_o - V(R_1) - V_o]/U_o\} U_o G_U(R_1, R_o) G(R, R_1) dR_1 \tag{3.23}$$

This last equation shows how the full Green's function is related to a "partial" Green's function satisfying (3.19-3.21) on a subdomain. This relation may be understood in the following way. First observe that if (3.20) is integrated over $D_o(R_o)$, we have

$$\int_{\partial D_o(R_o)} [-\nabla_n G_U(R', R_o)] dR' + U_o \int_{D_o(R_o)} G_U(R', R_o) dR' = 1 \qquad (3.24)$$

Since $G_U(R', R_o)$ and therefore $-\nabla_n G_U(R', R_o)$ are non-negative, they may be interpreted as probability density functions for a move in a random walk which may go either to some $R' \in D_o(R_o)$ or to $R' \in \partial D_o(R_o)$, the surface of the domain, respectively. Equation (3.23) is related to random processes of this kind. In particular it expresses the fact that $G(R, R_o)$ is the sum of $G_u(R, R_o)$ for the subdomain plus the expected value of $G(R, R_1)$ taken over an ensemble of random events. These events comprise one of the following two possibilities: 1) a move at random with density $-\nabla_n G_u(R_1, R_o)$ to R_1 on the boundary $\partial D_o(R_o)$: or 2) a move at random with density $U_o G(R_1, R_o)$ to R_1 on the interior of $D_o(R_o)$ with the averaging of $G(R, R_1)$ carried out with probability $[U_o - V(R_1) - V_o]/U_o$. It is true that in either case $G(R, R_1)$ is not known but we may now construct a domain $D_o(R_1)$ containing R_1. Then $G(R, R_1)$ may be expressed as in (3.23) as the sum of $G_u(R, R_1)$ plus the average of $G(R, R_2)$ taken over points R_2 reached by random steps to the boundary or interior of $D_o(R_1)$. The process may be iterated leading to a sequence of R_n with each chosen from its predecessor R_{n-1} by a move R_n on the boundary of $D_o(R_{n-1})$ drawn from $-\nabla_n G_u(R_n, R_{n-1})$ or to R_n on the interior of $D_o(R_{n-1})$ drawn from $G(R_n, R_{n-1})$ and propagated with

probability $[U_o - V(R_n) - V_o]/U_o$. $G(R, R_o)$ is the expected value of the sum of all the $G_u(R, R_n)$ for the R_n that are generated in this random walk. Each of these terms potentially makes a contribution to the set of points representing $\psi^{n+1}(R)$ in (3.11). The set of points are referred to as the next generation.That this procedure yields $G(R, R_o)$ can be proved formally, but we justify it here by a "physical" argument. Equation (3.7) has as its solution the expected density for observing at R an object which was started at R_o and which diffuses subject to an absorption process whose rate is $V + V_o$. Now at any stage of the diffusion process a domain $D_o(R) \subset D$ can be constructed. Green's function defined in (3.20,3.21) describes a diffusion in $D_o(R)$ subject to an absorption rate that is too large in the domain - cf. (3.19) - and to perfect absorption at the boundary. Diffusion continues until the first passage across that boundary. To describe the diffusion in the full domain such a first passage merely defines a surface source for subsequent diffusion. In addition the excess absorption owing to U_o is compensated by the reintroduction of the fraction. $\{[U_o - V(R) - V_o]/U_o\}$ of those objects absorbed in the interior.

It has been found useful to construct $D_o(R)$ as a cartesian product of subspaces, one for each particle. Taking each subspace to be a sphere is especially convenient. Then separation of variables permits the explicit calculation of G_u as a product and this, inturn, leads to an explicit algorithm for sampling G_u.

iii) Importance Sampling

The sampling algorithm embodied in (3.23) yields a population drawn from

$G(R, R_o)$ for any R_o. It must be altered to sample $\psi_T(R)G(R, R_o)/\psi_T(R_o)$ as indicated in (3.18). Equation (3.23) can be transformed by multiplying by $\psi_T(R)/\psi_T(R_o)$ to produce.

$$\psi_T(R)G(R, R_o)/\psi_T(R_o) = \psi_T(R)G_U(R, R_o)/\psi_T(R_o)$$

$$+ \int_{\partial D_o} [\psi_T(R_1)G_U(R_1, R_o)/\psi_T(R_o)]\psi_T(R)G(R, R_1)/\psi_T(R_1)dR_1$$

$$+ \int_{D_o} \{1 - [V(R_1) + V_o]/U_o\}U_o\psi_T(R_1)G_U(R_1, R_o)/\psi_T(R_o)$$

$$*\psi_T(R)G(R, R_1)/\psi_T(R_1)dR_1 \tag{3.25}$$

an integral equation for $\psi_T(R)G(R, R_o)/\psi_T(R_o)$. The new equation can also be sampled by a random walk in which the kernels which describe the passage from R' to R are modified by factors $\psi_T(R')/\psi_T(R)$. We now show that the use of ψ_T is of very great potential in increasing the efficiency of the method.

To see how this may be possible, we define $E_T(R)$ by

$$(-\nabla^2 + V + V_o)\psi_T(R) = [E_T(R) + V_o]\psi_T(R) \tag{3.26}$$

Combining this with (3.20) which defines Green's function G_U, we obtain

$$\int_{\partial D_o(R_o)} \{\psi_T(R')[-\nabla_n G_U(R', R_o)]/\psi_T(R_o)\}dR'$$

$$+ \int_{D_o(R_o)} \{[U_o - V(R') - V_o]\psi_T(R')G_U(R', R_o)/\psi_T(R_o)\}dR'$$

$$= 1 - \int_{D_o(R_o)} \{[E_T(R') + V_o]\psi_T(R')G_U(R', R_o)/\psi_T(R_o)\}dR' \tag{3.27}$$

Comparing with (3.23), the first integral on the left is the expected number of steps to the boundary of $D_o(R_o)$ which will be made when such steps are generated with density $\psi_T(R')[-\nabla_n G_u(R', R_o)]/\psi_T(R_o)$ in a random walk which generates $\psi_T(R)G_u(R, R_o)/\psi_T(R_o)$. The second integral on the left gives the expected number of steps to the interior of $D_o(R_o)$.

When $E_T(R) + V_o \geq 0$ (a weak condition since $V(R) \geq V_o$), the right side cannot exceed one. Thus the expected number of steps to boundary or interior of $D_o(R_o)$ made in the Green's function random walk is generally less than one and the random walk is guaranteed to terminate at some stage.

Now the n^{th} step in the random walk makes a contribution of $\psi_T(R)G_u(R, R_n)/\psi_T(R_n)$ to the full weighted Green's function $\psi_T(R)G_u(R, R_o)/\psi_T(R_o)$ and each partial contribution potentially contributes to the next generation of configurations. If $E_T(R)$ is replaced by E_t, then the integral on the right side of (3.27) is exactly the expected number of configurations in the next generation which results from the contribution of $G_u(R, R_o)$ for domain $D_o(R_o)$ to the full $G(R, R_o)$. Furthermore, if ψ_T were ψ_o, the lowest eigenfunction, then $E_T = E_o > V_o$, and we have the result that the three possible events have probabilities that add up exactly to one; the events are a move to the boundary of D_o, a move in the interior of D_o that continues the Green's function random walk, and the termination of the Green's function random walk with a configuration in the next generation. All three may then be sampled as mutually exclusive and exhaustive events. Thus one may arrange the algorithm so that the random walk terminates when and only

when a next generation configuration is produced. Under these circumstances , viz., $\psi_T = \psi_o$ and $E_T = E_o$, the random walk produces exactly one new configuration and is guaranteed to terminate.

In addition, if (3.26) is combined with (3.7) defining the full Green's function, and the periodic and any other boundary conditions for ψ_T are used, the result is

$$\int \{[E_T(R) + V_o]\psi_T(R)G(R, R_o)/\psi_T(R_o)\}dR = 1 \tag{3.28}$$

Again, if $\psi_T(R) = \psi_o(R)$ and $E_T(R) = E_o$,

$$\left\{ \int [\psi_o(R)G(R, R_o)/\psi_o(R_o)]dR \right\}^{-1} = E_o + V_o \tag{3.29}$$

The integral on the left in (3.29) is simply the expected size of the total population, say N_2, which results in the next generation after one configuration at $R_o(N_1 = 1)$ as in (3.15). With $E_t + V_o = 1$ in (3.15) we see that the energy estimate from growth of generations is identically E_o, independent of R_o or any distribution used in sampling R_o. The estimate of E then has zero variance, as does (3.16). Of course this ideal result requires knowing ψ_o, but we expect that "reasonable" ψ_T, such as those that prove useful in variational calculations will reduce the variance significantly. Much experience has borne this out.

Simplex Minimization of Multiparameter Functions

The problem of finding the optimum values of the parameters in the trial wave function, is essentially a multidimensional minimization problem. We use the *downhill simplex method* due to Nelder and Mead. The method requires only function evaluations, not derivatives.

A *simplex* is the geometrical figure consisting, in N dimensions, of $N+1$ points (oe vertices) and all their interconnecting line segments, polygonal faces, etc. In two dimensions, a simplex is a triangle. In three dimensions it is a tetrahedran, not necessarily a regular tetrahedran. In general we are only interested in simplexes that are nondegenerate, i.e. that enclose a finite inner N-dimensional volume. If any point of a nondegenerate simplex is taken as the origin, then the N other points define vector directions that span the N-dimensional vector space.

In one-dimensional minimization it is possible to bracket a minimum, so that the success of a subsequent isolation is guaranteed. There is no analogous procedure in multidimensional space. For multidimensional minimization, the best we can do is give our algorithm a starting guess, that is an N-vector of independent variables as the first point to try. The algorithm is then supposed to make its own way downhill thru the complexity of an N-dimensional typography, until it encounters a (local, at least) minimum.

The downhill simplex method must be started not just with a single point, but with $N + 1$ points, defining an initial simplex. If you think of one of these points (it matters not which) as being your initial starting point P_o, then you can

take the other N points to be

$$P_i = P_o + \lambda e_i \tag{3.30}$$

where the e_i's are N unit vectors, and where λ is a constant which is your guess of the problem's characteristic length scale. (Or, you could have different λ_i's for each vector direction.)

As the minimization proceeds the simplex volume decreases, until it reduces to a point within numerical tolerance. The minimum, then lies in the small region around this point.

We used the programs given in section 10.4 of the book Numerical Recipes by Press et. al. (1992).

CHAPTER IV : The Trial Wave Function

In this chapter we will first discuss the full 3-D liquid case that has been extensively studied, and then later introduce additional considerations to accomodate a description of helium on a surface.

Jastro-triplet

A successful trial wave function for studying liquid helium has been formulated in the following way. Since we are dealing with bosons, the wave-function should be totally symmetric under the exchange of any two particle coordinates. This can be accomplished by choosing the trial wave function to be a product of pair functions, the product being taken over all pairs.

$$\psi = \prod_{\substack{i<j \\ i<j=1}}^{N} f(r_{ij}), \qquad r_{ij} = \mid r_i - r_j \mid \tag{4.1}$$

Simple as this form may be, it has actually been shown (Bogoliubov and Zubarev, 1955) that in the weak coupling limit the exact ground state wavefuntion can be written in this form. Additionally, it has been shown (Hiroike, 1962) that this trial wave function reproduces the first two terms in the low density expansion of the ground state energy of the hard-sphere gas.

We may expect the probability distribution function

$$P_N(r_1, \ldots, r_N) = \psi^2(r_1, \ldots, r_N) = \frac{\prod_{i<j} f^2(r_{ij})}{\int \prod f^2} \tag{4.2}$$

to exhibit at least two phases: a disordered (gas or liquid) phase at low densities, and an ordered, solid phase at high densities, since the classical system with $exp[-V(r_{ij})/kT] = f^2(r_{ij})$ is expected to have this behaviour.

In order to obtain a reasonable value for $< V >$ in the many-body system, the wave-function must be small whenever the potential is large, that is, whenever any two atoms are less than about 2.6 Å (the distance below which the interatomic potential between helium atoms is positive) apart. Further, since the size of our simulation-box can only be finite, in fact not much larger than to accomodate about 100 atoms, the atoms furtherest away should feel no interaction else boundary effects may not be negligible. This requires that the pair function $f(r_{ij})$, be essentially a constant for r greater than about 6 Å. The small r asympotic solution of the two-body problem (two helium atoms), $f(r) = exp[-(2.51/r)^5]$, satisfies these requirements and provides a reasonable starting point for the calculation.

McMillan (1964) chose the pair function $f(r) = exp[-(b/r)^m]$ with b and m serving as variational parameters, to study the ground state of liquid helium with the Lennard-Jones interatomic potential and obtained a variational energy of 20% of the experimental value.

The trial wave-function used was of the Jastrow-Bijl form:

$$\psi_T(R) = exp\left[-\frac{1}{2} \sum_{\substack{i,j \\ i<j}} u(r_{ij}) \right] \tag{4.3}$$

where

$$u(r_{ij}) = \left(\frac{b}{r_{ij}} \right)^m \tag{4.4}$$

It has only two parameters, b and m. Typically the value of b is around 1.19 and the value of m is either taken to be 5 or 4. In figure 4.1 we plot the McMillan pair function for a selection of parameters in the typical range. Note from the graph that the pair function is essentially zero below 0.5σ and nearly 1 after 2σ.

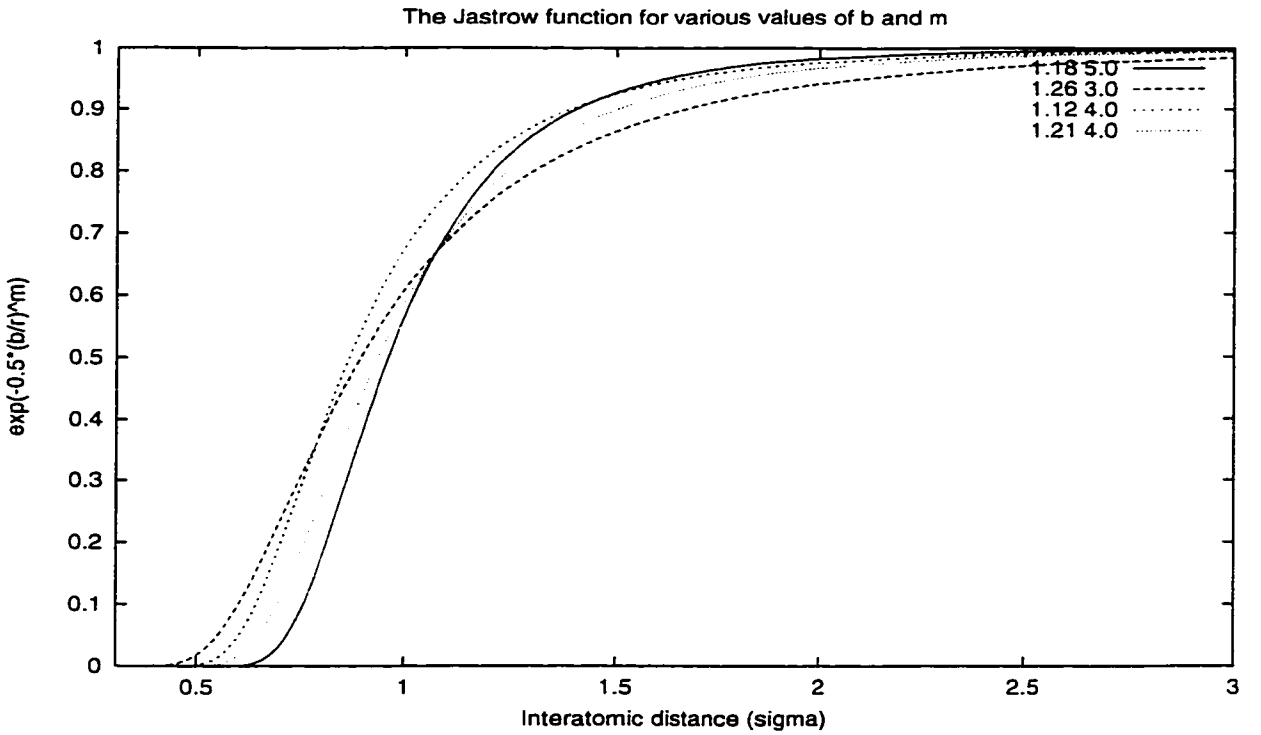

Fig. 4.1 The McMillan pair function for various values of the parameters b and m. The values of b and m are given in pairs at the top right corner of the figure.

We refer to $u(r)$ as the pseudopotential (in analogy to the probability function $exp(-V/kT)$), and the above form as the McMillan form. This wave-function contains only two-body correlations and efforts to include limited three-body correlations with a trial wave function of the form :

$$\psi_T(R) = exp\left[-\frac{1}{2}\sum_{\substack{i,j \\ i<j}} u(r_{ij}) - \frac{1}{2}\sum_{i<j<k} w_{ijk} \right] \qquad (4.5)$$

yielded significant improvement. Schmidt *et. al.*, (1980), for example, introduced triplet correlations resulting in about 7% improvement. To obtain more accurate results we have included these triplet correlations in our calculations.

Thus our trial wave function for studying the 3-D liquid phase is:

$$\psi_T(R) = exp\left[-\frac{1}{2}\sum_{\substack{i,j \\ i<j}} \tilde{u}(r_{ij}) - \frac{1}{4}\lambda \sum_{l} \vec{G}(l)\cdot\vec{G}(l)\right] \tag{4.6}$$

where

$$\begin{aligned} \vec{G}(l) &= \sum_{i\neq l} \xi_{li}\vec{r}_{li} \\ \tilde{u}_{ij} &= u_{ij} - \lambda\xi_{ij}^2 r_{ij}^2 \end{aligned} \tag{4.7}$$

with λ and ξ to be obtained variationally. The principal motivation for this choice is as follows. For an exact solution, $(H\psi_o)/\psi_o$ is a constant, but when one uses a pure Jastrow trial function $(H\psi_J)/\psi_J$ contains terms like $u'_{ij}u'_{ik}\vec{r}_{ij}\cdot\vec{r}_{ik}$. The form of ψ_T above permits the partial cancellation of such terms by terms arising from w_{ijk}. Additionally, it has been shown (Pandharipande, 1978) that a three-body form similar to the one considerd here includes effects of Feynman-Cohen backflow.

The form of these triplet terms require only two-body sums to be made, which does not significantly increase the computational burden. Three body sums would be computationally of order N times more time consuming than these terms.

Schmidt *et. al.*, 1980 obtained good results with $\xi(r)$ chosen to be of the form

$$\xi_{li}(r) = \left[exp\left(\frac{r_{li}-r_t}{\omega}\right)^2\right]\left(\frac{r_{li}-r_B}{r_B}\right)^3 \tag{4.8}$$

where r_t and w are new variational parameters. This form guarantees that the pseudopotentials go to zero at $r = r_B$, half the side of the simulation box. This is necessary, since we want each pair function in the product form trial wavefunction to go smoothly to a constant, at the edges of the simulation box.

Finite Film Width Considerations

In this thesis we are interested in studying helium films on a flat 2-dimensional surface ($z = 0$). The width in the z direction therefore is only at most a few atoms thick. whereas in the x-y plane the atoms are arrayed indefinitely. Since there are no external forces along the surface the number density of the atoms on the surface will not depend on the lateral coordinates (x,y). In the direction normal to the surface ($z > 0$) however the number density will fall rapidly to zero. as the film is traversed.

The atoms on the surface interact with the surface and with each other. On average the lateral forces on a particular atom must cancel out since the atoms are distributed uniformly laterally. The net force on an atom therefore mainly comes from the surface. A given atom in a monolayer film effectively sees the surface potential. as if no other atoms were present. Thus we expect that a good trial wave function for the fluid film in the presence of the surface to be of the form:

$$\psi_T = (\psi_T)_{3D} \times \psi_n(z_i) \tag{4.9}$$

where $\psi_n(z_i)$ is the solution of the one-dimensional Schrödinger wave equation with a single helium atom on the surface:

$$\Big[-\frac{\hbar^2}{2m}\nabla_i^2 + V_{surface}(z_i)\Big]\psi(z_i) = E\psi(z_i) \tag{4.10}$$

where $V_{surface}(z_i)$ is the potential that a single atom sees on the surface. Writing

$$\psi(z_i) = exp[-\frac{1}{2}h(z_i)] \tag{4.11}$$

we can finally write the trial wave function we used to study the helium monolayer.

$$\psi_T(R) = exp\Big[-\frac{1}{2}\sum_{\substack{i,j \\ i<j}} \tilde{u}(r_{ij}) - \frac{1}{4}\lambda \sum_{l} \vec{G}(l)\cdot\vec{G}(l) + \frac{1}{2}\sum_{i} h(z_i)\Big] \qquad (4.12)$$

The energy is computed from the identity

$$E = \frac{1}{N}\left\langle \frac{H\psi}{\psi} \right\rangle = \langle 2T_i + V_i - \vec{F}_i^2 \rangle \qquad (4.13)$$

where

$$\begin{aligned} T_i &= -\frac{\hbar^2}{4m}\nabla_i^2 ln\psi \\ \vec{F}_i^2 &= -\frac{\hbar^2}{2m}(\nabla_i ln\psi)^2 \\ V_i &= \frac{1}{2}\sum_{j\neq i} v_{ij} \end{aligned} \qquad (4.14)$$

where i refers to the coordinates of one particle, and angular brackets indicate an average over configurations. V_{ij} is the inter particle potential which we have taken to be the potential called HFDHE2, due to Ahlrichs *et. al.*, (1976) and Aziz *et. al.*, (1979). We describe this potential in Appendix III.

Single-Atom Solutions and the Fitted Function

Fig. 4.2 shows the wavefunctions for a single helium atom on an alkali metal surface. These have been used as the surface part of the trial wavefunction as described in equation (4.9). We have obtained these by solving the one-dimensional Schrödinger wave equation 4.10. The surface potentials used are those due to Cheng *et. al.* (1991), plotted in Fig. 6.1. We have plotted the wavefunctions for the surfaces of lithium, sodium, potassium, rubidium and cesium. The lithium surface is the strongest attracting surface and the cesium surface is the weakest. Note that

the lithium wavefunction is peaked closest to the surface and has the narrowest width. whereas the cesium wavefunction has its peak farthest from the surface and has the widest width. The sodium. potassium and rubidium wavefunctions are in between these and in this order. We have carried out calculations for the equation of states and the density profiles of helium on the surfaces for the cases of lithium and sodium. We present these results in chapter six. Note that the peaks of these wavefunctions are more than 4 Å away. This reflects the strongly repulsive nature of the surfaces towards helium. owing to the interaction of the two electrons of the helium atoms and the electrons of the outermost orbit of the alkali metal surfaces.

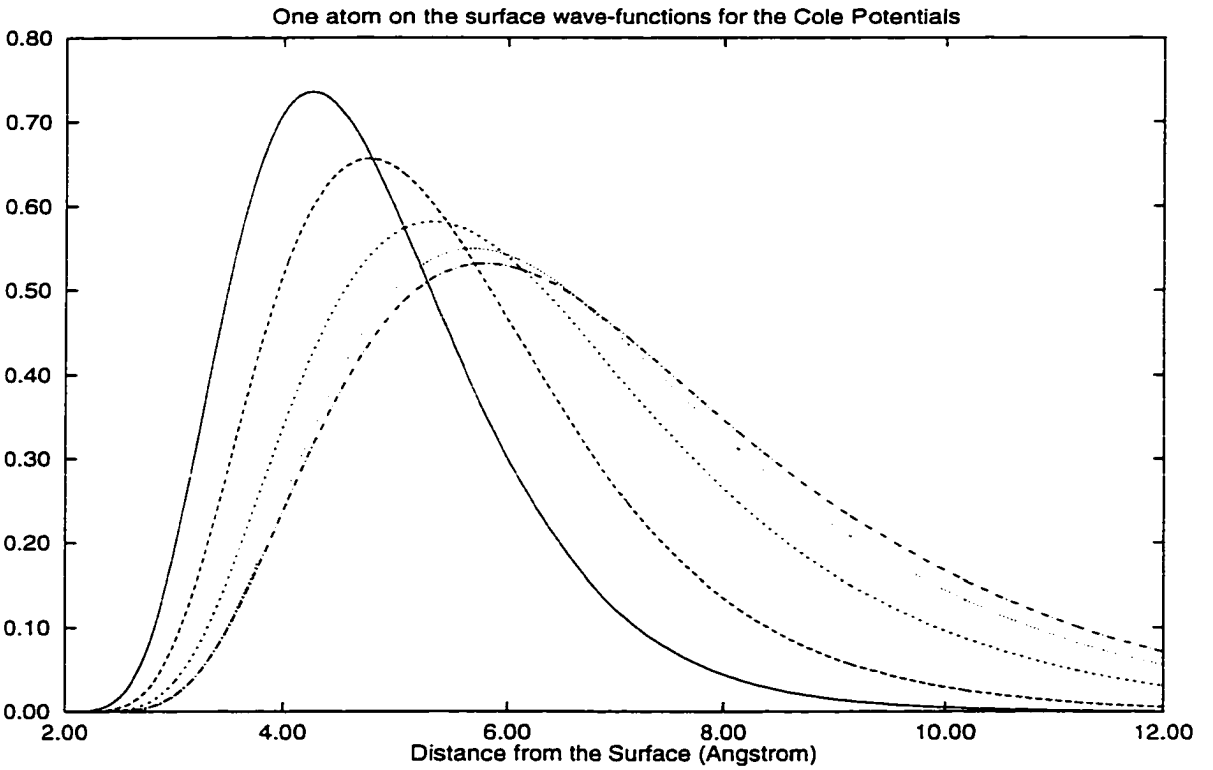

Fig. 4.2 Single atom wavefunctions for the surface potentials. From left to right: Li. Na. K, Rb. Cs.

In Fig. 4.3 we have plotted the squares of the wavefunctions plotted in Fig.

4.2, for reference. The wavefunctions in both these figures are square-normalized.

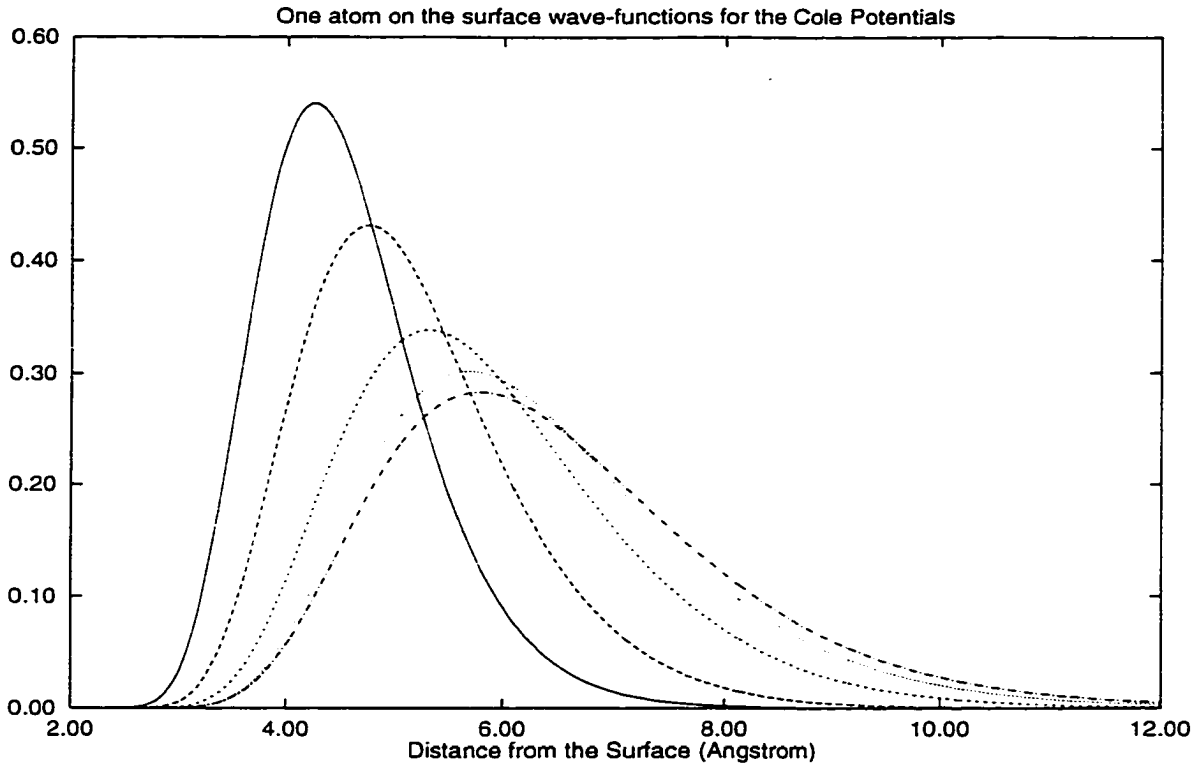

Fig. 4.3 The squares of Single atom wavefunctions for the Surface Potentials. From left to right: Li, Na, K, Rb, Cs

We have studied the liquid monolayer on lithium in detail. In order to obtain variational improvement on the ground state, we fitted the single atom wavefunctions to a parametric distribution function, $hz(x, n, m)$. We have plotted these functions in figures 4.4, 4.5 and 4.6. Equations (4.15) and (4.16) are two different algebraic forms of the same function. They are shown to highlight the way the parameters m and n enter in the expression.

$$hz(x,n,m) = \frac{n}{m} B\left(\frac{n}{2}, \frac{m}{2}\right) \frac{\left(\frac{xn}{m}\right)^{\frac{n}{2}-1}}{\left(1+\frac{n}{m}x\right)^{\frac{(n+m)}{2}}} \qquad (4.15)$$

$$hz(x,n,m) = n^{\frac{n}{2}} m^{\frac{m}{2}} B\left(\frac{n}{2},\frac{m}{2}\right) \frac{x^{\frac{n}{2}-1}}{(m+nx)^{\frac{(n+m)}{2}}} \tag{4.16}$$

These functions need to be shifted to the right to adjust to the small z behavior of the single atom wavefunction. These shifted functions (4.17), are plotted in Fig. 4.4, along with the single atom wavefunction for reference.

$$hzs(x,n,m,s) = hz(x-s,n,m) \tag{4.17}$$

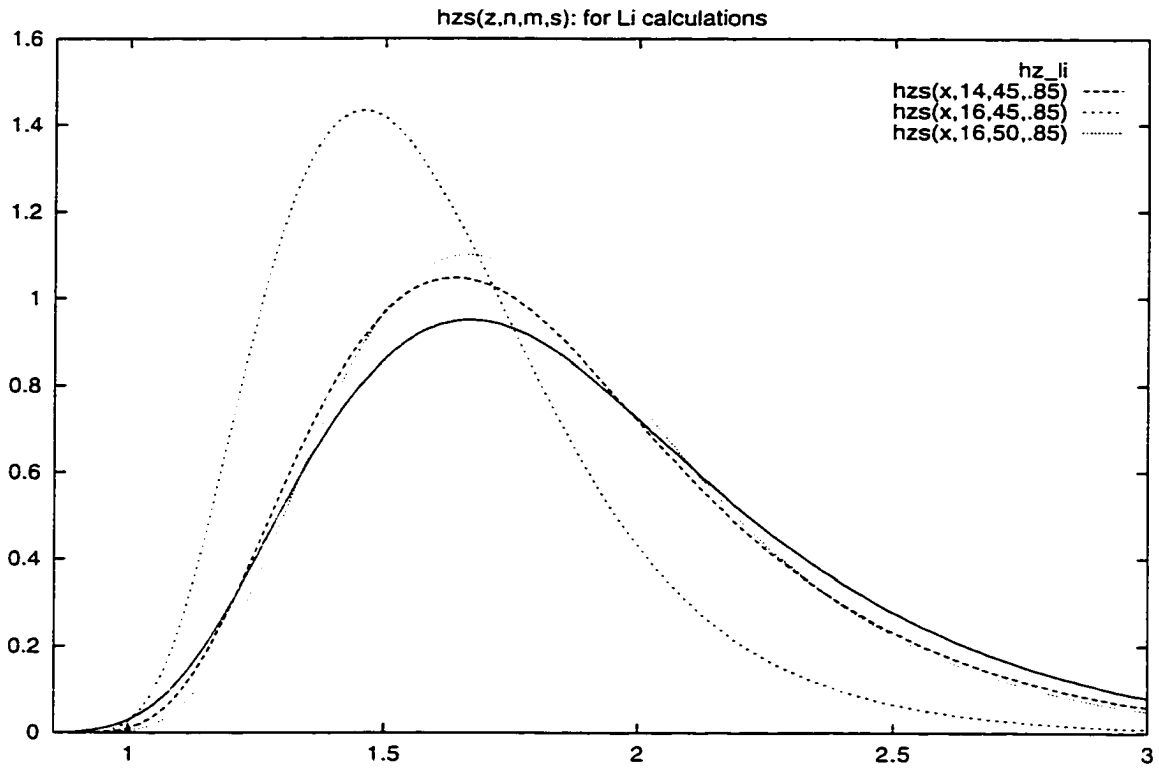

Fig. 4.4 Surface trial functions for Lithium: the parametric distribution function hzs(14,45,.85) is the best variationally

The optimum value of the shift parameter was found to be 0.85σ, or 2.17 Å. Fig. 4.5 shows the plots of the parametric surface function for values of the parameter n equal to 14, but for various values of m. Similarly, Fig. 4.6 plots these functions for $m = 45$, but for various values of n. The values $n = 14$ and $m = 45$

are the optimum values obtained by optimizing the total trial wavefunction for a liquid monolayer of helium on the surface of lithium. These optimised values were used in the Green's function Monte Carlo calculations for the helium monolayer. The optimized trial wave function is used as input (importance function) to the Green's function Monte Carlo calculations. A better importance function leads to lower variance in the Green's function Monte Carlo energy, but the estimated value of the energy should be the same.

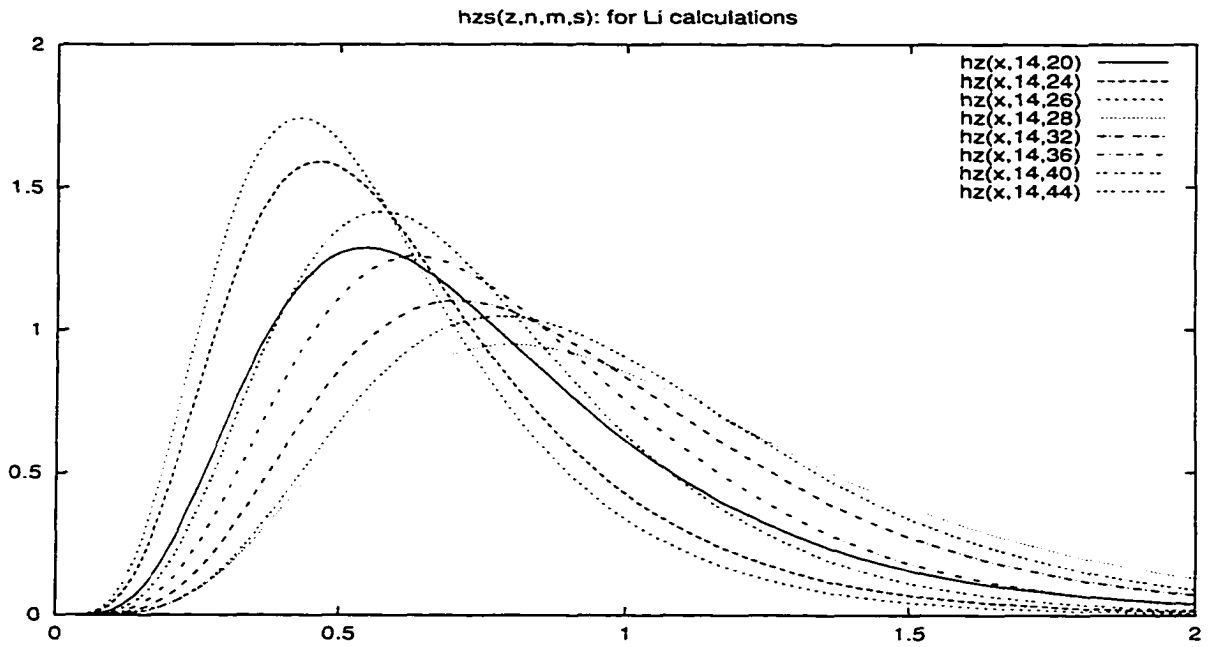

Fig. 4.5 Surface trial functions for Lithium: n=14 is the variational optimum

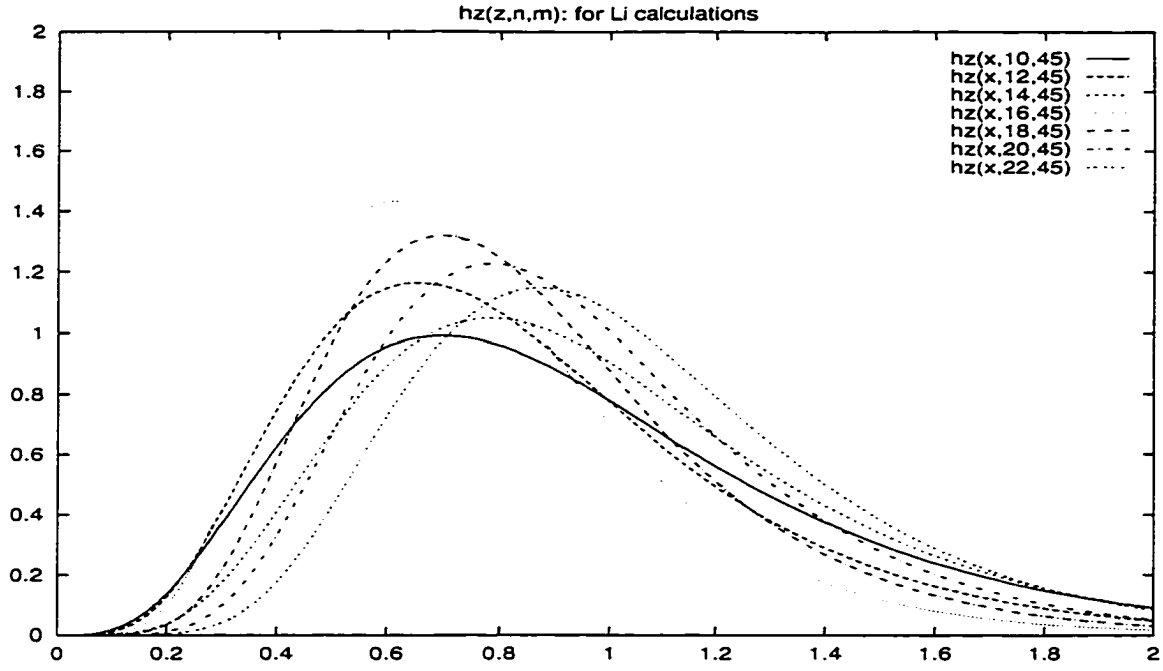

Fig. 4.6 Surface trial functions for Lithium: m=45 is the variational optimum

Gaussian localization for studying the solid phase

To study the solid phases of the helium systems we multiply the trial wave-function for the liquid phase (equation 4.6) with a product of gaussians localized at the lattice sites of the crystal structure that is being simulated.

$$\psi_{T_{solid}} = \psi_{T_{liquid}} \prod_i o_i \tag{4.18}$$

where,

$$o_i = e^{-\alpha(\vec{r}_i - \vec{l}_i)} \tag{4.19}$$

The $\vec{l}_i$ are the lattice points for the given crystal structure, and α is a variational parameter. This form of the localisation function was first considered by Nosanow (1966). It has been since widely used in simulations of the solid state.

Trial Wave-Functions for Studying Multilayers of Helium

At higher coverages layering of the helium atoms begins and the surface trial wave functions used for studying monolayers are no longer good enough. We need a surface trial wavefunction that can adequately represent multilayers, hz(z), before we can expect to have reasonable convergence in GFMC calculations.

One approach to obtain a class of functions with as many peaks or bumps as the number of layers we wish to study, is to consider a sum of Gaussian functions with varying heights and widths and displaced suitably from the origin.

$$hz(z) = \sum_{i}^{N} c_i f(z, \sigma_i, z_{o_i}) \tag{4.20}$$

where

$$f(z, \sigma_i, z_{o_i}) = \frac{1}{\sqrt{2\pi\sigma^2}} exp\Big[- \frac{(z - z_{o_i})^2}{2\sigma^2} \Big] \tag{4.21}$$

σ_i is a measure of the width of the i^{th} layer, and z_{o_i} is the location of the peak of the i^{th} layer.

This approach did not turn out to be fruitful. It seems that the value of the wavefunction near the surface (the small z part) is very important and must be close to the single atom wavefunction.

Another approach we considered is to use the histogram showing the z-profile of the distribution of atoms perpendicular to the surface, which we obtain with "bad" hz(z)'s (ones used for studying monolayers). At higher coverages the layering structure is evident in the histograms, even with monolayer hz(z)'s. By smoothing the histogram by some appropriate procedure we could extract an hz(z)

which can then be used in the optimization process.

We can consider shifted linear combinations of 1-atom. and multiple atom solutions of the Schrödinger wave equation in one dimension.

$$hz(z) = \sum_{i=1}^{N} c_i \psi_i(z - z_i) \tag{4.22}$$

where.

$$\psi_i(z) = \int \psi(z, z_2, z_3, ..z_i) dz_2 dz_3 .. dz_i \tag{4.23}$$

and $\psi(z, z_2, z_3, ..z_i)$ is the solution of the Schrödinger equation

$$\left[-\sum_{i=1}^{N} \frac{\hbar^2}{2m} \nabla_i^2 + V(z, z_2, ... z_i) \right] \psi(z, z_2, ... z_i) = E\psi(z, z_2, ... z_i) \tag{4.24}$$

and N is the number of layers one is studying.

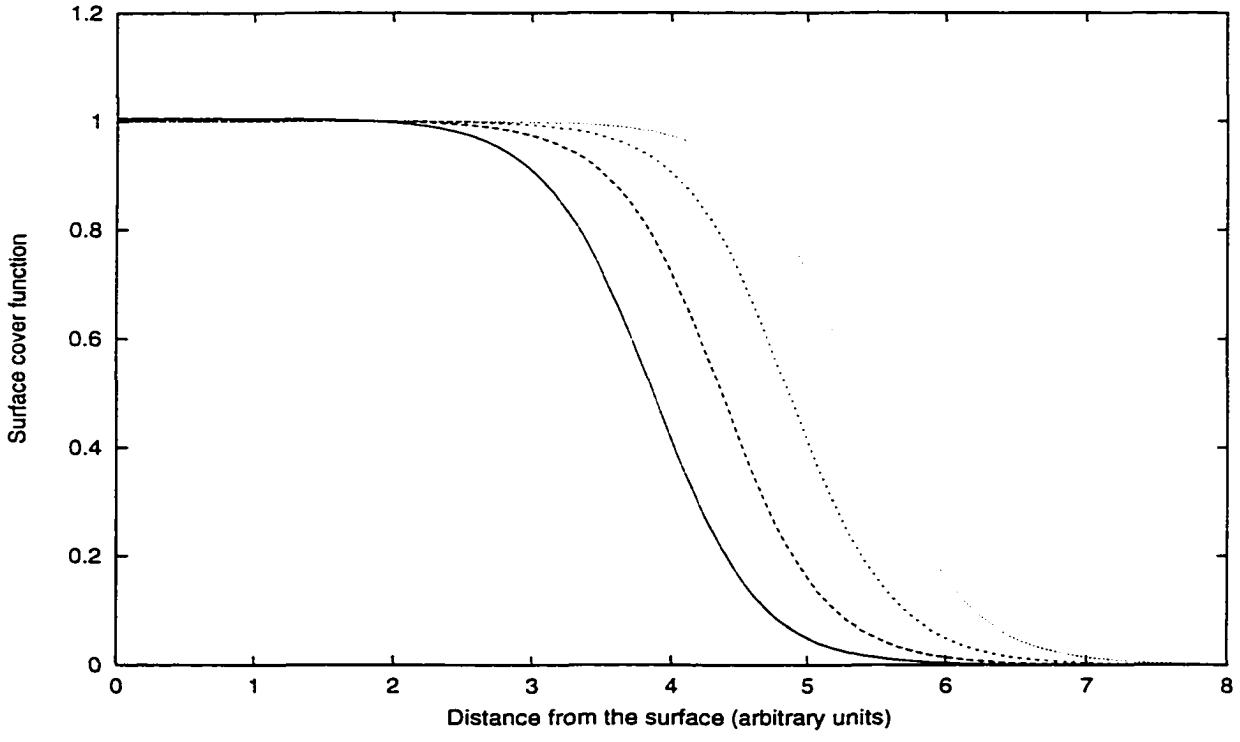

Fig. 4.7 Surface cover function, for different film widths.

CHAPTER V : Results: Helium on Solidifying Surfaces

In this chapter we first discuss helium films on the surface of graphite. We provide a method of studying film growth on the surface. Our calculations are in agreement with experimental data on layer promotion.

Helium on Graphite substrate

Clean (with no impurities), homogeneous (not presenting different crystallographic facets exposed for adsorption), samples of the graphite substrate material with good thermal properties and with large surface area need be available to obtain even moderately good results in surface studies. Such high quality samples of exfoliated graphite have been available for over 30 years. Typical figures for the available surface area are in the range 1-1000 m^2 in experimental sample volumes of 1-100 cm^3. The number of adsorbed atoms is then of the order of 10^{20}, which is several orders of magnitude below that usually found in studies of bulk helium. It has reasonably good thermal properties and can be studied down to milliKelvin and even sub-milliKelvin temperatures.

Adsorption of both ^{3}He and ^{4}He on exfoliated graphite has been well studied experimentally and several features are well established. In the present work we are only concerned with the bosonic ^{4}He.

Greywall (1993) has amassed specific heat data for coverages of helium from 0.0099 to 0.3500 $atoms/Å^2$, in the temperature range from about 3.5 K down to 100 mK. Up to five layers have been reported, layer promotion occuring at 0.120, 0.212, 0.288, 0.364, and 0.440 $atoms/Å^2$.

For sub-monolayer coverages, there are three distinct regimes: around 0.02 $atoms/\text{Å}^2$ a fluid film forms, at higher densities of about 0.0637 $atoms/\text{Å}^2$ several commensurate phases exist, with specific geometric arrangement of the atoms on the surface. These phases reflect the hexagonal ordered structure of the graphite surface and. At yet higher densities around 0.07 $atoms/\text{Å}^2$ an incommensurate triangular solid is formed, which does not seem to be affected by the surface structure, and seems to be due only to the helium-helium interatomic interaction. At around 0.12 $atoms/\text{Å}^2$ a second helium layer begins to form. The crystalline ordered state of the surface seems to destroy the superfluidity in the first layer.

Crowell and Reppy (1996) have completed a torsional-oscillator study of superfluidity in thin films of ^{4}He adsorbed on the basal plane of graphite for coverages from 1.5 to 7 atomic layers, in the temperature range 20mK and 1.2 K. In contrast to superfluidity in films adsorbed on amorphous substrates, they find several different regimes of superfluid behaviour. No superfluidity is experimentally observed in the first layer.

At a coverage of just above one and a half layers, superfluidity appeares and then later disappears before the completion of the second layer which solidifies. Superfluidity later reappears early in the third layer. The superfluid film appears to coexist with a two dimensional surface gas for low coverages in the third layer. Just before the completion of the third layer they see evidence of a phase transition that they think may be due to structural changes in the underlying second layer. Modulation of the superfluid signal with coverage is seen through the completion

of the sixth layer.

The present work does not study these and other phenomena arising out of the order in the adsorbing surface structure. Our work concentrates on the physics of the structureless surface (amorphous substrates), which must be completed with satisfaction, before studying these effects. The effects due to surface structure can then be studied as additional enhancements to the basic picture already understood.

In this thesis we consider the graphite potential averaged over the surface as our working representation of the surface, and only study a homogenous fluid state.

The fluid monolayer

Whitlock and Chester (1997) have carried out a study of the monolayer with an averaged surface potential. They find a fluid phase and a triangular solid phase at a higher density, as would be expected from the homogeniety of the system. The surface being strongly attractive, the monolayer is essentially two dimensional, and compares well with their earlier study of the hypothetical 2-D helium. For studying multi layers they suggest following the layer-by-layer approach outlined in the introduction. In this thesis we have considered trial wave functions that should adequately describe multilayers. Whitlock and Chester (1997) assume that the surface is structureless and that the interatomic helium-helium potential is well represented by the Aziz potential. A stable monolayer is found at a density (coverage) 0.0443 $atoms/\text{Å}^2$, in their GFMC calculation and at 0.0389 $atoms/\text{Å}^2$

in their variational calculation. Earlier, Gottlieb and Bruch (1993) have carried out a more realistic calculation for studying the monolayer. They considered the effects of corrugation (surface structure) and the effects of elastic distortion of the substrate by the adsorbed helium atoms. They estimate the density in a variational calculation to be 0.0216 $atoms/\text{Å}^2$ which is only about half of the density calculated by the structureless surface approach of Whitlock and Chester (1997). The monolayer density obtained by Gottlieb and Bruch (1993), seems to be consistent with the data of Greywall (1993). Thus it seems clear that surface structure effects play a significant role at monolayer coverages.

To solve the multilayer problem we used the averaged surface potential due to Carlos and Cole (1980) :

$$V_o(z_i) = \left(\frac{4\pi\epsilon\sigma^6}{a_s d^4}\right)\left[\frac{2}{5}\left(\frac{\sigma}{d}\right)^6 \zeta(10, \frac{z_i}{d}) - \zeta(4, \frac{z_i}{d})\right] \tag{5.1}$$

with $\epsilon = 16.24K$, $\sigma = 2.74$ Å, $d = 3.37$ Å, and $a_s = 5.24$ Å^2. $\zeta(n, z)$ is the generalised Riemann zeta function arising out of lattice sums in the calculation of the potential. The binding energy of a single atom in this potential is -140.738 K as compared to the bulk helium per atom binding energy of about -7.12 K. A single atom thus is bound 20 times more strongly to the graphite surface than when in the bulk liquid. It is this overwhelming strength that sustains several layers of helium (with the first two layers solidifying), before the film reaches bulk coverages.

In figure 5.1 we plot this potential as well as another used more recently due

to Brahmi, Joly and Lhuillier (1992).

$$V(z) = Ae^{-\alpha z} - \frac{C_3}{z^3} - \frac{C_4}{z^4} \tag{5.2}$$

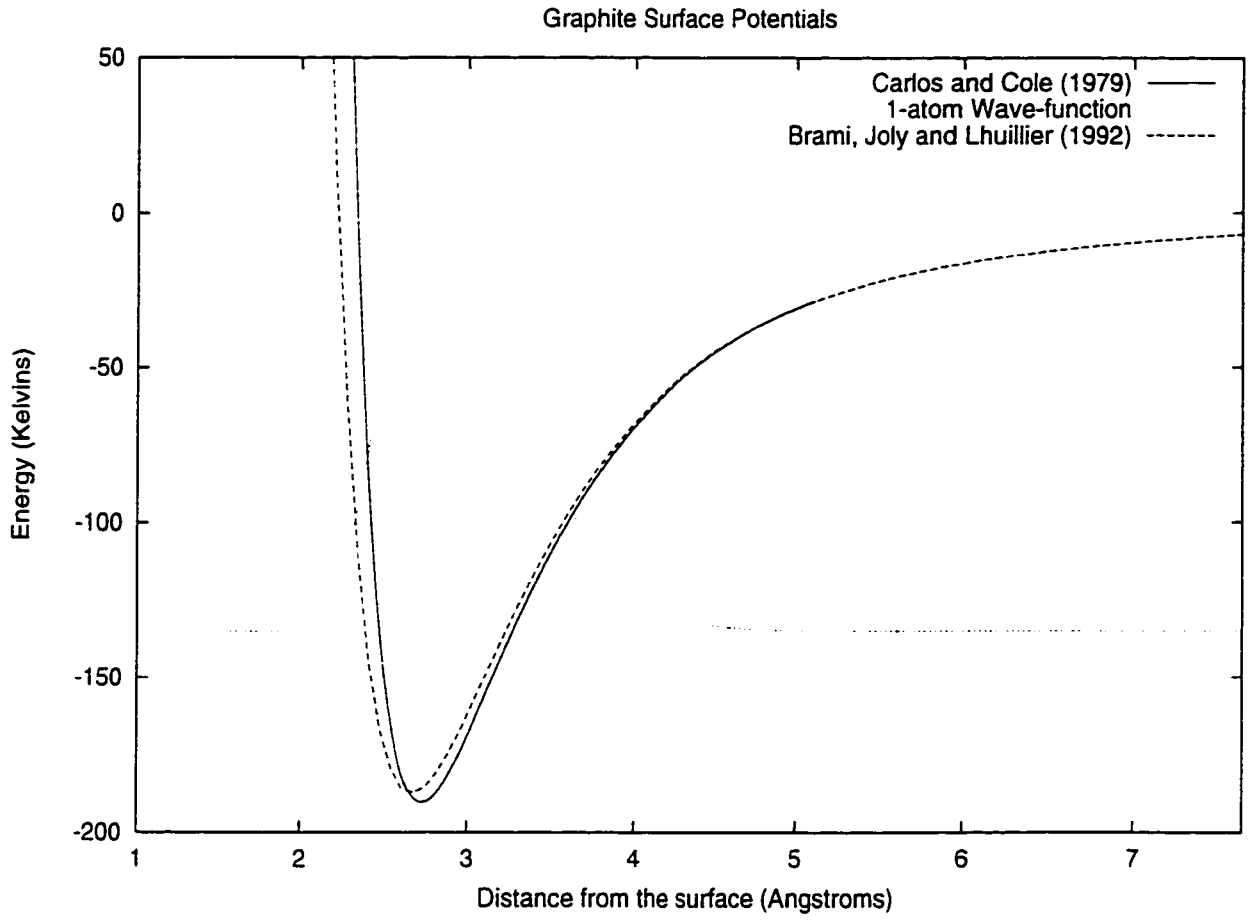

Fig. 5.1 The Surface potentials for a graphite surface commonly used. The slightly deeper one is due to Carlos and Cole (1979), and the other one is due to Joly, *et. al.* (1992). The single atom wave function for the former potential is plotted too.

The single atom wave-function shown in Fig. 5.1 is for the first potential. It has a maximum at 2.85 Å(1.116σ) and the width of its square at half height is about $0.626A$ (0.245σ), which is about 12% of the interparticle spacing in the film at the equilibrium density. Thus the helium atoms are very tightly bound to the

surface and their motion away from the surface is very small. Physically this is because the helium atoms are very strongly bound to the graphite surface.

Discussion of results

Table 5.1 summarises our results of variational optimization with the single-atom wavefunction used as the surface part of the trial wavefunction. As seen from the second column for E, the minimum density is at a coverage of 0.250 atoms/σ^2, though clearly the minimum seems to be very flat, particularly above the minimum. At this coverage the minimum energy is the minimum energy is -141.48 K. The single atom binding energy is -140.738 K and when subtracted from the total energy gives the *excess binding energy*, BE_{ex}, due to the interatomic interactions. This is tabulated in the second column.

Coverage	BE_{ex}	E	*P.E.*	$P.E._s$	$P.E._{int}$	*K.E.*
0.245	-0.740	-141.478	-166.357	-162.414	-3.942	24.878
0.250	-0.742	-141.480	-166.440	-162.392	-4.048	24.960
0.255	-0.741	-141.479	-166.535	-162.369	-4.166	25.055
0.260	-0.741	-141.479	-166.606	-162.334	-4.271	25.127
0.265	-0.738	-141.476	-166.679	-162.295	-4.384	25.203
0.270	-0.733	-141.471	-166.753	-162.253	-4.500	25.282

Table 5.1 Minimum Density with triplet strength, $\lambda = -1.3$.$b = 1.20$, $m = 5.0$. sampling error in E, $BE_{ex} = 0.002$ sampling error in PE, $PE_s = 0.014$. The shift parameter is 3.

We see, that the minimum BE_{ex}, is -0.742 K. We see that the potential energy per particle, *P.E.*, the potential energy per particle due to the surface, PE_s, as well as the potential energy of interatomic interaction per atom, tabulated in the 4^{th}, 5^{th} and 6^{th} columns, decrease monotonically with coverage. The kinetic

energy, $K.E.$, on the other hand monotonically increases. This is expected due to the uncertainty principle. 80 atoms were used in the simulation.

Table 5.2 shows variations of energy near the minimum density, at a smaller value, $\lambda = -0.5$, of the triplet strength parameter. The values obtained for the energies are clearly higher, for $\lambda = -0.5$ than for $\lambda = -1.3$.

Coverage	BE_{ex}	E	$P.E.$	$P.E._s$	$P.E._{int}$	$K.E.$
0.235	−0.717	−141.455	−166.235	−162.468	−3.767	24.780
0.245	−0.728	−141.466	−166.423	−162.447	−3.976	24.957
0.255	−0.725	−141.464	−166.610	−162.402	−4.208	25.146
0.265	−0.721	−141.459	−166.762	−162.333	−4.429	25.303
0.275	−0.707	−141.444	−166.924	−162.267	−4.657	25.480

Table 5.2 Energy variations around the minimum density, with $\lambda = -0.5$, $b = 1.20$, $m = 5.0$, sampling error in E, $BE_{ex} = 0.002$ sampling error in PE, $PE_s = 0.014$. The shift parameter is 3.

In Table 5.3 we present our calculations for variational optimisation of the triplet strength parameter, λ, at a fixed coverage, 0.255σ, selected near where the minimum density seems to be. The best value of $\lambda = -1.2$, yields the excess binding energy of $-0.746K$. The shift parameter is 2.

Coverage	BE_{ex}	E	$P.E.$	$P.E._s$	$P.E._{int}$	$K.E.$	*Shift*	λ
0.255	−0.701	−141.439	−166.637	−162.414	−4.222	25.198	3	−0.2
0.255	−0.725	−141.464	−166.610	−162.402	−4.208	25.146	3	−0.5
0.255	−0.738	−141.477	−166.526	−162.351	−4.175	25.049	2	−1.1
0.255	−0.746	−141.484	−166.522	−162.356	−4.166	25.038	2	−1.2
0.255	−0.741	−141.479	−166.534	−162.369	−4.166	25.055	3	−1.3
0.255	−0.735	−141.474	−166.489	−162.332	−4.157	25.015	2	−1.4
0.255	−0.733	−141.471	−166.496	−162.350	−4.146	25.025	2	−1.5

Table 5.3 Optimizing the triplet strength parameter λ. $b = 1.20$, $m = 5.0$, sampling error in E, $BE_{ex} = 0.002$ sampling error in PE, $PE_s = 0.014$.

Table 5.4 presents our calculations for the variations in energy with the shift parameter, at the fixed coverage, 0.255σ. The optimum value of the shift seems to be in the range 2-3. The effect of the shift parameter is to move the trial wavefunction as a whole the surface in the direction normal to the surface. A positive value means the atoms in the film prefer to stay away from the surface than a single atom does. The value of 1 means 0.001 σ (0.0026 Å). The value of 2 or 3 seems very small, but we can still see the variation in energy. This is an indicator of how sensitive the energy is close to the surface. We shall see that this is an important parameter at higher coverages.

Coverage	BE_{ex}	*E*	*P.E.*	$P.E._s$	$P.E._{int}$	*K.E.*	*Shift*
0.255	−0.661	−141.400	−166.649	−162.417	−4.232	25.250	0
0.255	−0.677	−141.415	−166.671	−162.432	−4.239	25.256	2
0.255	−0.674	−141.413	−166.651	−162.423	−4.228	25.239	3
0.255	−0.669	−141.407	−166.670	−162.433	−4.236	25.262	4
0.255	−0.660	−141.398	−166.628	−162.401	−4.227	25.230	5

Table 5.4 Energy variations due to the shift parameter with no triplet terms in the trial wavefunction . $\lambda = 0$, $b = 1.20$, $m = 5.0$, sampling error in E, $BE_{ex} = 0.002$ sampling error in PE, $PE_s = 0.014$.

Table 5.5 presents our calculations for variations in energy over a much wider range of the shift parameter. Negative values of the parameter mean that the trial wavefunction is shifted towards the surface. An atom in the film, due to its binding with the atoms of the film seems not to go closer to the surface than it would have if it were the only atom on the surface. This is therefore a many-body effect. The calculations have been done with $\lambda = -0.5$. Note that now the minimum energy is −0.726 K, which is lower than that for $\lambda = 0$ (no triplets) (−0.677). The minimum

energy for $\lambda = -1.2$ is still lower, $-0.746K$. Thus the triplet contribution to the film binding energy is $(-0.746) - (-0.677) = -0.069$ K which is 9.2% of the total (-0.746 K).

In bulk helium, the triplet strength parameter is -1.0 at the equilibrium density, and the triplet contribution is about 10% .

Coverage	BE_{ex}	*E*	*error*	*P.E.*	$P.E._s$	$P.E._{int}$	*K.E.*	*Shift*
0.255	−0.608	−141.346	0.003	−166.467	−162.266	−4.202	25.121	−4
0.255	−0.675	−141.413	0.003	−166.554	−162.350	−4.204	25.141	−2
0.255	−0.711	−141.449	0.002	−166.606	−162.403	−4.203	25.156	0
0.255	−0.715	−141.454	0.002	−166.579	−162.376	−4.203	25.125	1
0.255	−0.726	−141.464	0.002	−166.596	−162.397	−4.199	25.132	2
0.255	−0.725	−141.464	0.002	−166.610	−162.402	−4.208	25.146	3
0.255	−0.706	−141.445	0.002	−166.581	−162.377	−4.204	25.136	5
0.255	−0.609	−141.347	0.003	−166.474	−162.272	−4.202	25.127	9

Table 5.5 Energy variations due to the shift parameter with $\lambda = -0.5$, $b = 1.20$, $m = 5.0$, sampling error in E, $BE_{ex} = 0.002$ sampling error in PE, $PE_s = 0.014$.

It is considerably difficult to study the monolayer as the binding energies are very low, of the order of -0.75 K, and the Monte Carlo fluctuations are large. It is necessary to make very large runs. All the runs reported for the calculations in the tables have been for half a million Metropolis passes.

Multilayers on Graphite

Using a simple cover function we studied the growth of multilayer helium films on graphite. Our results indicate that the growth of the second layer does not affect the first layer significantly. We also obtain results which indicate a third layer formation.

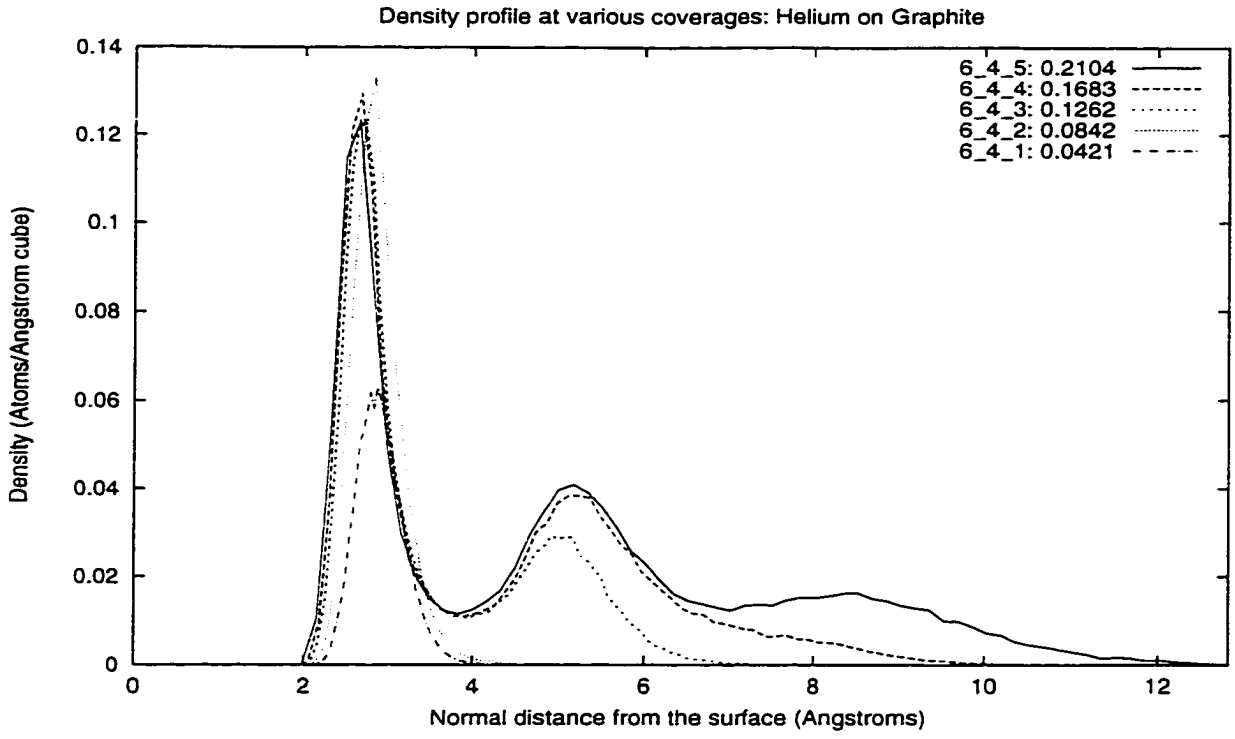

Fig. 5.2 Density profiles of Helium atoms on a Graphite surface, at various coverages, from a variational calculation. A simple cover function has been used as the surface part of the trial wave-function.

The density of the ground state is a lot more than the equilibrium bulk density (about three times). We do not expect superfluidity in the first layer. This is experimentally observed too, as pointed out earlier.

Note that as the second layer grows, the density crosses the superfluid density region approximately midway. This suggests that superfluidity will appear in the second layer when the it is about half full. Towards layer completion the density is about twice the equilibrium bulk density and superfluidity is expected to be lost. This phenomena has been reported by Crowell and Reppy (1992,1996).

Table 5.6 presents our calculations of the data plotted in Fig. 5.3.

N	*coverage*	*energy*	*error*	k	$z0$
80(8_5_1)	0.0390	−141.484	0.002	− − −	− − −
160(8_5_2)	0.0842	−133.78	0.40	11.0	0.1
144(6_4_3)	0.1262	−91.45	0.15	5.0	0.0
192(6_4_4)	0.1683	−74.24	0.19	3.5	0.0
240(6_4_5)	1.3750	−61.38	0.13	2.6	0.0

Table 5.6 Per particle energies at various coverages: Helium on graphite. $\lambda = -1.3$. $shift = 3$. $b = -1.20$. $m = 5.0$

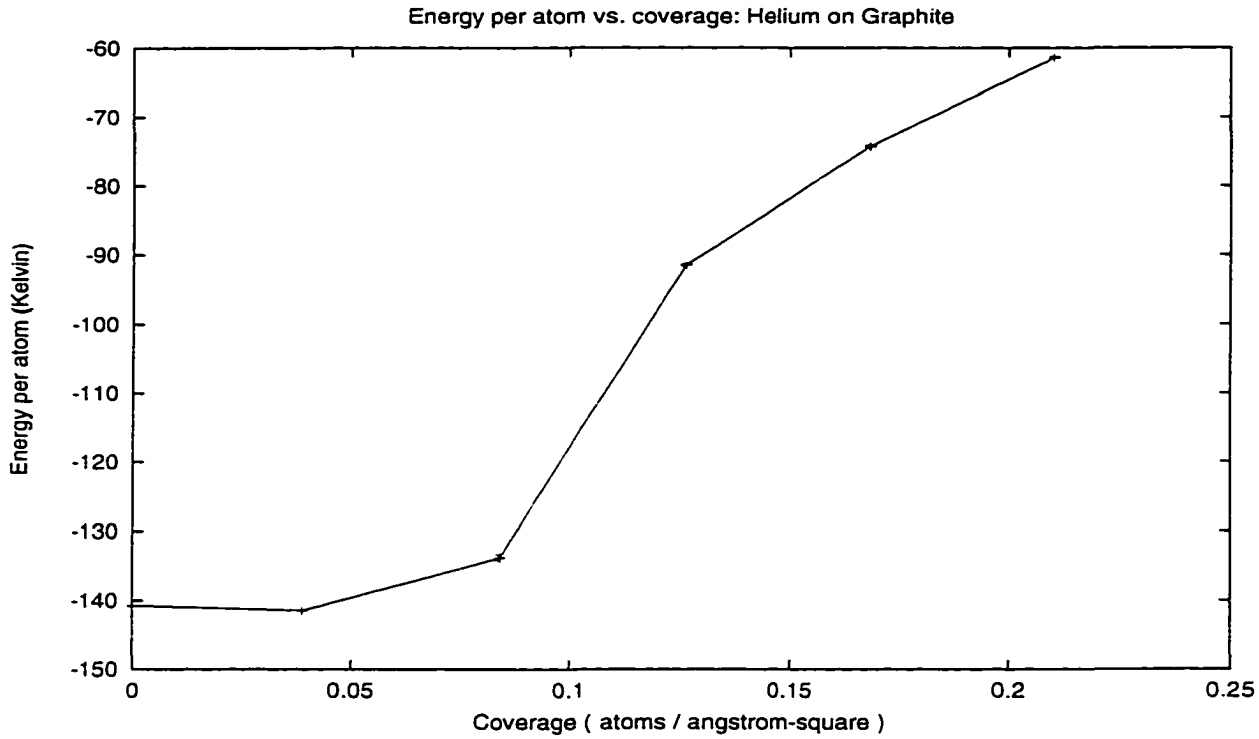

Fig. 5.3 Equation of state for helium films on the surface of graphite. The energy is plotted against coverage. The graphite surface is of Type I for helium adsorbate.

Non-Formation of a solid monolayer

We studied the disappearance of the monolayer solid as a function of well-depth. The equations of state for potentials of various depth shows that a surface with well-depth less than about 25 K will not support a monolayer solid.

We studied four potentials with varying depths. For the case of lithium we had found that no monolayer solid formed. For the case of graphite with a well depth of about 10 times that of lithium, it is well-known that at least two solid layers form. In order to locate the depth around which the solid monolayer no longer forms we performed calculations for four potentials with different well-depths: 4 times, 2 times, 1.5 times and 1.25 times the well-depth of the lithium potential. The equations of state are plotted in Fig. 5.4 for both the solid and the liquid state.

We find that for the third of these potentials (1.5 times the lithium potential), the solid and liquid states are close in energies at a high coverage (around 0.52 atoms/σ^2). We conclude that the solid monolayer will no longer form at depths less than around 25 K (the well-depth of lithium being about 17 K).

Fig. 5.4 shows the equation of states for the potentials discussed above.

We used gaussian localization in constructing the trial wavefunction for simulation of the solid state.

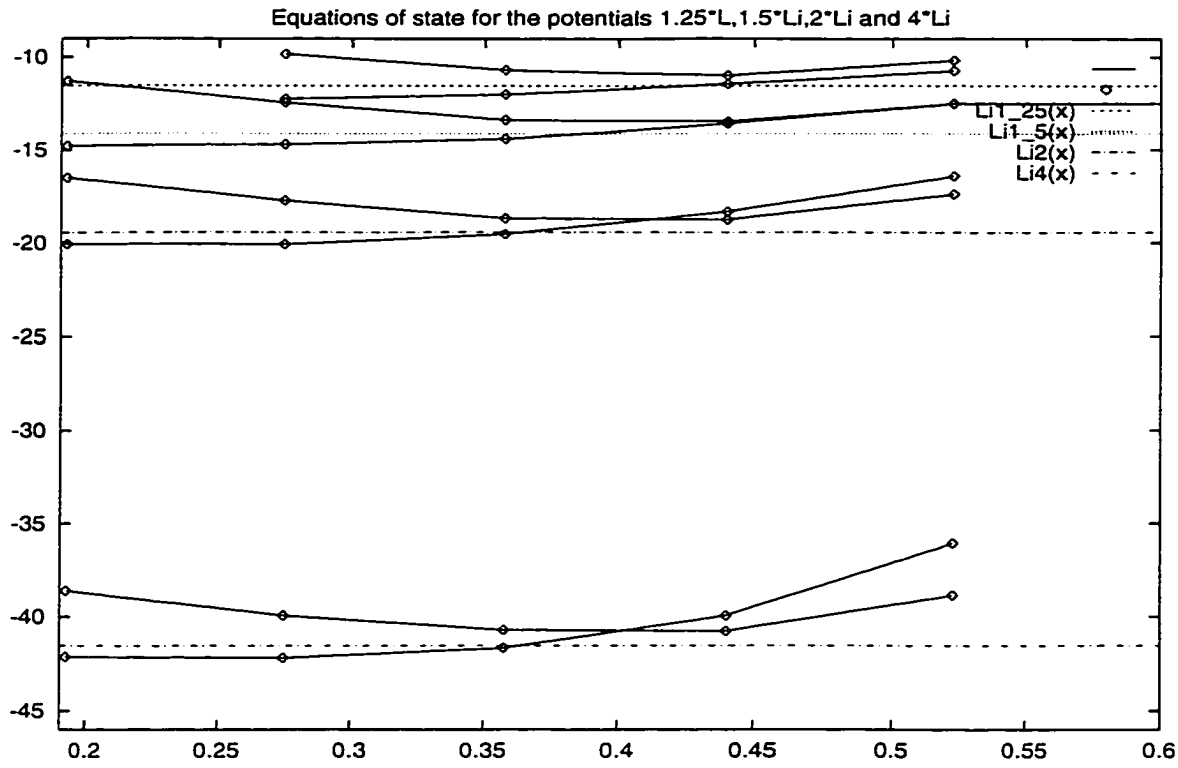

Fig. 5.4 Equation of states for various potentials of varying strengths: (depth. be) ..... The depths of these potentials are 4, 2, 1.5, 1.25 times the well-depth of the Lithium surface potential (-17.1 K). For the third case, the solid state is not preferred even at higher densities.

CHAPTER VI : Results: The Weak Binding Substrates

The Weak-Binding Alkali Surfaces

In this chapter we discuss our calculations for the alkali metals. These surfaces present a much weaker binding to the helium atoms, as compared to the graphite surface.

The weak-binding alkali surfaces are very difficult to prepare experimentally, due to their high chemical activity. Even under very high vacuum the surface is often not clean enough to get reproducible results. Thus the theoretical potentials derived from surface physics, may be inaccurate by as much as 50%. In the discussions and results presented in this chapter the potential family for the alkali surfaces, provided by Cheng, *et. al* (1991) have been used. Even though we may be discussing "lithium" or "cesium" what we really mean is the magnitude of the potential. The atomic symbols in Fig. 6.1, can be viewed as mere labels to the potential function plotted. It may well turn out, in the end, when the alkali surfaces can and are studied well enough that what is labeled as sodium may be a better representation for the potential of cesium. Or that the potential we are labeling lithium may have a well-depth of 25 K rather than the 17.1 K in the potential we use for calculation in the thesis.

This uncertainty in our knowledge of the potential, thus is a limitation to all our considerations. We are able to calculate qualitatively different phenomena for one potential than for another. If these are experimentally observed on different alkali surfaces experimentally, then our thesis provides the basis for reducing the

uncertainty in our knowledge of the potential. Thus we have tried to present our results which indicate qualitatively different regimes that these potentials give rise to. Our numerical results therefore cannot be used to get quantitative results at this time. but can be used as a guide to obtain some surface potential which may correspond or can be extrapolated to actual alkali surfaces.

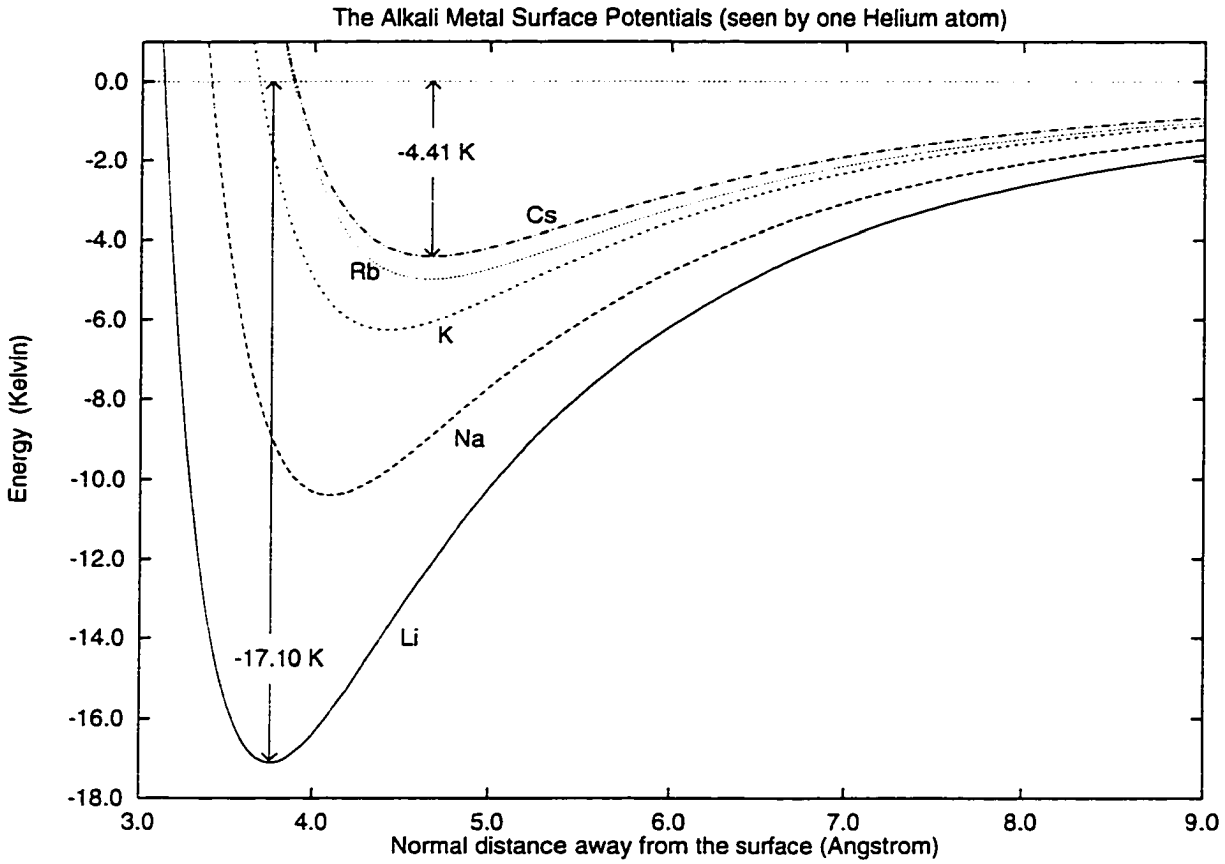

Fig. 6.1 The alkali-metal surface potentials due to Cole et. al (1991)

Figure 6.1 plots the Cole potentials for the alkali metal surfaces. The potential for lithium is the deepest. about 17 K. and the potential for the cesium surface the shallowest, about 4.4 K. In between is the potential for sodium, with a well depth of about 10 K. The model calculations presented in this thesis are mainly

for the potentials corresponding to lithium and sodium surfaces. Note also that the potentials for rubidium and cesium are very nearly the same and also that the width of the potential increases as the depth decreases.

A key question in studying the surfaces represented by these potentials is: Will helium wet these surfaces ? In our calculations we find that a monolayer film forms only on the relatively stronger lithium surface. The minimum stable coverage calculated for the sodium potential is more than a monolayer, more like a two layered structure. On the cesium surface our calculation indicates that the minimum stable coverage has about three layers. Thus, we conclude that helium wets these surfaces at progressively higher coverages. Our calculations are for an infinite system in the x-y plane. However, we can see from the energetics and film structure, that if a finite system, say a big droplet is placed on the sodium surface, the atoms will try to arrange themselves in two layers, rather than spread out in a monolayer, thus showing non-wetting.

Element	*At.No.*	E_{var}	E_o	*B.E.*	$Density_{min}$	b
H_2	1	−11.34	−10.65416	−0.68	0.2340	1.18
Li	3	−9.79	−9.00164	−0.79	0.3575	1.19
Na	11	−5.97	−4.81643	−1.16	0.4400	1.18
K	19	−4.42	−2.43950	−1.98	0.8113	1.19
Rb	37	−4.20	−1.81043	−2.39	1.0175	1.19
Cs	55	−4.12	−1.48781	−2.63	1.1000	1.19

Table 6.1 Binding energies obtained by using the single atom wavefunction as the surface cover function

The investigations of these weakly bound systems start with the surface part of the trial wave functions taken as the product of one-atom on the surface wave-

functions. The results we obtained are summarised in table 6.1.

The single atom binding energies for each surface are tabulated in the fourth column, E_o. The variational best energy is in the third column. The fifth column is the variational energy with the one atom binding energy subtracted out. This is the binding energy due to the interatomic interactions of the helium atoms.

First we note that the binding energy per atom, tabulated in the fifth column, decreases as the surface potential gets weaker. This is because there is greater binding between He atoms than between He and the surface, and it is advantageous for the atoms to form multiple layers, thus providing more interatomic interaction between the He atoms. We also note that the density (coverage) at which the minimum in energy occurs, tabulated in the sixth column, increases as the surface attraction weakens. This is to be expected too.

The density calculated in column six, is the areal density of atoms on the surface, and not the 3-dimensional density which varies with the distance away from the surface. The particle configurations calculated show that for lithium there is a clear monolayer. Our results indicate a clear second layer building for sodium, and our results for the cesium potential indicates that there are at least three distinct layers.

Lithium: Liquid Monolayer

Table 6.2 summarizes our variational results for a helium monolayer on lithium. The second column gives the variational minimum energies at the coverage shown in the first column. The third and the fourth columns, give the estimates of the

expectation values of the potential and kinetic energies.

Density	E_v	$< V >_v$	$< T >_v$
0.1925	-9.669 ± 0.005	-14.901 ± 0.011	5.232 ± 0.013
0.2750	-9.810 ± 0.007	-16.114 ± 0.012	6.304 ± 0.015
0.3575	-9.791 ± 0.003	-17.290 ± 0.008	7.499 ± 0.010
0.4400	-9.414 ± 0.005	-18.286 ± 0.008	8.871 ± 0.010
0.5225	-9.022 ± 0.006	-19.317 ± 0.008	10.30 ± 0.010

Table 6.2 Variational energies. for a helium monolayer on lithium at various coverages

The single-atom to the surface binding energy for the lithium potential. is -9.00 K. The minimum variational energy is obtained at 0.2750 atoms/$\sigma^2$and is about -9.81 K. The excess binding energy is therfore. -0.81 K. We note that the potential energy decreases with increasing density while the kinetic energy increases with density. This is in accordance with our general expectations. The particle configurations we obtain from the Monte Carlo sampling of the trial wavefunction at the density shows a clear monolayer structure.

Our results indicate clearly that a monolayer of helium forms on the lithium surface. To obtain a more accurate understanding we performed Green's function Monte Carlo calculations for this system. Green's function Monte Carlo convergence if achieved, would give an exact value of the energy. up to statistical sampling errors.

Table 6.3 summarizes our Green's function Monte Carlo results for the ground state of helium on a lithium surface. at four different values of the density. The choice of these values was guided by where we expect the minimum to be. and

here the earlier variational results are useful even though they are approximate.

Density	E_g	$< V >_g$	$< T >_g$	E_{grow}	*Gen*
0.1925	− − −	− − −	− − −	− − −	− − −
0.2750	-10.140 ± 0.002	-16.319 ± 00	6.179 ± 00	-10.132 ± 0.062	500
0.3575	-10.262 ± 0.002	-17.690 ± 00	7.428 ± 00	-10.256 ± 0.057	430
0.4400	-10.161 ± 0.003	-18.550 ± 00	8.390 ± 00	-10.145 ± 0.069	500
0.5225	-10.085 ± 0.004	-19.340 ± 00	9.255 ± 00	-10.064 ± 0.093	440

Table 6.3 GFMC energies. for a helium monolayer on lithium at various coverages

The best Green's function Monte Carlo energy we obtain we obtained is at the density, 0.3575 atoms/σ^2, and is -10.262 K. We note again that the potential energy decreases with density while the kinetic energy increases. This is what we would expect on general grounds. Squeezing the atoms, to a smaller space, as would happen when the density is increased, causes the momentum and thus the kinetic energy to increase, according to the uncertainty principle. Since the atoms, when under pressure will tend collect close to the well (the potential energy minimum) the potential energy will fall.

In Fig. 6.2 we plot the data presented in Table 6.3 to obtain the equation of state in a functional form. The data is fitted to the form:

$$E = E_o + B\left[\frac{\rho - \rho_o}{\rho_o}\right]^2 + C\left[\frac{\rho - \rho_o}{\rho_o}\right]^3$$

We chose this form because then E_o will be the minimum energy and ρ_o will be the density at this minimum. Furthermore, B and C are dimensionless quantities. The result of the fit plotted in Fig. 6.2 is:

$$E/N = -10.2687 + 22.5473(\rho - 0.339)^2 - 87.9666(\rho - 0.339)^3$$

The minimum energy, is $-10.2687K$. at a density 0.339 atoms/σ^2. The excess binding energy is about -1.3 K. The excess binding energy for the graphite surface is -0.9 K. This difference is due to the greater z-motion of the helium atoms in the much weaker lithium surface potential.

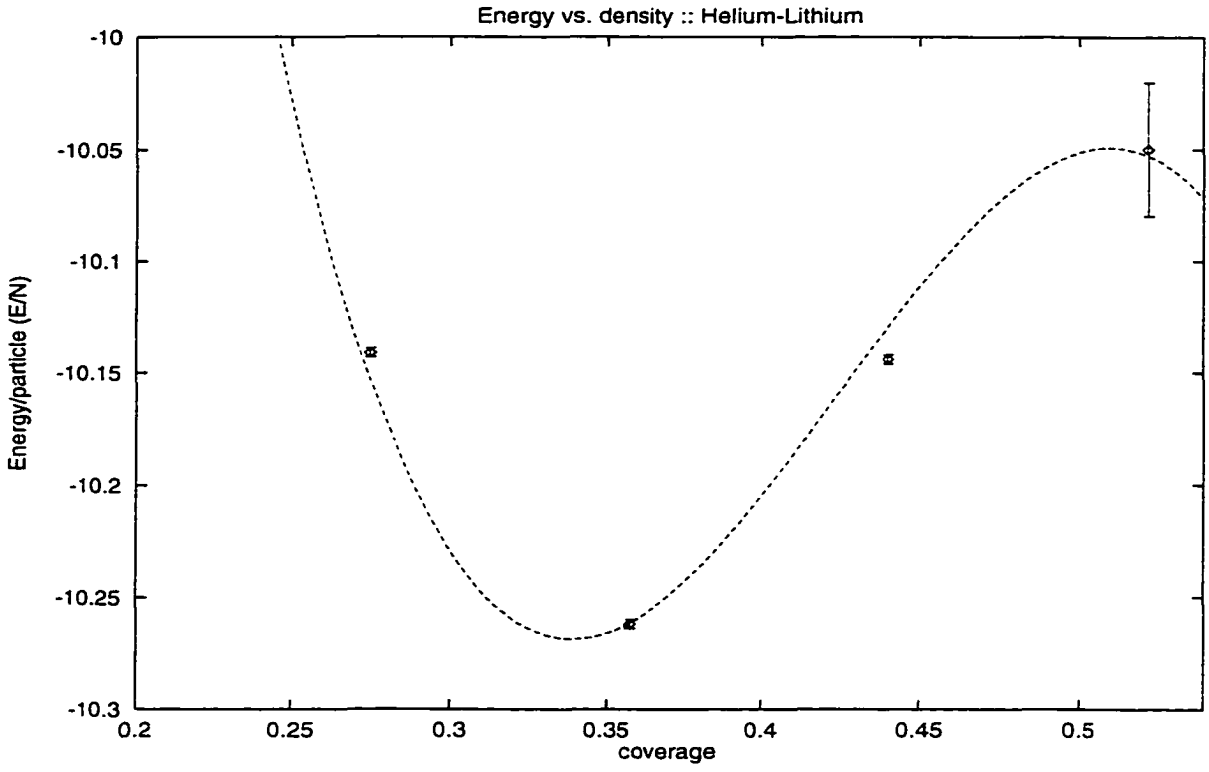

Fig. 6.2 The equation of state for the helium monolayer on the lithium surface. From GFMC data.

The variational binding energy we calculated was about -0.8 K. So, our GFMC result gives an improvement of -0.5 K. Thus the variational energy is off by, about 38%. This is indicative that there is much room for improvement in the trial wavefunction , or that the optimization of the trial wavefunction needs further work.

The importance function we used in the Green's function Monte Carlo cal-

culations, was the trial wavefunction with the parameters at the variational minimum. As we have described earlier, this trial wavefunction , is simply a product of the bulk helium trial wavefunction and a product of single-atom wavefunction s, to represent the surface part. The single atom wavefunction we used was a parametric form, that was optimized for the parameters in the variational calculations. We have obtained a clear minimum in the energy, and the minimum energy is an improvement over the variational estimate, and so our expectations seem to be correct. There is one subtle point however that requires further consideration. The GFMC method has been extensively used in studying bulk helium in three dimensions, with various interatomic potentials (Lennard-Jones, Aziz, etc...) as we have noted earlier. A variety of importance functions have been used and the convergence to the ground state has been satisfactorily achieved with each one. The bulk helium is also a case that is experimentally well known. So for bulk helium, our confidence in the GFMC convergence also comes from our ability to compare with experimental numbers. In the case of helium on weak-binding surfaces as we have discussed at the beginning of the chapter, we are not so fortunate. Experimental studies of helium on weak binding surfaces are not so definite, as to provide immediate support or confirmation for our theoretical result. Furthermore, in this thesis the first time that GFMC calculations have been used for a weak-binding surface. With poor experimental numbers available for comparison, the theoretical results cannot be compared with experiment. The suggestion (Chester, personal communication), has been made that the GFMC calculations be carried out for

various sets of parameters in the surface part of the trial wave function. That is we vary the importance function a little and see if the GFMC random walk converges to the same minimum energy, though maybe with a slightly more or less variance. If it does converge to the same minimum energy then we can have greater confidence in the efficacy of the method. The point is well taken, and we shall endeavour to do that in the future.

For the present however, we accept the minimum in the equation of state obtained, and take it as a *definite signal of the existence of the ground state of the system.*

We plot in Figures 6.3, 6.4, 6.5, 6.6, and 6.7, the energies versus the generations (iteration number) in the random walk, at all the four densities at which we performed the calculations. They are typical of Monte Carlo calculations.

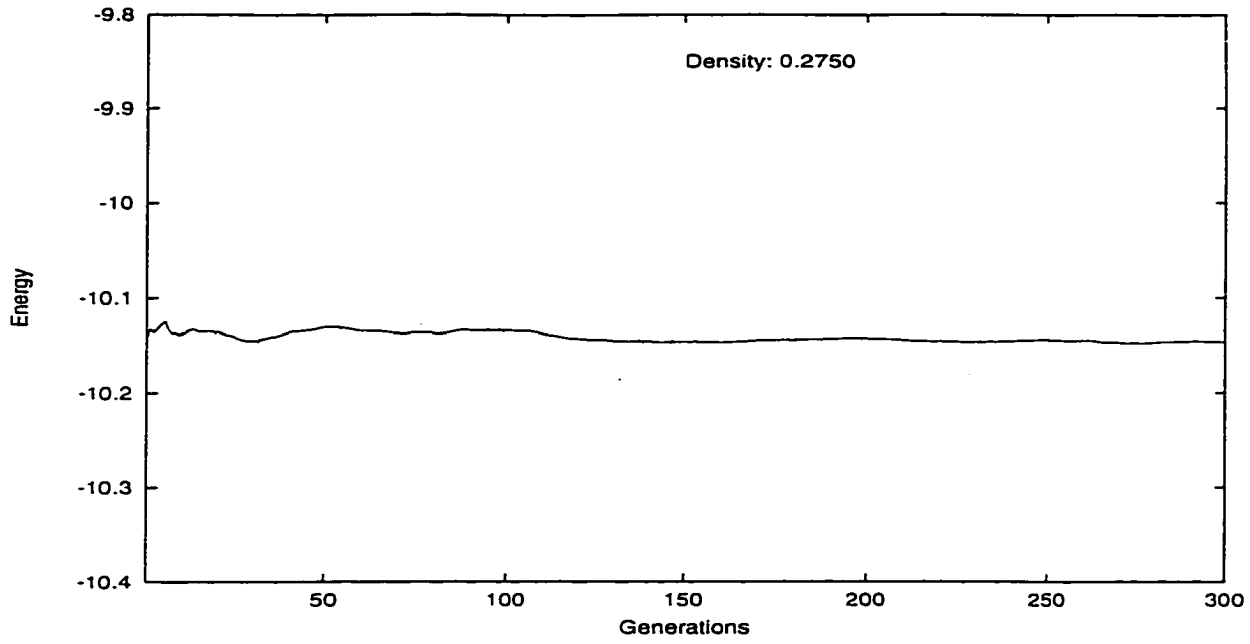

Fig. 6.3 Green's function Monte Carlo Energy estimation at 0.2750 atoms/σ^2

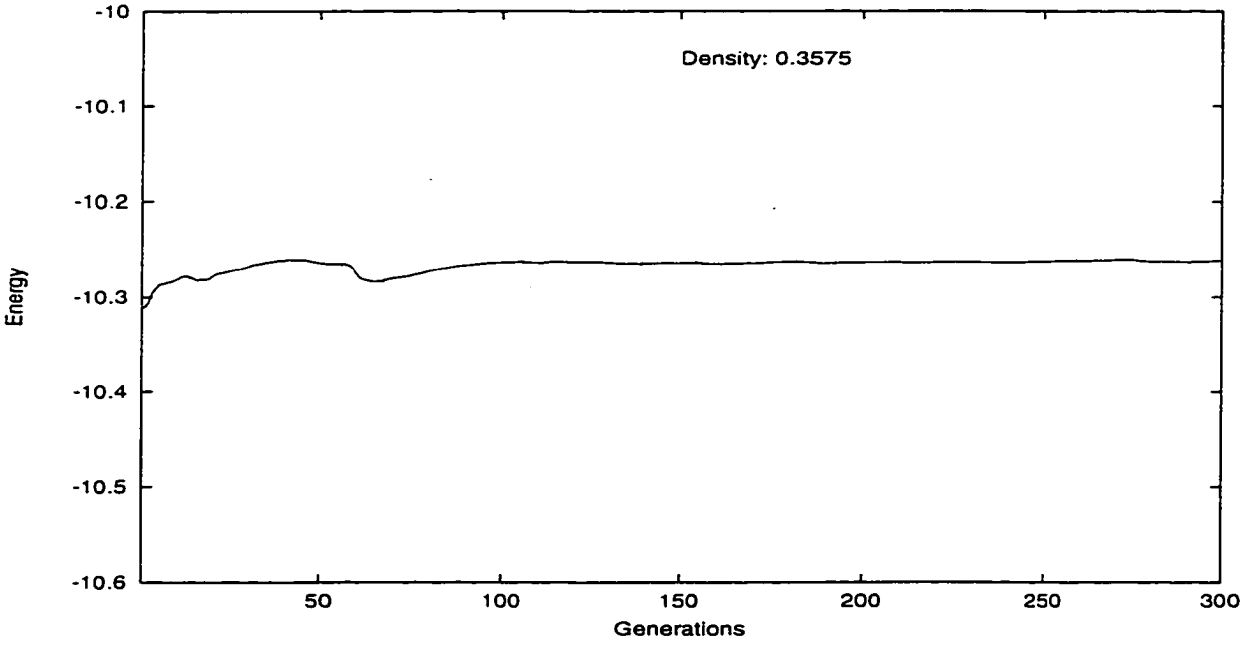

Fig. 6.4 Green's function Monte Carlo Energy estimation at 0.3575 atoms/σ^2

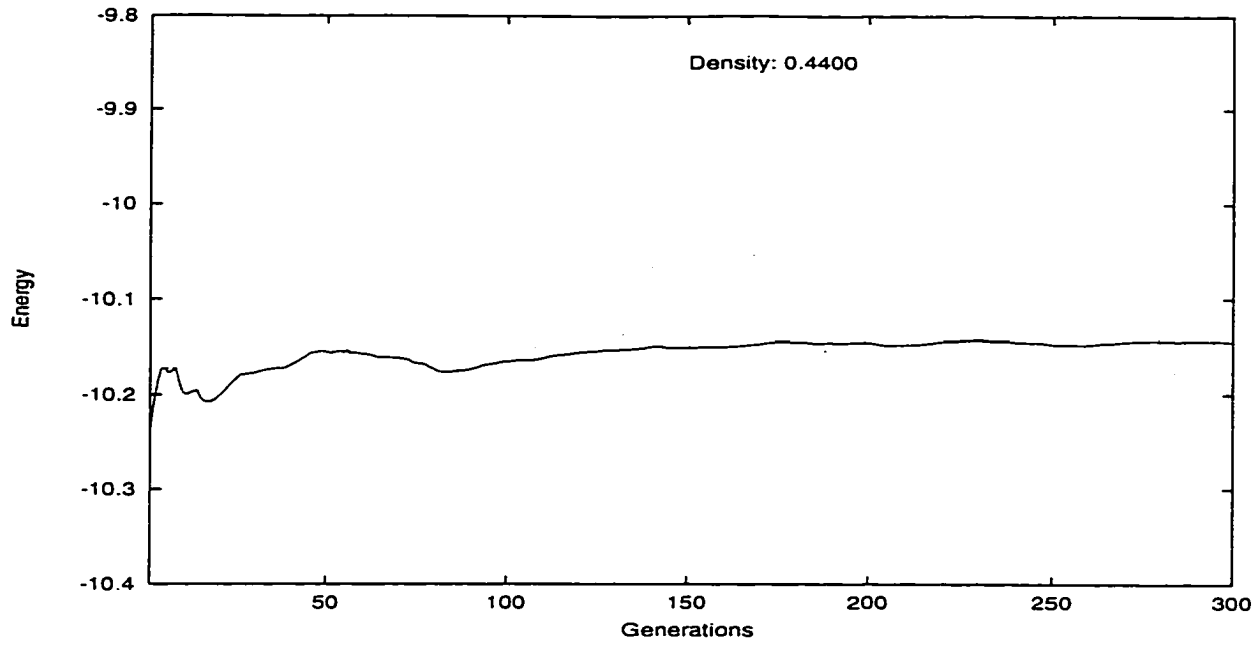

Fig. 6.5 Green's function Monte Carlo Energy estimation at 0.4400 atoms/σ^2

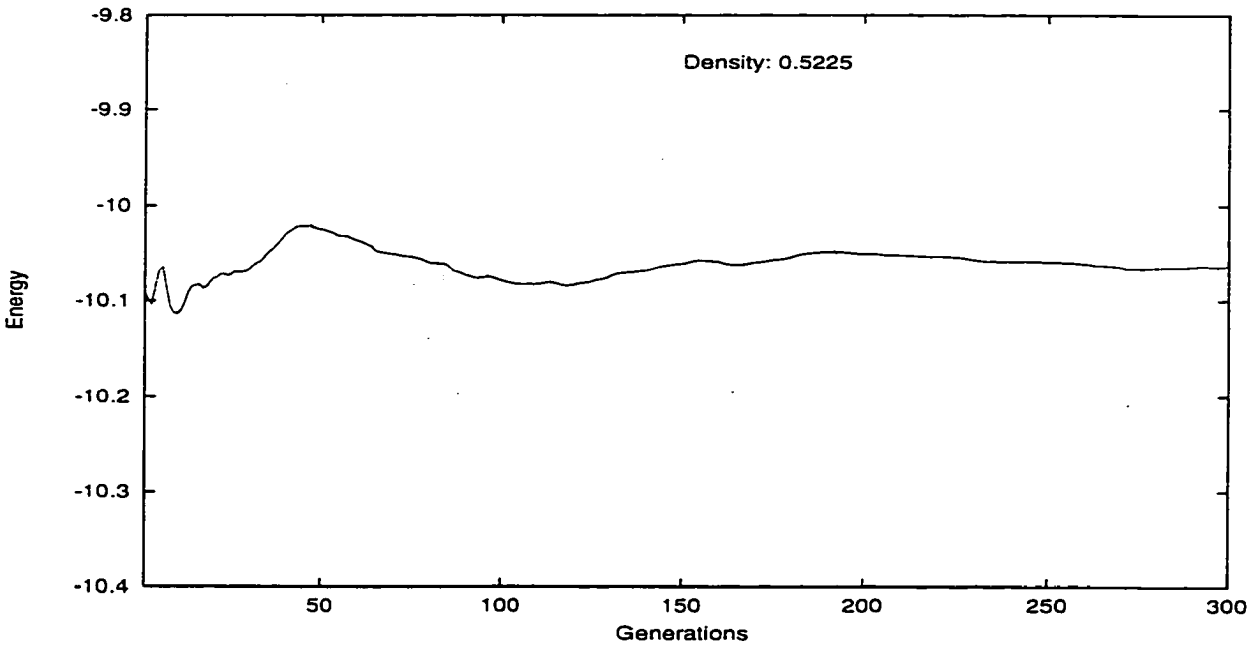

Fig. 6.6 Green's function Monte Carlo Energy estimation at 0.5225 atoms/σ^2

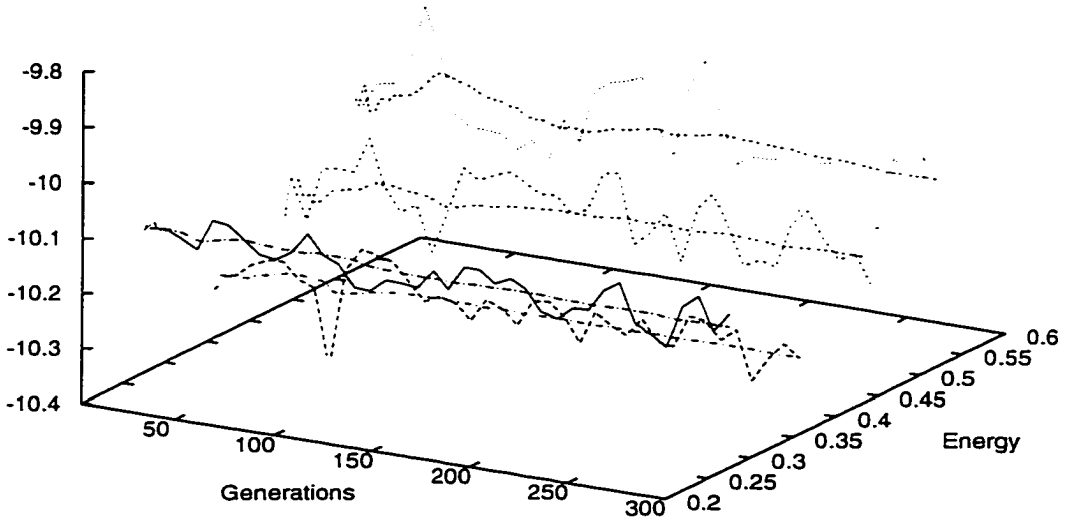

Fig. 6.7 Green's function Monte Carlo Energy estimation at all the four densities. This figure plots all the four separately drawn plots in one, to provide a comparative view.

Note that the energy estimate, as the average of the energy at every iteration, stabilises and that the fluctuations are around it.

Fig. 6.8 presents our calculations of the density profile of the atoms on the surface, plotted for all the four densities studied, in Fig. 6.8 below. The first most striking feature of our results is that as the coverage increases more and more atoms get adsorbed in the monolayer, until the second layer begins to form. The coverage at which layer promotion occurs seems to be around 0.065 $atoms/\text{Å}^2$. Above that coverage there are indications in the plot for 0.07998 $atoms/\text{Å}^2$ that a second bump appears indicating second layer formation. The diffuse way in which the second

layer seems to be developing suggests that the potential that the second layer sees is very weak. The density increase at the maximum. shows that more atoms get soaked up in the monolayer. before a second layer develops. The maximum density. occurs around 4 Angstroms. The equilibrium density interestingly is around the bulk equilibrium density.

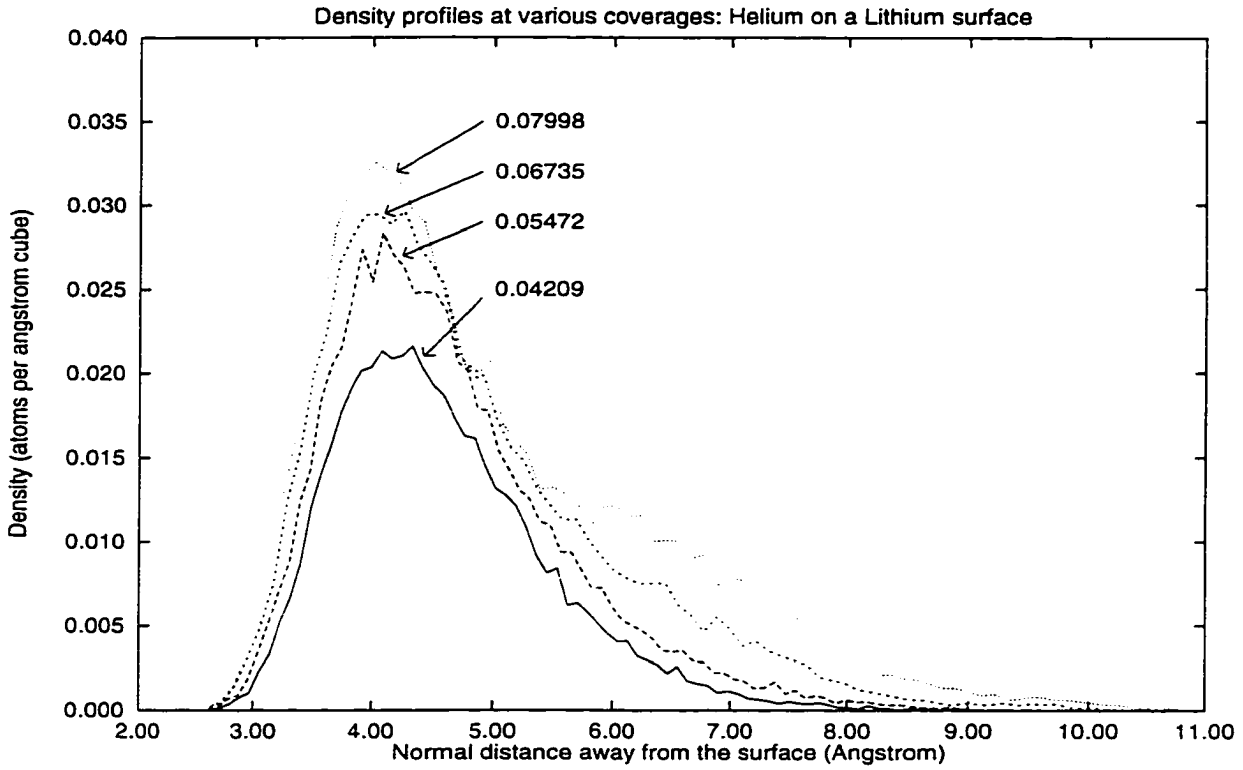

Fig. 6.8 Green's function Monte Carlo Density profiles of helium atoms on a lithium surface. at various coverages (indicated by arrows). The configurations have been obtained by Green's function Monte Carlo

Fig. 6.9 shows the plots of the one-body distribution function $\rho(z:z)$. The single-atom on the surface probability function is also plotted for reference. The equilibrium curve we calculate is close to this curve.

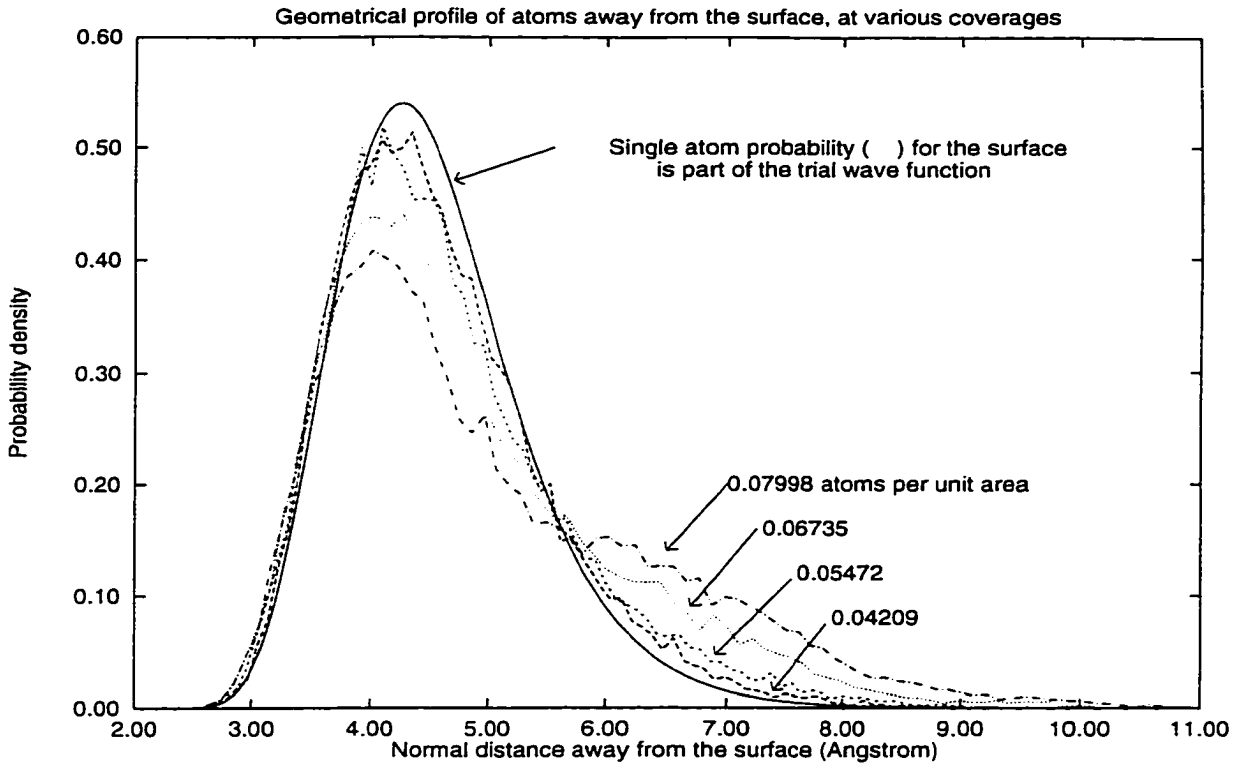

Fig. 6.9 Green's function Monte Carlo One-body density distribution of helium atoms on a lithium surface, at various coverages (indicated by arrows). The single atom probability distribution which has been used as part of the Importance function in the Green's function Monte Carlo calculation is also shown

Multiple layers of Helium on a Lithium surface

N	n_x	n_y	n_z	*Coverage*	E	k	z
48	4	3	2	0.1530(1.0)	-9.02 ± 0.021	2.6	1.6
72	4	3	3	0.2296(1.5)	-8.45 ± 0.012	2.8	3.1
96	4	3	3	0.3061(2.0)	-8.05 ± 0.011	2.8	5.0
120	4	3	5	0.3826(2.5)	-7.90 ± 0.016	2.8	6.1
144	4	3	6	0.4592(3.0)	-7.77 ± 0.015	2.5	7.5
168	4	3	7	0.5357(3.5)	-7.63 ± 0.015	2.5	8.8
192	4	3	8	0.6122(4.0)	-7.55 ± 0.012	2.5	10.3
216	4	3	9	0.6888(4.5)	-7.47 ± 0.011	2.5	11.6

Table 6.4 Variational energies, for helium films on lithium at various coverages: With the flat cover trial hz()

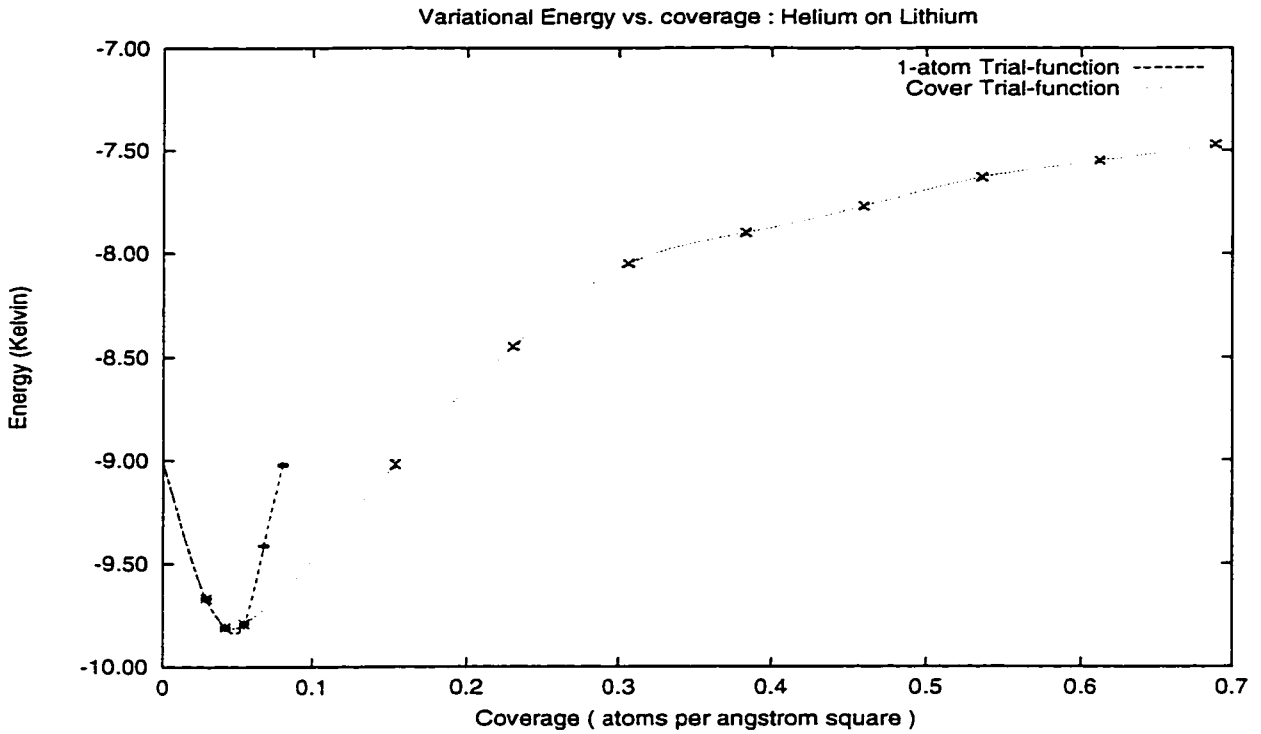

Fig. 6.10 Equation of state for helium films on a lithium surface. The energy per atom is plotted against coverage. The coverages are given in $atoms/\text{Å}^2$. The energy estimates have been obtained by Variational Monte Carlo .

Sodium : Bilayer stable coverage

In this section we describe our results which seem to indicate monolayer non-wetting of helium on the surface of sodium. The surface to atom potential for the sodium surface being of the same order as the helium interatomic potential, prevents a stable monolayer formation.

Sodium surface and the Aziz potentials

There is something unique about the sodium surface potential. Its well depth is about the same as that of helium-helium interatomic potentials. The sodium surface potential has a 1-atom binding energy of -4.81 K, which is higher than the

bulk value of -7.12 K, and it is therefore of Type II according to the classification presented earlier. Fig. 6.11 is a plot of the interatomic potential and this potential on the same scale for comparison.

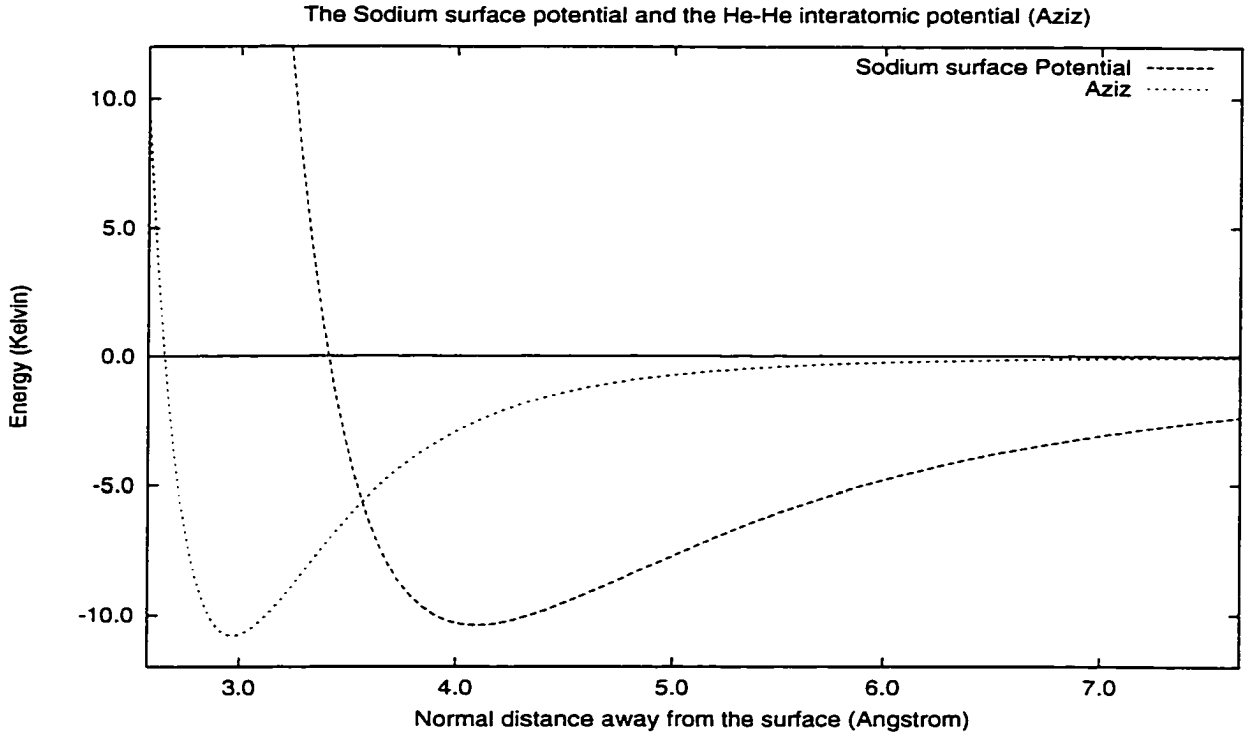

Fig. 6.11 The helium interatomic potential (Aziz) and the sodium surface-potential plotted together. Note that the range of the surface potential is about twice the range of the interatomic potential.

Table 6.5 shows our results for the energy minimization with the single atom wavefunction for the surface. The minimum occurs around -6.32 K at a coverage of 0.6 atoms/σ^2. The optimum value of the triplet strength is 0.5 and the shift away from the wall is 100. The simulation has been carried out with 80 atoms, with 8x5 unit cells in the simulation area.

The configurations show a second layer developing. This shows that a wider

surface trial wavefunction must be tried. The flat cover function was used, as the surface trial wavefunction .

coverage	*energy*	*error*	*b*	*alamt*	*shift*	*N*
0.4400	−6.18570	0.02102	1.19	0.5	100	80
0.5225	−6.27669	0.01020	1.19	0.5	100	80
0.6050	−6.32580	0.01117	1.19	0.5	100	80
0.7700	−6.21582	0.01227	1.19	0.5	100	80

Table 6.5 Variational energies, for helium films on sodium at various coverages: single atom surface cover function used. Note the minimum at 0.605 atoms/σ^2

Table 6.6 summarizes our optimization results with the flat cover function. This table shows the calculations starting from the coverage of 0.6050 atoms/σ^2, at which we had obtained a minimum earlier with the single-atom trial wavefunction, upto a coverage of 1.6150 atoms/σ^2. The energy monotonically falls, throughout the entire range.

coverage	*energy*	*error*	*k*	*Z*	*N*
0.6050	−6.42443	0.01092	2.7	1.1	80
0.6875	−6.51594	0.00954	2.7	1.2	80
0.7700	−6.54550	0.01225	2.7	1.2	80
0.8525	−6.58512	0.01110	2.7	1.6	80
0.9350	−6.61836	0.00996	2.7	1.7	80
1.1000	−6.63026	0.01024	2.7	2.0	108
1.2650	−6.62979	0.01083	2.7	2.8	120
1.6150	−6.63895	0.01009	2.7	3.8	120

Table 6.6 Variational energies, for helium films on sodium at various coverages: With the flat cover trial wavefunction

In order to quickly locate the minimum, we optimised the energy at coverages of 0.5, through 3.0 atoms/σ^2in steps of 0.5 atoms/σ^2, for a simulation area con-

taining only 4x3 unit cells. The result is shown in Table 6.7. npart is the number of atoms in the simulation. We notice that the energy reaches a minimum plateau around 2.0 atoms/σ^2.

coverage	*energy*	*error*	k	Z	*npart*
0.5	−6.32031	0.03579	2.0	0.5	24
1.0	−6.72424	0.01637	2.6	1.8	48
1.5	−6.79058	0.01519	2.6	3.1	72
2.0	−6.77238	0.01083	2.6	4.8	96
2.5	−6.77894	0.00899	2.6	6.0	120
3.0	−6.77838	0.01080	2.6	8.0	144

Table 6.7 Variational energies, for helium films on sodium at various coverages: smaller area of box. Note the systematic error.

We then carried out optimisations with a larger simulation area, accomodating a larger number of atoms, at the same coverage. The results are summarized in Table 6.8. There was a systematic error of about 0.14 K, in the previous case, due to tail corrections caused by using a smaller number of atoms in the simulation box.

coverage	*energy*	*error*	k	Z	N
1.0	−6.63071	0.01156	2.6	1.9	96
1.5	−6.63300	0.00755	2.6	3.3	144
2.0	−6.63234	0.00942	2.6	4.8	192
3.0	−6.61253	0.00819	2.6	7.6	288

Table 6.8 Variational energies, for helium films on sodium at various coverages: large enough area of simulation box

Fig. 6.12 plots the variational energy versus coverage for the various trial wavefunctions used in the calculations. The parabolic curve at the top left corner

is for the single-atom trial wave function. Of the two other curves the lower one is for the cover function with a large enough number of atoms used in the simulation. The curve above it shows a systematic error due to a smaller number of atoms used in the simulation. At higher coverages the curves are essentially flat since the well-depth of the interatomic potential is comparable to the surface to atom potential.

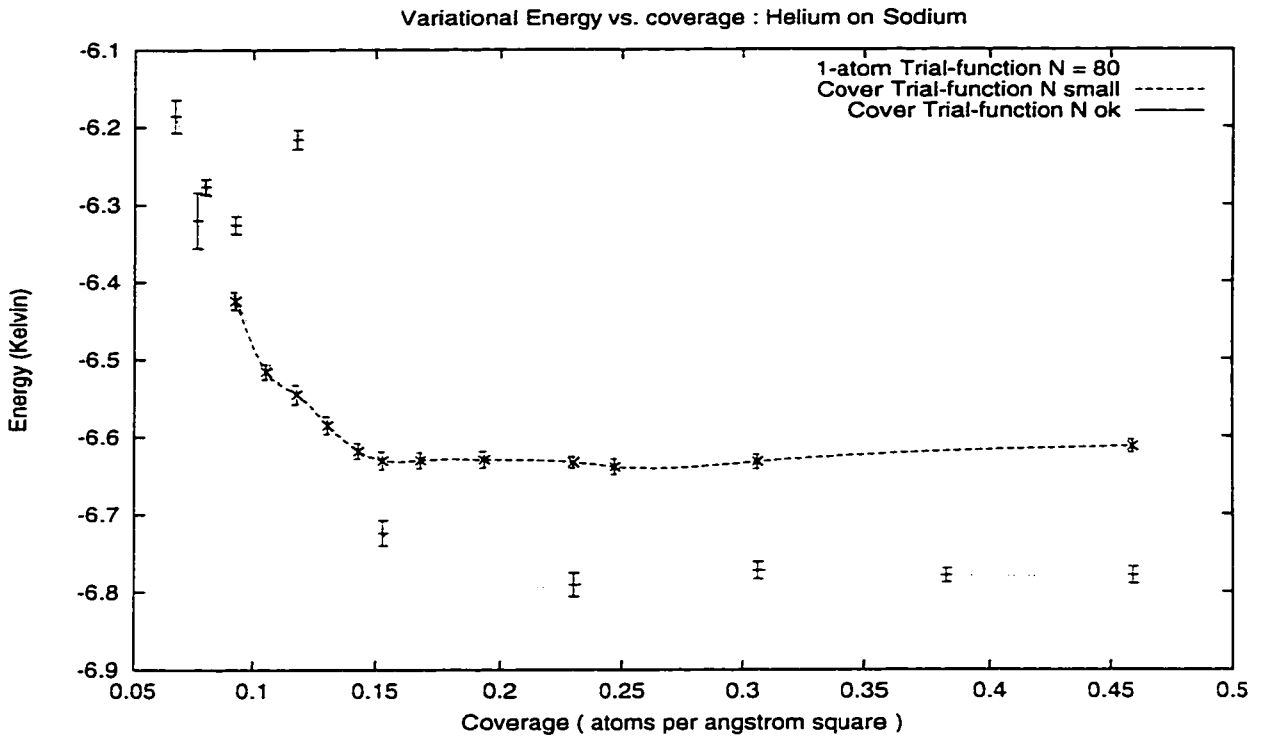

Fig. 6.12 Equation of state for helium films. The energy per atom is plotted against coverage. The coverages are given in $atoms/\text{Å}^2$. The energy estimates have been obtained by Variational Monte Carlo .

The density profiles obtained from the particle configurations at various coverages, are shown in Fig. 6.13. No stable monolayer forms and the minimum stable coverage is for a bilayer. This clearly demonstrates monolayer non-wetting.

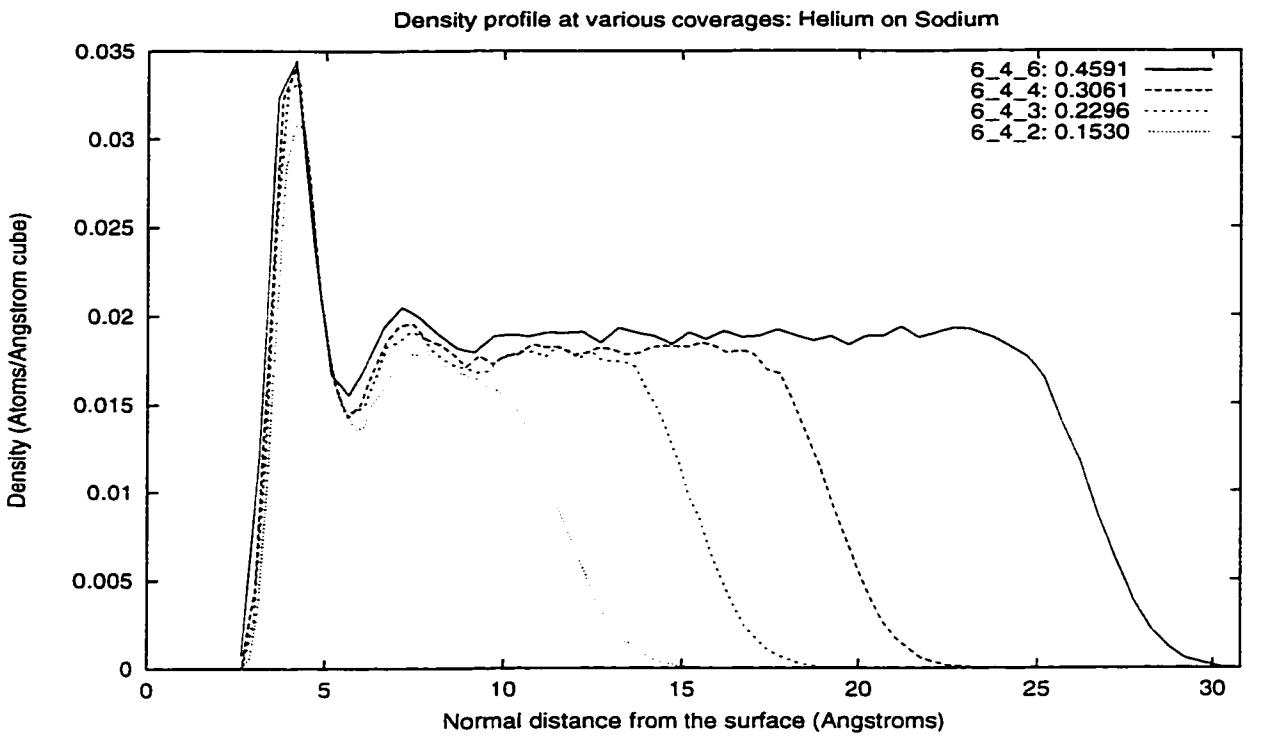

Fig. 6.13 Density profiles of helium films on a sodium Surface. The coverages are given in $atoms/\text{Å}^2$. The configurations have been obtained by Variational Monte Carlo .

In our study of the weak-binding substrates we have been able to establish a few results. We find that for the strongest attracting surface of lithium there is no solid monolayer formation, but a stable liquid monolayer does form. We established this result by Green's function Monte Carlo calculations. For the weaker surface of Sodium we establish that the minimum stable coverage is a bilayer, and that no monolayer wetting takes place. The results presented are the first based on Monte Carlo Simulations.

CHAPTER VII : Conclusions and Future Directions

In this thesis we presented our calculations and results on the ground state of helium films on a range of surfaces. We established a program for studying film growth using Monte Carlo simulations. We studied film growth and layer formation on the surfaces of graphite, lithium and sodium. For the problem of helium on graphite we established formation of upto three layers. The coverages at which layer promotion occurs compares well with experiment. Higher coverages can be studied in a straightforward way, only requiring more computation time. On the lithium surface, we established that helium will form a stable liquid monolayer. We used Green's function Monte Carlo calculations to establish this result. For the sodium surface which is weaker than lithium, we establish monolayer non-wetting.

As a result of our investigations of helium films at very low temperatures we can suggest a few directions for fruitful research. We list them below.

- **Optimising the pair-function with density dependent parameters.**

The maxima and minima of the pair correlation function are measures of how likely pair distances occur in the system. These are density dependent. It would be interesting to see if the coordinates of these are taken as parameters, with smooth functions connecting them, whether one gets a better pair function. It just might.

- **Optimising the film cover-function with density dependent parameters.**

We have used a very simple cover function to envelop the film. Structure information from the density profiles, can be used to improve it. We expect the

energies to get better, though the structure may not change much, which depends more on the potentials. An optimisation procedure similar to the one suggested above may be attempted.

- **Green's function Monte Carlo studies of the weak binding regime.**

Green's function Monte Carlo studies to obtain accurate confirmation of the qualitative results discussed in this work, will enhance our confidence in the understanding we have obtained principally using Variational Monte Carlo . Moreover fast microprocessors available today make long Green's function Monte Carlo runs feasible.

- **Wetting-Non wetting transition be modeled.** The transition is expected around a weak-binding surface with the single atom binding energy of about -7.12 K.

- **Gas-Liquid coexistence region.**

At low coverages before stable coverage is reached we expect the finite system to be prone to clustering and non-wetting. This seems to be an entirely open regime, and our understanding seems to be very poor. Our methods and models cannot be a guide as the system is thermodynamically unstable and splits up into liquid gas phases.

- **Multithreaded and distributed computing.**

Multithreaded and object oriented paradigms and the availablity of fact multiprocessor computers should be exploited to write codes for larger systems. Ability to make several million metropolis passes may help to resolve the sampling noise

that drowns the distinction between states with small energy difference.

APPENDIX 1 : Testing the Variational Code

Single atom of Helium on alkali-metal surfaces

For each of the alkali-element surfaces studied 80 atoms have been used in the simulation. The variational code was run with only one atom and using the one-dimensional wavefunction obtained from the numerical solution of the 1-d problem. and excellent match was obtained with the exact one-atom energies calculated by using one-dimensional methods. The following table summarises the results.

The simulation Box-Size was: 96.11246σ x 104.04479σ. and 2.000.000 Metropolis steps were used in each case.

$Surface$	E_o	E_{var}	$Acceptance$
Li	-9.00164	-9.00165 ± 0.00014	0.81353
Na	-4.81643	-4.81655 ± 0.00010	0.85014
K	-2.43950	-2.43957 ± 0.00006	0.88189
Rb	-1.81043	-1.81049 ± 0.00004	0.89440
Cs	-1.48781	-1.48789 ± 0.00004	0.90090

Table A 1.1 Single atom of Helium on alkali-metal surfaces. Comparison of Variational energies with the exact values

Scaling with repect to the number of simulation atoms

Several calculations were done with $N = 64$ and $N = 108$. All the results were within the statistical error.

random number lists used

Several calculations carried out with different random number lists all yielded the same results upto statistical sampling errors.

Reproducing results for a graphite surface

Both the variational and the Green's function Monte Carlo codes have reproduced the results for a graphite surface that were produced on the CRAY

APPENDIX 2 : Random Number Generator Used

RANNYU() :

The following is a listing of the FORTRAN code of the random-number generator used for the present work.

```
      function rannyu()
      real*8 rannyu
      integer*4 m1,m2,m3,m4,l1,l2,l3,l4,i1,i2,i3,i4
      common /rnyucm/ m1,m2,m3,m4,l1,l2,l3,l4
      i1=l1*m4+l2*m3+l3*m2+l4*m1
      i2=l2*m4+l3*m3+l4*m2
      i3=l3*m4+l4*m3
      i4=l4*m4
      l4=mod(i4,2**12)
      i3=i3+i4/2**12
      l3=mod(i3,2**12)
      i2=i2+i3/2**12
      l2=mod(i2,2**12)
      l1=mod(i1+i2/2**12,2**12)
      rannyu=2.0**(-12)*(dfloat(l1)+
     + 2.0**(-12)*(dfloat(l2)+
     + 2.0**(-12)*(dfloat(l3)+
     + 2.0**(-12)*(dfloat(l4)))))
      return
      end
      block data dtseed
      integer*4 m(4),l(4)
      common /rnyucm/ m(4),l(4)
      data m / 502,1521,4071,2107/
      data l / 3340, 2254, 6352, 4015/

      end
```

APPENDIX 3 : Interatomic potentials for Helium

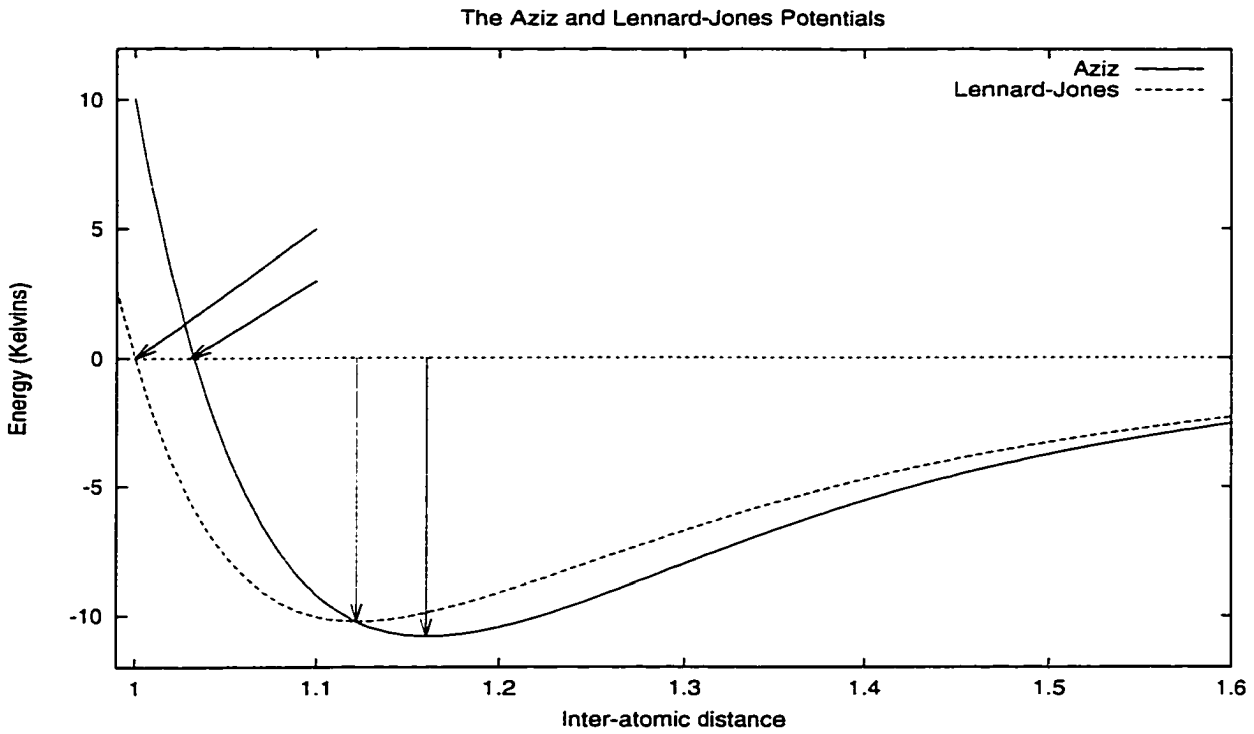

Fig. A 3.1 The Lennard-Jones and Aziz Potentials

Lennard Jones

This was the earliest somewhat successful potential proposed by de Boer and Michels (1938) which was fitted to second virial coefficients above 60 K This potential arose from an estimation of the gas corrections involved in helium gas thermometry. McMillan used this potential to study the ground state of liquid helium, which was the first attempt to use variational methods.

$$V(r) = 4\epsilon[(\sigma/r)^{12} - (\sigma/r)^{6}]$$
$$\epsilon = 10.22K.$$
$$\sigma = 2.556A$$

Later, more accurate potentials were proposed that were fits to viscosity, molecular beam and thermal conductivity data. We use a potential due to Aziz *et. al.* (1978), which we describe below.

Ahlrichs-Aziz potential, 1979

This is the interatomic potential for helium used in all calculations in the present work. It was proposed by Ahlrichs *et. al.* (1976) and later improved upon by Aziz *et. al.* (1979) and is referred to as HFDHE2. Ahlrichs *et. al.* used a combination of *ab initio* calculation of the self-consistent-field Hartree-Fock repulsion between closed shell systems, an empirical estimate of the correlation energy and semi-emperically determined dispersion coefficients C_6, C_8 and C_{10}. The form of the potential is

$$V(r) = Aexp(-\alpha x) - \left\{\frac{C_6}{x^6} + \frac{C_8}{x^8} + \frac{C_{10}}{x^{10}}\right\}F(x).$$

where

$$F(x) = exp - \left[\left\{\frac{D}{x} - 1\right\}^2\right] \qquad for \quad x < D$$

$$= 1 \qquad for \quad x \geq D$$

and $D = 1.28$ and $x = r/r_m$.

The function $F(x)$, which was considered to be universal for all spherical systems, was obtained by fitting a potential of this form to the accurately known potential curve of the $^3\Sigma_u^+$ state of H_2. This fixed the value of parameter D at 1.28.

The input data for this potential are the Self-Consistent-Field Hartree Fock calculations of the repulsive interactions due to McLaughlin and Schaefer (1971)

restricted to the range 4.0-6.0 a.u. and the dispersion coefficients of Tang *et. al.* (1976). (C_6 = 1.47 a. u. and C_8 and C_{10} rounded off to 14 and 170 a. u. respectively). There are no adjustable parameters and the values of ϵ/k = 10.6 K and r_m = 2.98 result from constraints on the value of the reduced potential and its slope at its minimum.

Aziz *et. al.* (1979) improved the fit of the high temperature bulk properties and interestingly the resulting potential turned out closer to *ab initio* calculations. This potential, named HFDHE2 (after Ahlrichs's HFDHE1) was later found to be the "best" potential in a comprehensive study of available potentials (Kalos *et. al.*, Modern potentials and the properties of condensed ^4He), and has since been used in Monte Carlo studies of Helium. We too have used this potential in all our calculations.

The parameters for this potential are:

$A = 0.5448504 \times 10^6$	$\epsilon/k = 10.8K$
$\alpha = 13.353384$	$C_6 = 1.37732412$
$D = 1.241314$	$C_8 = 0.4253785$
$r_m = 2.9673A$	$C_{10} = 0.178100$

Aziz *et. al.*, 1987 report a newer potential which they call HFD–B form. This potential gave slightly lower energies (0.04/9.80) for a variational run, but we have not extensively used this potential. It has been fitted to low temperature second virial coefficient data and recent accurate room temperature viscosity data, while at the same time pinning the repulsive wall to the value calculated by Ceperley and

Partridge at 1 Bohr. It possesses a well-depth of 10.948 K. considerably deeper than many of the recent emperical or *ab-initio* potentials.

BIBLIOGRAPHY

Ahlrichs, R., P. Penco, and G. Scoles, Chem. Phys. 19, (1976): 119.

Andersen, Hans C., *Molecular dynamics simulation at constant pressure and/or temperature*, J. Chem. Phys., Vol. 72, No. 4, (15 Feb. 1980): 2384-93.

Arnow, David, *Doctoral Dissertation*, New York University, New York, 1981.

Aziz, Ronald A., F. R. W. McCourt and C. C. K. Wong, *A new determination of the ground state interatomic potential for* He_2, Molecular Physics 61, (1987): 1487.

Aziz, Ronald A., Martin J. Slaman, *An examination of ab initio results for he helium potential energy curve*, J. of Chem. Phys. 94, (1991): 8047.

Aziz, Ronald A., V. P. S. Nain, J. S. Carley, W. L. Taylor, and G. T. McConville, *An accurate intermolecular potential for helium*, J. of Chem. Phys. 70 (9), (1 May 1979): 4330-42.

Belić, A., and S. Fantoni, *Variational Monte Carlo study of* ^4He *in two dimensions*, Physica 194-196B, (1994): 517.

Bijl, A., Physica 7, (1940): 869.

Bogolyubov, N. N., J. Phys. U.S.S.R. 11, (1947): 23.

Bogolyubov, and N. N., Zubarev, JETP 1, 83 (1955).

Brueckner, K. A., and Sawada, K., *Bose-Einstein Gas with Repulsive Interactions: General Theory*, Phys. Rev., Vol. 106, No. 6, (15 June 1957): 1117.

Brueckner, K. A., and Sawada, K., *Bose-Einstein Gas with Repulsive Interactions: Hard Spheres at High Density*, Phys. Rev., Vol. 106, No. 6, (15 June

1957): 1128.

Carlos, E. William, and Milton W. Cole. *Interaction between a He atomand a graphite surface*. Surface Science 91, (1980): 339-357.

Carraro, C., M. W. Cole. *Existence and nature of a helium monolayer film*. Phys. Rev. B 46, (1992): 10947-10951.

Callen, H. B., *Thermodynamics*. John Wiley and Sons, New York, 1960.

Ceperley, D. M., *Path integrals in the theory of condensed helium*. Reviews of Modern Physics, Vol. 67, No. 2, (April 1995): 279-355.

Ceperley, D. M., R. O. Simmons, and R. C. Blasdell, *Kinetic Energy of Liquid and Solid* ^4He. P.R.L. Vol 77, No. 1, (1996): 115-118.

Ceperley, and D. M., H. Partridge, *The* He_2 *potential at small distances*. J. Chem. Phys. 84 (2), (15 Jan. 1986): u20-1.

Cheng, Chizmeshya, Cole, Klein, Ma, Saam and Treiner. *New Phenomena predicted for films on weak-binding surfaces*. Physica A 177 (1991): 466-373.

Cheng, E., Milton W. Cole, W. F. Saam, J. Treiner, Phys. Rev. Lett., *Helium Prewetting and Nonwetting on Weak-Binding Substrates*. Phys. Rev. Lett. 67, (1991): 1007.

Cheng, E., Milton W. Cole, J. Dupont-Roc, W. F. Saam, J. Treiner, *Novel wetting behaviour in quantum films* . Rev. Mod. Phys. 65, (1993): 557-567.

Cheng, E., A. Chizmeshya, M. W. Cole, J. R. Klein, J. Ma, W. F. Saam and J. Treiner, *New phenomena predicted for films on weak-binding surfaces*, Physica 177A, (1991): 466.

Chester, G. V., Phys. Rev. 100, (1955): 455.

Chester, G. V., *Speculations on Bose-Einstein Condensation and Quantum Crystals*, Phys. Rev. A, Vol 2 No. 1 (1970): 256-58

Ciccotti, G., D. Frenkel, I.R. McDonald (editors), *Simulation of Liquids and Solids. Molecular Dynamics and Monte Carlo Methods in Statistical Mechanics.* This is a selection of important papers between 1953 and 1985.

Clements, B. E., E. Krotscheck, H. J. Lauter, and M. Saarela, *Temperature Dependence of Third Sound in Helium Monolayers*, Physica 194-196B, (1994): 657.

Clements, B. E., H. Forbert and E. Krotscheck and M. Saarela, J. ^4He *on Weakly Attractive Substrates: Structure, Stability, and Wetting Behavior*, Low Temp. Phys. 95, (1994): 849.

Clements, B. E., H. Forbert, E. Krotscheck, H. J. Lauter, and C. J. Tymczak, *Dynamics of Quantum Films*, Physica 194-196B, (1994): 659-60.

Clements, B. E., E. Krotscheck, H. J. Lauter, and M. Saarela, *Structure and Growth of Quantum Films*, Physica 194-196B, (1994): 655-56.

Clements, Krotscheck and Lauter, *Growth Instability in Helium Films*, PRL, Vol 70, No. 9, (1 Mar 1993): 1287-90.

Clements, Epstein, Krotscheck and Saarela, *Structure of boson quantum films*, Phys. Rev. B, Vol. 48, No. 10, (1 Sep 1993): 7450-7470.

Crowell, P. A., and J. D. Reppy, *Superfluidity and film structure in* ^4He *ad-sorbed on graphite*, Phys. Rev. B, Vol. 53, No. 5, (1996): 2701-18.

Crowell, P. A., J. D. Reppy, *Superfluidity in thin ^4He films adsorbed on graphite*. Physica 197B, (1994): 269-77.

Crowell, P. A., J. D. Reppy, *Reentrant Superfluidity in ^4He Films Adsorbed on - Graphite*. PRL, Vol 70, No. 21, (24 May 1992): 3291-94.

Cole, Milton W. *The Extraordinary Phenomena of Weak Adsorption* . J. of Low Temp. Phys., Vol 101, Nos. 1/2, (1995): 25-30.

deBoer, J., and A. A. Michiels, Physica 5, (1938): 945; 6, (1939): 97.

Dingle, R. B., Phil. Mag. 40, (1949): 573.

Feynman, R. P., Phys. Rev., 91, (1953): 1291.

Feynman, R. P., Phys. Rev., 94, (1954): 262.

Greywall, D. G., *Heat capacity and the commensurate-incommensurate transition of ^4He adsorbed on graphite*. Phys. Rev. B 47, No. 1, 309 (1993).

Hansen, Jean P. and Ian R. McDonald, *Theory of Simple Liquids*. Academic Press, London, 1976.

Hansen, Jean-Pierre, and Loup Verlet, *Phase Transitions of the Lennard-Jones System*, Phys. Rev., VOl 184, No. 1, (5 Aug. 1969): 151-61.

Huang, Kerson, *Statistical Mechanics*, Wiley Eastern Ltd., New Delhi, 1963.

Hulpke, E. (ed.), *Helium Atom Scattering from Surfaces*, Springer-Verlag, (1995): 25-40.

Jastrow, Robert, Phys. Rev. 98, (1955): 1479.

Kalos, M. H., *Energy of a Boson Fluid with Lennard-Jones Potentials*, Phys. Rev. A, Vol. 2, No. 1, (July 1970): 250-55.

Kalos, M. H., M. A. Lee, P. A. Whitlock, and G. V. Chester, *Modern potentials and the properties of condensed ^4He*, Phys. Rev. B 24, (1981): 115.

Kalos, Malvin H. and Paula A. Whitlock, *Monte Carlo Methods*, John Wiley and Sons, New York, 1986.

Kalos, M. H., D. Levesque and L. Verlet, *Helium at zero temperature with hard-sphere and other forces*, Phys. Rev. A Vol. 9 No. 5, (1974): 2178-2195.

Ketola, K.S., S. Wang and R. B. Hallock, *Anomalous Wetting of Helium on Cesium*, Phys. Rev. Lett. 68, (1992): 201-4.

Lee, T. D., Kerson Huang, and C. N. Yang, *Eigenvalues and Eigenfunctions of a Bose System of Hard Spheres and Its Low-Temperature Properties*, Phys. Rev., Vol. 106, No. 6, (15 June, 1957).

London, F., Nature 141, (1938): 643.

London, F., *Superfluids*, (John Wiley and Sons, Inc., New York, 1954.

MacFarland, T., G. V. Chester, M. H. Kalos, L. Reatto and S. A. Vitiello, *An Improved Shadow Wavefunction for Bulk He-4*, Physica 194-196B, (1994): 525-26.

MacFarland, T., S. A. Vitiello, L. Reatto, G. V. Chester, M. H. Kalos, *Trial shadow wave function for the ground state of* ^{4}He, Phys. Rev. B, Vol. 50, No. 18, (1 Nov. 1994): 13,577-93.

Masserini, G. L., L. Reatto, *Maximum-overlap Jastrow wave function for liquid* ^{4}He., Phys. Rev. B, Vol. 35, No. 13, (1 May 1987): 6756-61.

Matsubara, T., Progr. Theoret. Phys. Japan 6, (1951): 714.

Metropolis, N., A. W. Rosenbluth, M. N. Rosenbluth, A. H. Teller, and E. Teller. *Equation of State Calculations by Fast Computing Machines*. J. Chem. Phys. 21 (6), (June, 1953): 1087-93.

McMillan, W. L. *Ground State of Liquid He^4*. Phys. Rev. 138 2A, (1965): A442.

Mochel, Jack M., Ming-Tang Chen. *Superfluid helium on solid hydrogen*. Physica 197B, (1994): 278.

Moroni, Saverio, Stefano Fantoni, and Gaetano Senatore, *Euler Monte Carlo calculations for liquid ^4He and ^3He.* . Phys. Rev. B. Vol 52. No. 18, (1995): 13.547-58.

Mott, N. F., Phil. Mag. 40, (1949): 61.

Nacher and Dupont-Roc. *Experimental Evidence for Nonwetting with Superfluid Helium*. PRL. Vol 67. No. 21. (18 Nov 1991): 2966-69.

Nosanow, N. H., Phys. Rev. 146, (1966): 120.

Pederiva, F., A. Ferrante, S. Fantoni, and L. Reatto, *Variational Monte Carlo Calculations for Solid-Liquid Coexistence and Interface in ^4He with Shadow Wave Function*. Physica 194-196B, (1994): 967.

Pederiva, F., A. Ferrante, and S. Fantoni, L. Reatto, *Quantum Theory of Solid-Liquid Coexistence and Interface in ^4He* . Phys. Rev. Lett. 72, (1994): 2589.

Pederiva, F., A. Ferrante, and S. Fantoni, L. Reatto, , Phys. Rev. B, Vol. 52 (1995): 7564.

Penrose, Oliver and Lars Onsagar, *Bose-Einstein Condensation and Liquid He-*

lium, Phys. Rev. Vol 104, No. 3, (Nov. 1 1956): 576-84.

Press, William H., Saul A. Teukolsky, William T. Vetterling, and Brian P. Flannery, *Numerical Recipes in Fortran*, Cambridge University Press, Cambridge, 1992.

Pricaupenko, L., and J. Treiner, *Quantum Prewetting Transitions in Liquid ^3He*, Phys. Rev. Lett. 72, (1994): 2215.

Rahman, A., *Correlations in the Motion of Atoms in Liquid Argon*, Phys. Rev., Vol. 136, No. 2A, (19 Oct. 1964): A405-412.

Romano, S., and K. Singer, *Calculation of the entropy of liquid chlorine and bromine by computer simulation*, Molecular Physics, Vol. 37, N0. 6, (1979): 1765-72.

Rosenbluth, M. N., and A. W. Rosenbluth, J. Chem. Phys. 22, (1954): 881.

Saarela, M., B. E. Clements, E. Krotscheck and F. V. Kusmartsev, *Phase Transitions in the Growth of ^4He Films*, J. Low Temp. Phys. 93, (1993): 971.

Schmidt K., M. H. Kalos, and Michael A. Lee and G. V. Chester, *Variational Monte Carlo Calculations of Liquid ^4He with Three-Body Correlations*, Phys. Rev. Lett. 45, (1980): 573.

Shirron, P. J., and J. M. Mochel, *Atomically Thin Superfluid Helium Films on Solid Hydrogen*, Phys. Rev. Lett. 67, (1991): 1118.

Taborek, P., J.E. Rutledge, *Wetting transitions of helium on weak binding substrates*, Physica 197B, (1994): 283.

Tisza, L., Nature 141, (1938): 913.

Verlet, Loup *Computer "Experiments" on Classical Fluids. I. Thermodynamical Properties of Lennard-Jones Molecules*, Phys. Rev., Vol. 159, No. 1, (5 July 1967): 98-103.

Vitiello, Silvio, Karl Runge, and M. H. Kalos, *Variational Calculations for Solid and Liquid* ^{4}He*with a "Shadow" Wave Function*, PRL, Vol 60, No. 19, (9 May 1988): 1970-72.

Whitlock, P. A., G. V. Chester, M. H. Kalos, *Monte Carlo study of* ^4He *in two dimensions*, Phys. Rev. B 38, (1988): 2418.

Whitlock, P. A., G. V. Chester, *Monte Carlo study of a* ^4He *film on Graphite*, provisionally accepted by Phys. Rev. B.

Wu, Fa Yueh and Eugene Feenberg, *Ground State of Liquid Helium (Mass 4)*, Phys. Rev., Vol 122, No. 3 (1961) 739-742.

Wood, W. W., and F. R. Parker, *Monte Carlo Equation of State of Molecules Interacting with the Lennard-Jones Potential. I. A Supercritical Isotherm at about Twice the Critical Temperature*, J. of Chem. Phys., Vol 27, No. 3, (Sept. 1957): 720-33.

Wyatt, Klier and Stefanyi, *Prewetting of* ^4He *on Rb: The Coexistence of Two Superfluid Films?*, PRL, Vol 74, No. 7, (13 Feb 1995): 1151-4.

Zaremba, E., W. Kohn, Phys. Rev. B, 13, (1976): 2270.

Zhang, Shiwei, M. H. Kalos, G. V. Chester, S. A. Vitiello, and L. Reatto, *A Self-Bound Wavefunction for Clusters of* ^4He, Physica 194-196B, (1994): 523.

Zimmerli, Mistura and Chan. *Third-Sound Study of a Layered Superfluid Film.* PRL, Vol 68, No. 1, (6 Jan 1992): 60-63.

IMAGE EVALUATION TEST TARGET (QA-3)

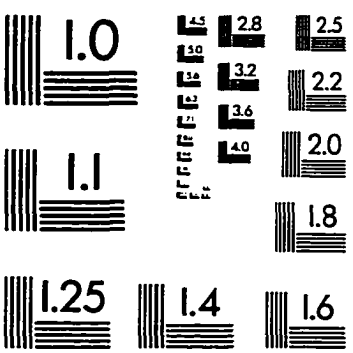

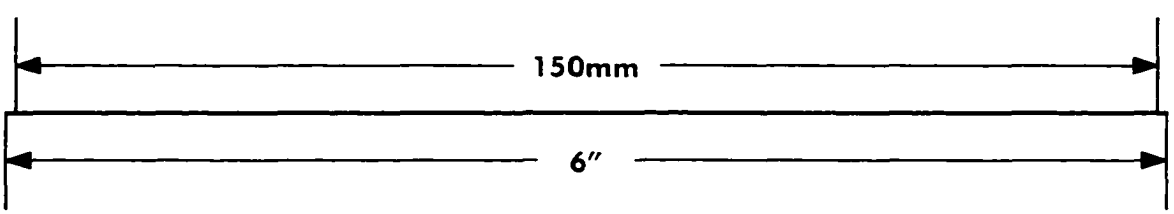

APPLIED IMAGE, Inc
1653 East Main Street
Rochester, NY 14609 USA
Phone: 716/482-0300
Fax: 716/288-5989